

# Use of Achiral and Meso Ligands To Convey Asymmetry in Enantioselective Catalysis

Patrick J. Walsh,<sup>\*,†</sup> Alice E. Lurain,<sup>†</sup> and Jaume Balsells<sup>‡</sup>

*P. Roy and Diana T. Vagelos Laboratories, Department of Chemistry, University of Pennsylvania, 231 South 34th Street, Philadelphia, Pennsylvania 19104-6323, and Department of Process Research, Merck Research Laboratories, P.O. Box 2000, Rahway, New Jersey 07065*

Received January 20, 2003

## Contents

1. Introduction and Scope	3297	6.2.2. Diimine Ligands with Meso Backbones	3334
2. The Use of Achiral Salen Ligands in Asymmetric Catalysis	3305	6.2.3. Diimine Ligands with Atropisomeric Biphenyl Backbones	3334
3. Use of Achiral Biphenol-Based Ligands in Asymmetric Catalysis	3308	6.2.4. Simple Achiral Diamine Ligands	3336
3.1. Asymmetric Carbonyl–Ene Reaction	3308	6.2.5. Diamine Ligands That Form Stereogenic Centers on Binding to Metals	3336
3.2. Asymmetric Addition of Methyl Groups to Aldehydes	3309	6.2.6. Diamine Ligands with Pendant Atropisomeric Substituents	3336
3.3. Asymmetric Baeyer–Villiger Oxidation	3309	6.2.7. Impact of Achiral and Meso Ligands on Catalyst Efficiency	3337
4. Atropisomeric Biphenyl-Based Phosphines and Related Ligands in Asymmetric Catalysis	3310	6.3. Geometry-Induced Ligand Asymmetry	3338
4.1. Asymmetric Hydrogenation Reactions Using BIPHEP-Derived Ligands	3311	7. Concluding Remarks	3340
4.2. Asymmetric Diels–Alder and Carbonyl–Ene Reactions with BIPHEP-Derived Ligands	3313	8. Acknowledgments	3340
4.3. Interconversion of Diastereomeric Catalysts and Catalyst Precursors Containing BIPHEP Derivatives	3315	9. References	3340
4.4. Mechanistic Aspects of Atropisomerization of BIPHEP	3317		
4.5. A Potentially Useful New Class of Achiral Diphosphine Ligands (NUPHOS)	3319		
4.6. Complexes of a Meso Cyclohexane-Based Diphosphine	3320		
4.7. Spontaneous Resolution of an Asymmetric Catalyst Bearing a Bis(phosphole) Ligand	3320		
4.8. A Metallocene Catalyst with a Biphenyl Backbone	3322		
4.9. Use of Bis(diphenylphosphino)ferrocene and Related Ligands in Asymmetric Catalysis	3323		
4.10. Dynamic Resolution of Bis(phosphoryl)–Zr Complexes	3325		
5. Examination of the Barrier to Atropisomerization in Biphenyl-Based Diamines	3326		
5.1. 1,1'-Biphenyl-2,2'-diamine (DABP) Derivatives	3326		
5.2. Atropisomeric Bisoquinolines and Bipyridines	3327		
5.3. 2,2'-Bis(2-imidazole)biphenyl Ligands	3330		
6. Catalyst Optimization with Achiral and Meso Ligands Having Chiral Conformations	3331		
6.1. Achiral and Meso Bis(sulfonamide) Ligands with Chiral Titanium Alkoxides	3331		
6.2. Achiral and Meso Diamine and Diimine Ligands with Zinc(BINOLate)	3333		
6.2.1. Simple Achiral Diimine Ligands	3334		

## 1. Introduction and Scope

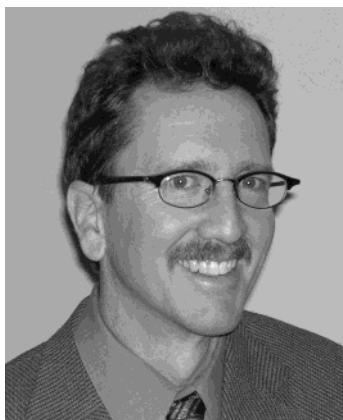
The field of asymmetric catalysis has progressed rapidly since the early 1980s, as judged by the increasing number of reports each year and the greater frequency with which enantioselective catalysts are employed in industry.<sup>1–3</sup> This intense research effort has greatly expanded the variety of reactions that can be performed with good substrate generality and in a highly enantioselective fashion. Despite this remarkable success, most asymmetric catalysts do not meet the criteria required to be attractive to industry, such as high turnover frequency, long catalyst lifetimes, tolerance of air and moisture, and high enantioselectivity. Therefore, new catalysts will need to be developed.

The approach to developing new catalysts has not changed greatly since the early days of asymmetric catalysis. In general, chemists rely on their intuition to design and optimize new catalysts. Research in asymmetric catalysis has been driven by the need to develop and optimize enantioselective processes. As a result, investigations into the reaction mechanisms have received less emphasis, and our understanding is not well developed. Further contributing to this deficiency is the complexity exhibited by many catalytic systems. Thus, the era of rationally designed catalysts may be in the distant future.

Emerging strategies to develop asymmetric catalysts based on combinatorial methods hold great promise.<sup>4–29</sup> Several research groups have successfully synthesized families of ligands and catalysts for use in asymmetric catalysis, while others have used

<sup>†</sup> University of Pennsylvania.

<sup>‡</sup> Merck Research Laboratories.



Patrick J. Walsh hails from El Cajon, CA. He received his B.A. from the University of California, San Diego (1986), where he was mentored by Prof. Charles Perrin. He graduated from the University of California, Berkeley (Ph.D., 1991), where he synthesized and examined the reactivity of Zr–N double bonds under the direction of Prof. R. G. Bergman. He was an NSF postdoctoral fellow with Prof. K. B. Sharpless at the Scripps Research Institute. Moving across town in 1994, he was an assistant professor at San Diego State University. In 1999, he moved to his current position at the University of Pennsylvania, where he was promoted to associate professor in 2002.



Alice E. Lurain was born in Portsmouth, VA, and raised in Chicago, IL. She graduated Phi Beta Kappa with a B.A. degree from Wesleyan University in Middletown, CT, in 1998. While there, she received a Tishler Scholarship for undergraduate research and worked under the direction of Professor Joseph W. Bruno on the asymmetric nitroaldol reaction. After testing her mettle as a high school chemistry teacher in New York City, Alice began work on her Ph.D. at the University of Pennsylvania in 2000. She is currently a fourth-year graduate student in the laboratory of Professor Patrick J. Walsh, with a research focus on zinc-mediated asymmetric reactions.

hits generated in a combinatorial screening approach as a starting point in the design of new catalysts.

Computational methods are being developed to evaluate “chirality content” of catalyst systems, with the goal of understanding how differences in ligand geometry impact catalyst enantioselectivities within a family of ligands.<sup>30–33</sup> Novel approaches to computer-aided ligand design for asymmetric catalysis have also met with initial success.<sup>34–37</sup> Clearly, these methods will play an increasing role in the advancement of asymmetric catalysis; however, the conventional methods of catalyst synthesis and screening will continue to be central to this field.

The traditional approach to asymmetric catalysis with metal-based catalysts is an iterative operation that revolves around the synthesis of chiral ligands



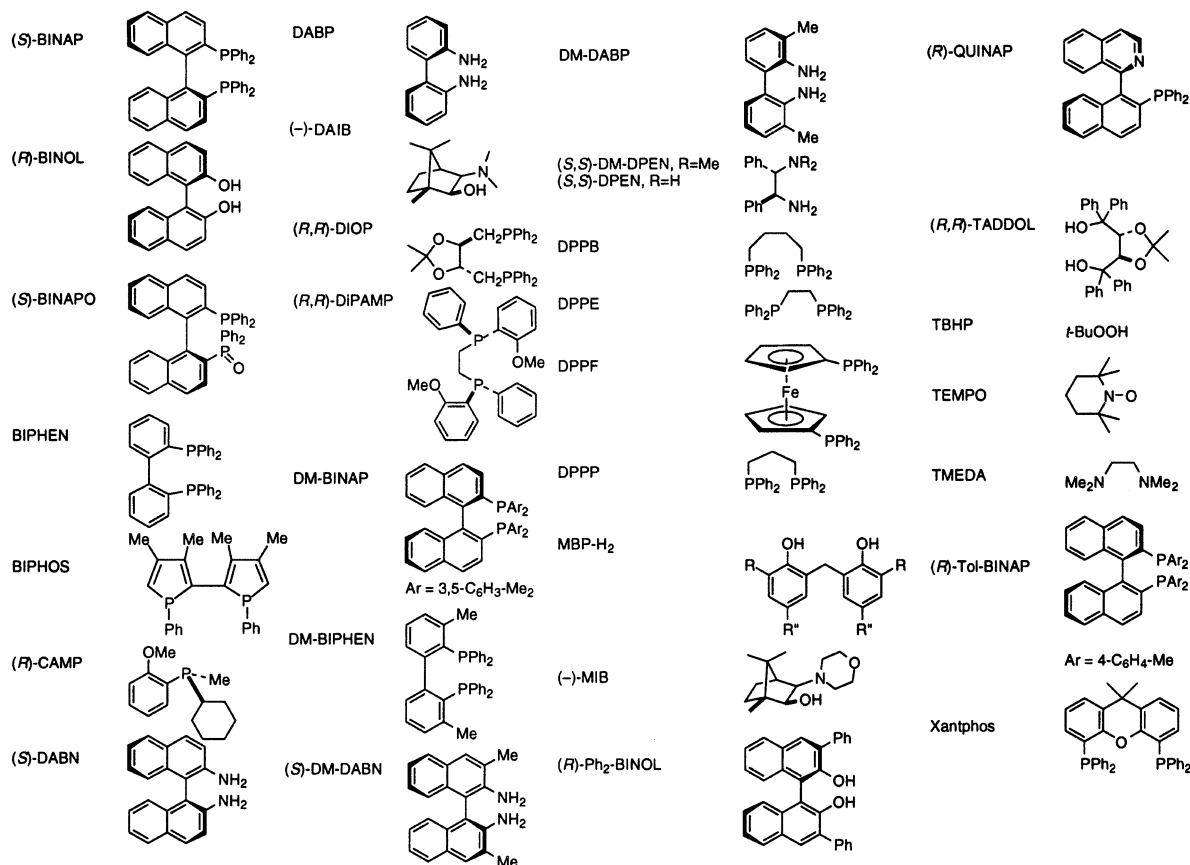
Jaume Balsells received his B.Sc. in chemistry at the Universitat de Barcelona in 1993 and stayed to study for his M.Sc. and Ph.D. degrees in organic chemistry (1998) with Professor Miquel A. Pericàs, working on the development of asymmetric versions of the Pauson–Khand reaction. He then joined the laboratory of Professor Patrick J. Walsh at the University of Pennsylvania as a postdoctoral fellow, where he worked on the use of achiral ligands for asymmetric catalysis. After two years he joined the laboratory of Professor Gary A. Molander at the University of Pennsylvania as a NATO postdoctoral fellow, where he worked on the total synthesis of varicocolin. He is currently a Senior Research Chemist in the Department of Process Research at Merck & Co., Inc., Rahway, NJ.

of high enantiopurity.<sup>1–3</sup> Once the chiral ligands have been bound to the metal center, the new catalysts are examined to determine their enantioselectivities and activities. Results of these studies are evaluated, and the next generation of ligands is designed. In this process, the key to efficient reaction optimization is often rapid access to numerous catalysts with diverse chiral environments. Unfortunately, the synthesis of enantiopure ligands can be an arduous task, severely hampering the optimization of the asymmetric process.<sup>38</sup>

A different approach to asymmetric catalysis is the use of an enantiopure ligand ( $L^*$ ) in combination with achiral or meso ligands ( $L$ ) in a catalyst  $M(L)L^*$ . The degree of interaction between the chiral ligand and the achiral or meso ligand in the complex  $M(L)L^*$  depends on the nature and the proximity of the ligands. The enantiomeric conformations of the achiral or meso ligand in  $ML$  become diastereomeric in  $M(L)L^*$  and differ in energy. If the interactions between  $L$  and  $L^*$  are strong, the chiral ligand  $L^*$  can bias the conformation of the achiral or meso ligand  $L$  such that it preferentially adopts a chiral conformation. The chiral conformation of  $L$  can play an integral part, or a dominant role, in the transmission of asymmetry from the catalyst to the substrate.<sup>39–46</sup> The advantage of this approach to asymmetric catalysis over the traditional approach is that catalysts can be optimized by the synthesis of achiral and meso ligands instead of enantiopure ligands.<sup>39,41,44–46</sup> In general, achiral ligands are more easily prepared than enantiopure ligands and are significantly less costly.

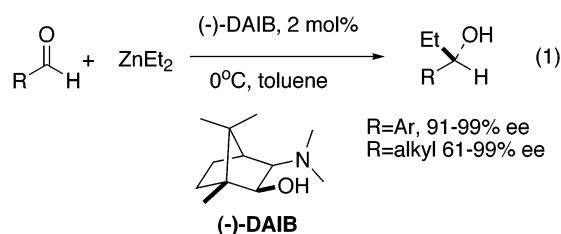
This review addresses the potential uses and documented applications of large, flexible achiral and meso ligands in asymmetric catalysis. Emphasis is placed on studies of the interaction between chiral ligands of defined stereochemistry and stereochemically dynamic ligands within the coordination sphere of a metal. An understanding of the factors that

## Chart 1. Abbreviations



impact these interligand interactions is crucial to efficient optimization of catalysts of the type  $M(L)_2$ . To aid in the understanding of these interactions, a brief examination of transmission of asymmetry within a given ligand (intraligand) is presented. The systems outlined in this section were chosen to illustrate the ways in which asymmetry can be transmitted within a metal–ligand adduct. The examples are not intended to be comprehensive, nor do they necessarily represent the most enantioselective catalysts currently known.

**Stereochemically Rigid Ligands with Defined Chiral Environments.** The simplest types of chiral ligands to understand are those that have little or no conformational freedom. An important example of this class is the  $\beta$ -amino alcohol ligand, (–)-3-*exo*-(dimethylamino)isoborneol [(–)-DAIB; see Chart 1 for a list of the abbreviations used in this review], introduced by Noyori and co-workers.<sup>47,48</sup> This ligand was shown to be highly efficient at promoting the asymmetric addition of dialkyl zinc reagents to aldehydes, as shown in eq 1.



The mechanism of the DAIB-catalyzed alkylation of aldehydes has been studied extensively.<sup>37,49–57</sup> The

initial studies by Noyori have had an enormous impact in defining our current understanding of catalytic asymmetric reactions. The DAIB system was one of the first to exhibit strong positive nonlinear behavior<sup>58</sup> and has become a cornerstone of nonlinear effects in asymmetric catalysis.<sup>59</sup> On binding of the DAIB ligand to zinc, a rigid structure is formed. Experimental and computational results point to a highly ordered transition state for this reaction and for related additions.<sup>60</sup> One possible transition state structure is illustrated in Figure 1.

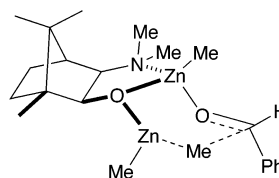


**Figure 1.** Possible transition state for alkyl addition to benzaldehyde.

In spite of the well-defined geometry of the DAIB catalyst, further optimization of the enantioselectivity of this system based on the same amino alcohol framework was not to come for several years, until the MIB ligand (Figure 2) was developed by Nugent.<sup>61</sup> Although structurally very similar to DAIB, MIB

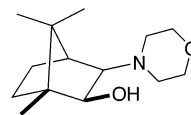


**Figure 2.** Nugent's MIB.

gives significantly higher enantioselectivities with  $\alpha$ -branched aldehydes (97–99% ee).

**Transmission of Asymmetry within a Metal–Ligand Adduct.** Early in the development of asymmetric catalysis, it was believed necessary to position the stereocenter or centers of the ligand as close to the reactive metal center as possible.<sup>62</sup> Thus, initial chiral phosphines were stereogenic at phosphorus, as exemplified by Knowles's CAMP ligand (Figure 3).<sup>63</sup>

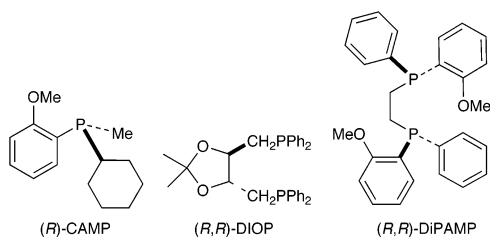


**Figure 3.** Important early chiral phosphine ligands.

In retrospect, rhodium complexes of this ligand were surprisingly enantioselective, given the high degree of rotational freedom about the P–C and the M–P bonds. It was not until Kagan's introduction of DIOP (Figure 3),<sup>64,65</sup> a chiral bidentate phosphine with two stereogenic centers far removed from the metal center, that chemists began to appreciate the importance that ligand conformations could play in asymmetric catalysis. The chelating DiPAMP ligand (Figure 3) then became the basis of the commercial production of L-DOPA, used in the treatment of Parkinson's disease.<sup>62</sup>

**Conformations of Chiral Metalloccycles: BINAP and TADDOL.** One of the most successful ligands in asymmetric catalysis is the axially chiral BINAP (Figure 4).<sup>66</sup> Although this ligand is best known for

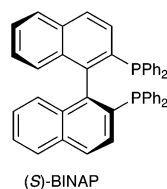


**Figure 4.** Structure of (S)-BINAP.

its application in catalytic enantioselective hydrogenations of olefins and ketones,<sup>67,68</sup> metal complexes of BINAP have found many applications in asymmetric reactions with a broad range of metals. The effectiveness with which BINAP-based catalysts convey asymmetry to substrates is a result of the projection of the axial chirality of the binaphthyl backbone to the orientations and positions of the phenyl groups. The conformation of the skewed seven-membered metalocycle causes the phenyl groups to adopt pseudoaxial and pseudoequatorial positions (Figure 5).<sup>69</sup> The pseudoequatorial phenyl rings are thrust forward, extending beyond the metal center, while the pseudoaxial phenyl groups are directed away from the metal. It is the pseudoequatorial phenyl groups that are thought to be responsible for the exquisite enantiocontrol in this ligand system.<sup>1</sup> There is also an edge–face interaction between the phosphorus-bound aryl groups.<sup>70,71</sup> The observation that substituents in the para positions

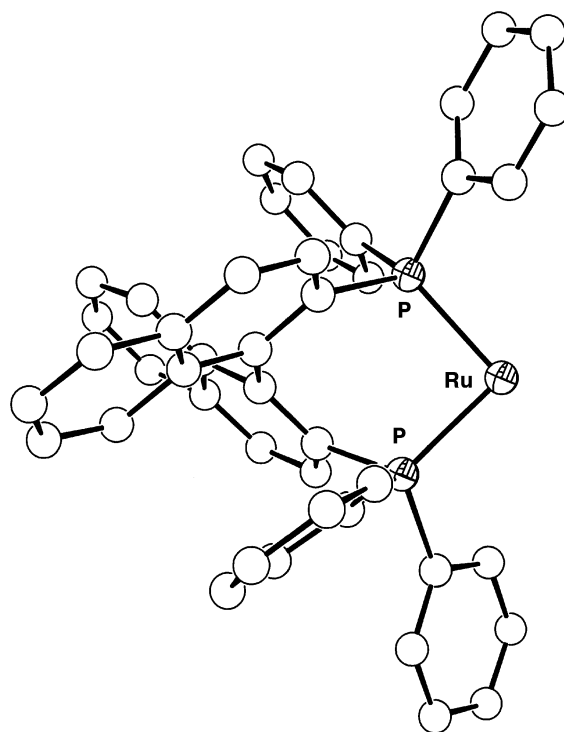


**Figure 5.** Partial structure of (BINAP)Ru(O<sub>2</sub>C-*t*Bu)<sub>2</sub>, with carboxylate ligands removed for clarity. The pseudoequatorial rings are directed forward, while the pseudoaxial phenyls are pointed away from the metal.

of the phenyl groups can impact the enantioselectivity of the catalyst is consistent with this hypothesis, although a stereoelectronic effect in such cases may be important.<sup>72</sup>

Another ligand that has frequently been employed with outstanding results is Seebach's tartaric acid-based TADDOL (Figure 6). The introduction of the

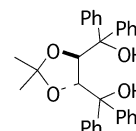


**Figure 6.** Seebach's TADDOL ligand.

original TADDOL ligand was followed by a large number of analogues with different aromatic substituents and acetal moieties.<sup>73</sup> The TADDOL family of ligands has found applications in a number of asymmetric Lewis acid-catalyzed reactions.<sup>73</sup>

The many crystal structures of the free ligands and structures of the metal-bound TADDOLate (Figure 7)<sup>74,75</sup> that have been reported provide insight into the characteristics that make these ligands outstanding.<sup>73</sup> The free rotation of the diphenylmethanol moiety of the unbound ligand is constrained upon metalocycle formation to give a trans-fused bicyclo-[5.3.0]decane ring system. The stereocenters of the dioxolane are too far removed from the metal center to have a stereodiscriminating effect. Nonetheless, they exert a powerful conformational preference on the adjacent metalocycle, effectively directing the diastereomeric aromatic substituents to adopt pseudoequatorial and pseudoaxial positions. As a result, the asymmetry of the stereogenic centers is projected

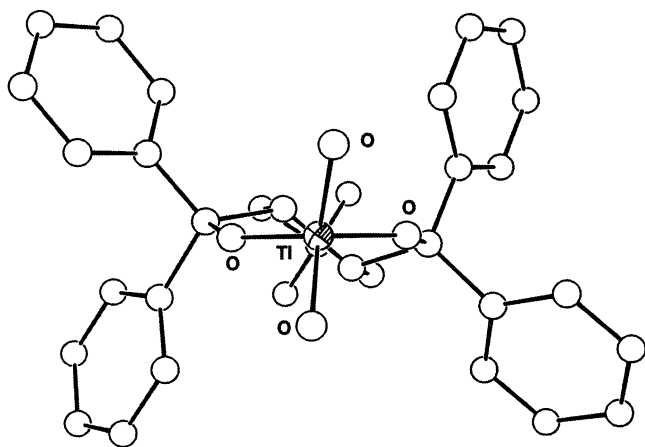


**Figure 7.** Partial structure of  $\text{Ti}(\text{TADDOLate})_2$ , with all of one ligand removed, except for the oxygens.

forward, toward the metal center. The asymmetrically disposed aryl groups define the chiral environment of the catalyst and the preferential orientation of binding of a substrate, as shown in Figure 8.<sup>76</sup>

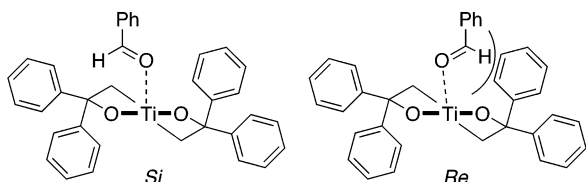
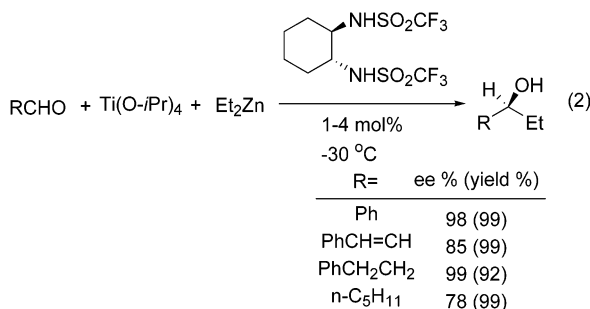


**Figure 8.** Effect of TADDOLate aryl groups on the binding of a substrate aldehyde. The dioxolane moiety has been omitted for clarity.

**Binding of Diastereotopic Groups and Lone Pairs.** The number of stereocenters in a ligand can be increased by interaction of a diastereotopic atom or lone pair with metal centers.<sup>77</sup> This interaction can limit the degrees of rotational freedom within the metal–ligand framework, thus extending and rigidifying the asymmetric environment about the reactive metal.

A class of ligands in which coordination of one of two diastereotopic atoms to metals may be important is the sulfonamide-based ligands. Bis(sulfonamide) ligands form efficient and highly enantioselective catalysts for a number of reactions, including the asymmetric addition of alkyl groups to aldehydes.<sup>78,79</sup> The reaction provides a route to prepare highly functionalized secondary alcohols with excellent enantioselectivity (eq 2).<sup>80</sup>



The titanium complexes of these bis(sulfonamide) ligands have been proposed to be the catalytically active species in this reaction.<sup>78,79,81,82</sup> Solid-state

structure determination revealed a bonding interaction between the metal center and one of the diastereotopic oxygen atoms on each sulfonamide moiety.<sup>82</sup> This  $\text{Ti}-\text{O}(\text{sulfonyl})$  interaction renders the sulfur atoms chiral, rigidifying the  $C_2$  symmetry of the complex, as seen in Figure 9. Since the chiral

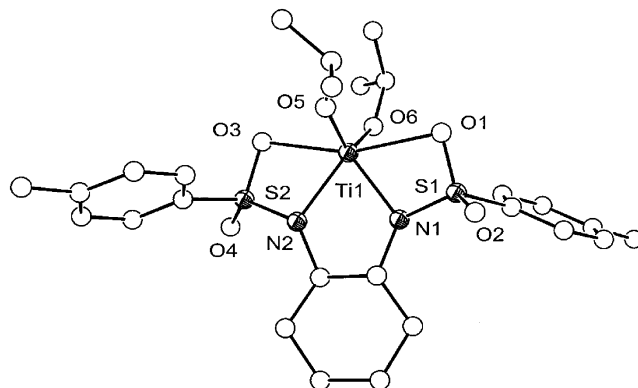


**Figure 9.** Structure of bis(sulfonamido) $\text{Ti}(\text{O}-i\text{Pr})_2$ , showing the  $\text{Ti}-\text{O}(\text{sulfonyl})$  interaction.

centers of the cyclohexane ring backbone are responsible for the orientation of the sulfonamide substituents,<sup>82–85</sup> the ligand can, in a sense, extend its chiral environment upon diastereoselective coordination of the sulfonamide oxygens. The sulfonamide substituents are closer to the reactive metal center and appear to exert a significant impact on the enantioselectivity of these catalysts.<sup>78,86</sup>

Bis(sulfonamide) ligands are also highly effective in the asymmetric amination of *N*-acyloxazolidinones with magnesium catalysts,<sup>87</sup> asymmetric cyclopropanation of allylic alcohols with zinc catalysts,<sup>88–91</sup> and the asymmetric Diels–Alder reaction with aluminum catalysts.<sup>92</sup> The Lewis acidic magnesium bis(sulfonamido) complex can potentially coordinate the sulfonyl oxygens, and evidence exists for this interaction in related systems;<sup>93</sup> however, it is unlikely that aluminum<sup>92</sup> and zinc<sup>94</sup> catalysts will bind the sulfonyl oxygens. In these latter cases, a gearing of the sulfonyl group with the chiral ligand backbone may account for the high enantioselectivity in these systems.

A related bidentate N,O-binding mode in the copper nitrene intermediates,  $L^*\text{CuNSO}_2\text{Tol}$ , generated from  $\text{PhINSO}_2\text{Tol}$ , has been proposed to be important in a mechanistic study of the enantioselective aziridination of alkenes (Figure 10).<sup>95</sup>

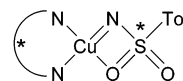


**Figure 10.** Intermediate nitrene proposed in the asymmetric aziridination of alkenes.

The number of stereogenic centers on a ligand can be increased by diastereoselective coordination of an  $\text{sp}^3$ -hybridized lone pair, usually on nitrogen or sulfur. One such example is the mixed phosphorus/sulfur ligands introduced by Evans (Figure 11).<sup>96,97</sup> The corresponding palladium complexes of these ligands are effective catalysts for asymmetric allylic substitution reactions. Under optimized conditions, the authors carried out the alkylation of 1,3-diphenyl-

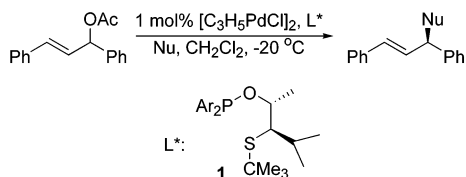


**Figure 11.** Asymmetric allylic substitution with P/S ligands.

2-propenyl acetate with dimethyl malonate in 98% yield and 97% enantioselectivity. Allylic amines could likewise be obtained in 95% yield and 97% enantioselectivity using benzylamine as the nucleophile (Figure 11).

Palladium binds to ligand **1** in a bidentate manner by coordination of one of the diastereotopic sulfur lone pairs (Figure 12). Solid-state and solution studies

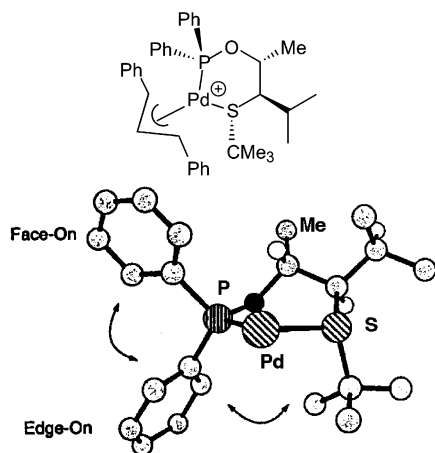
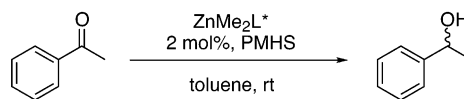


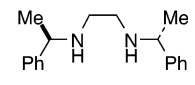
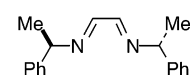
**Figure 12.** Structure of the allyl–Pd complex of **1** (top), with partial structure showing the stereogenic sulfur and the interaction of the substituents to create the chiral environment.

indicate that the isopropyl group adjacent to the sulfur causes the *S*-*t*Bu group to orient opposite the isopropyl substituent, resulting in detection of a single diastereomer at low temperature. The gearing, or buttressing, effect of the isopropyl group on the ligand backbone greatly increases the energy difference between coordination of the diastereotopic lone pairs of the sulfur atom, such that the chirality of the ligand backbone is effectively transmitted to the sulfur. The sulfur is closer to the reactive center of the catalyst and can have a profound effect on the enantioselectivity of the reaction.

Mimoun and co-workers have used chiral diamine zinc complexes as catalysts for the asymmetric reduction of ketones with polymethylhydrosiloxane.<sup>98</sup> The catalyst was obtained in quantitative yield by combining *N,N*-ethylenebis(1-phenylethylamine) (**2**, Figure 13) and dimethylzinc. In the structure of the resulting complex, the stereochemical information in the chiral *N*-phenethyl groups is effectively relayed to the nitrogen centers, which are rendered configurationally stable (Figure 13). The close proximity of the stereogenic nitrogens to the zinc is expected to impact the enantioselectivity in the ketone reduction reactions.

When the reduction of acetophenone was performed using a catalyst derived from diamine **2** and



L*	Yield (%)	e.e. (%)
 <b>2</b>	100	75 ( <i>R</i> )
 <b>3</b>	98	48 ( <i>S</i> )

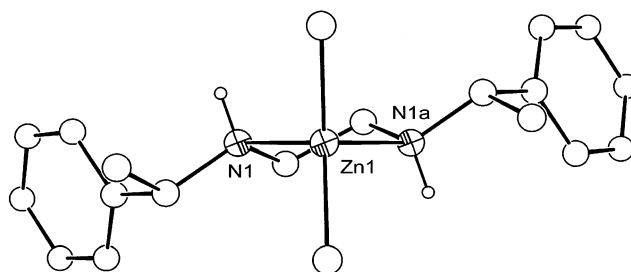


**Figure 13.** Enantioselective reduction of ketones by polymethylhydrosiloxane in the presence of chiral zinc catalysts (above), and structure of  $\text{ZnMe}_2$  coordinated to diamine **2** (below).

dimethylzinc, quantitative formation of the (*R*)-alcohol product was observed in 75% enantioselectivity (Figure 13). Interestingly, the dimethylzinc complex of chiral diimine **3** was also shown to promote the reaction, but it gave the reduced product with the *opposite absolute configuration* in modest enantioselectivity (48%, Figure 13). Since the nitrogen atoms in the diimine ligand are  $\text{sp}^2$  hybridized, the side chains are the only groups responsible for controlling the transfer of asymmetry in the reaction.

#### Catalysts That Are Chiral at the Metal Center.

As illustrated above, positioning the chiral centers of the asymmetric ligand as close to the metal as possible can have a significant impact on the enantioselectivity of the catalyst. It is reasonable, therefore, to expect that a chiral metal center<sup>99,100</sup> would further increase the level of catalyst enantiocontrol. Key to this strategy is choosing a chiral ligand such that, on binding to the metal center, a single configuration at the metal is preferred. This can be a challenge, because the coordination number of the metal will likely change throughout the course of the reaction and may permit epimerization of the metal center.

Faller's group has explored this strategy and recently reported the use of complexes **4** and **5** (Figure 14), with central chirality at the metal, in the Diels–Alder reaction of cyclopentadiene and methacrolein with excellent enantioselectivity.<sup>101–104</sup>

The ruthenium complex **4** was obtained as a 5:1 mixture of diastereomers by reacting (*R*)-QUINAP with  $[\text{CyRuCl}_2]_2$ . An attempt to recrystallize **4** led to the equilibration of the mixture to a single diastereomer. The reaction of  $[\text{CyRuCl}_2]_2$  with (*S*)-BINPO afforded complex **5** as a single diastereomer. The Lewis acidic forms of the catalysts are generated in situ by treatment of the precatalysts **4** and **5** with  $\text{AgSbF}_6$  to generate the corresponding aquo com-

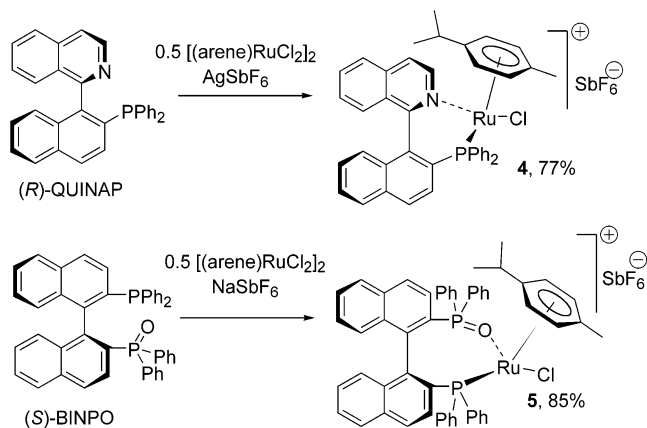


**Figure 14.** Complexes for asymmetric catalysis with central chirality at the metal center.

plexes. The authors also showed that a single diastereomer of the aquo derivative of **4** could be obtained from the kinetic 5:1 mixture of diastereomers. The Diels–Alder adducts of methacrolein and cyclopentadiene were obtained in very high diastereo- and enantioselectivity (Figure 15).

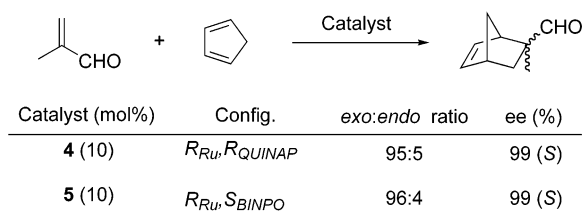


**Figure 15.** Asymmetric Diels–Alder reactions catalyzed by complexes with central chirality at the metal center.

**Ligands That Can Adopt Atropisomeric Conformations.** *Biphenyl-Based Ligands.* Axial chirality has also proven to be very effective in controlling stereoselection with several classes of ligands. The transmission of central chirality to an axially chiral group that undergoes atropisomerization within a given ligand has been successfully demonstrated.<sup>77</sup> Reetz and co-workers<sup>105</sup> reported the use of diphosphite ligands **6a–d** in the rhodium-catalyzed hydrogenation of dimethyl itaconate to afford chiral diesters (Figure 16).

The sugar-derived diol was derivatized as a bis-(phosphite) in which the phosphorus centers bear a stereochemically fixed binaphthyl or a stereochemically dynamic biphenyl group that adopts axially chiral conformations. When (*R*)- or (*S*)-BINOL was incorporated into the ligands (**6a** and **6b**), products of opposite configuration were obtained with high ee, indicating that the axially chiral portion of the ligand was responsible for the sense of enantioselectivity.

When ligand **6c**, based on atropisomerically flexible biphenyl, was used in the reaction, product of 39% ee was obtained, showing poor control of enantioselectivity. The best results were obtained with ligand **6d**, which afforded product having higher enantiomeric excess (96.8%) than the BINOL-based ligands (87.8% with (*S*)-BINOL and 94.5% with (*R*)-BINOL).

With no structural information on the catalyst, the excellent performance of ligand **6d** could be the result

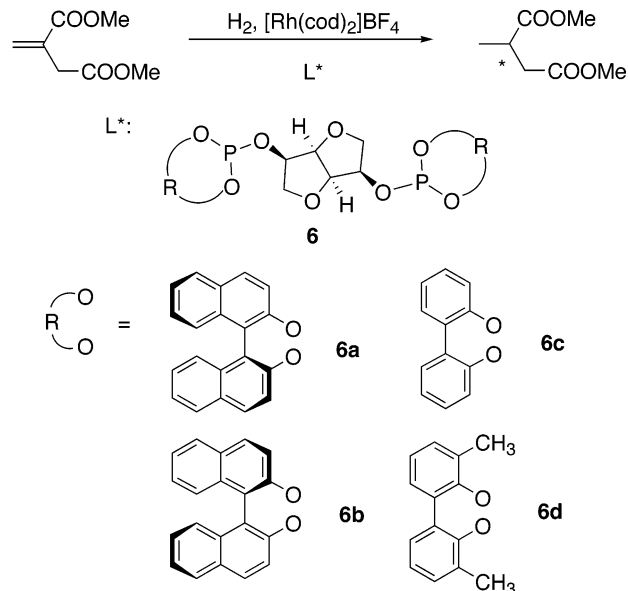


**Figure 16.** Asymmetric hydrogenation of dimethyl itaconate with chiral diphosphite ligands.

of two limiting situations: the generation of a dynamic mixture of diastereomeric catalysts having markedly different reaction rates or a high control of the axial chirality of the biphenyl group, generating a single highly enantioselective catalyst.

*Atropisomeric Amides.* The vast majority of atropisomeric ligands used in asymmetric catalysis are biaryl derivatives; however, recent advances in the use of atropisomeric amide-based ligands highlight the ability of these ligands to convey asymmetry.<sup>106</sup> Given that the synthesis of atropisomeric amides with only axial chirality is not trivial,<sup>107–109</sup> central chirality at the tetrahedral carbon atom bearing the amide nitrogen can be used to influence dynamic axial chirality and provide entry into ligands containing atropisomeric amides.<sup>110,111</sup>

With this goal in mind, Mino and co-workers have reported the use of the atropisomeric amide-based ligand **7** for the palladium-catalyzed allylic alkylation.<sup>110</sup> Under their optimized conditions, they have carried out the alkylation of 1,3-diphenyl-2-propenyl acetate with dimethyl malonate in 94% yield and 85% enantioselectivity (Figure 17). Although they have

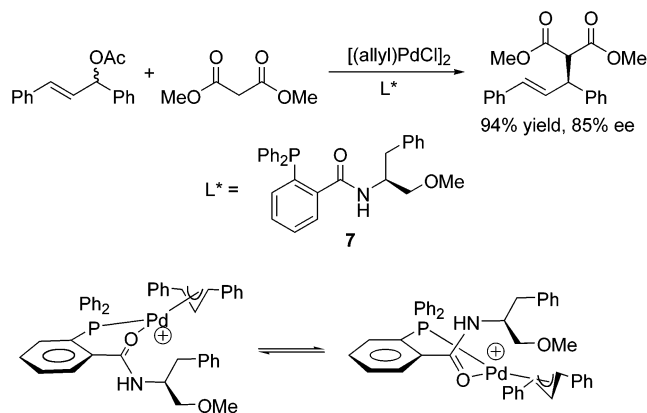


**Figure 17.** Asymmetric allylic alkylation using atropisomeric amides as chiral ligands (top) and possible diastereomeric allyl intermediates.

not reported the structure of the ( $\pi$ -allyl)Pd complex involved in the reaction, their NMR data suggest that a P–O chelate is formed.

The central chirality of this ligand is distant from the metal center and is unlikely to be responsible for the high enantioselectivity in the allylation reaction. It is more probable that the central chirality biases the conformation of the amide and that the asymmetry of the ligand is relayed through the axial conformation of the amide and the positioning of the diastereotopic *P*-phenyl groups.

**Ligand–Substrate Chiral Amplification.** A complementary approach to transmission of stereochemical information within a ligand has been recently reported by Sibi and co-workers.<sup>112</sup> In this clever approach, a rapidly racemizing amino group is incorporated into the substrate. Rather than directly controlling the enantioselectivity of the reaction, the role of the asymmetric catalyst is to bias the configuration of the chiral relay group in the substrate, which in turn determines the stereochemical outcome of the reaction. In this approach, the interaction of the chiral ligand with the substrate temporarily transforms a stereochemically labile nitrogen into a chiral auxiliary (Figure 18).

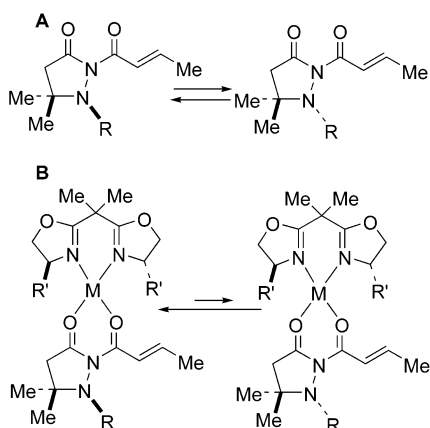


**Figure 18.** (A) Enantiomeric substrates interconvert through nitrogen inversion. (B) Diastereomeric substrate-catalyst adducts may have very different energies.

Sibi and co-workers have examined the asymmetric Diels–Alder reaction catalyzed by bis(oxazoline)copper(II) complexes. The substrates for this reaction are butenoyl-pyrazolidinones **8** (Figure 19), having different *N*-alkyl relay groups (R). In one scenario, the

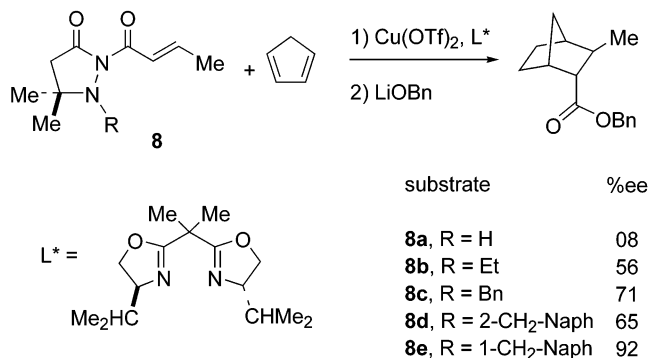


**Figure 19.** Asymmetric Diels–Alder reactions with chiral relay groups.

bound substrate can undergo inversion and preferentially equilibrate to the lower energy configuration, thus minimizing steric interactions with the chiral catalyst. It is also conceivable that one enantiomer of an equilibrating pair selectively binds to the chiral catalyst and is activated to react (Figure 18).

The authors compared different relay groups **8a–e** and showed that enantioselectivities gradually increased when bulkier relay groups were used (Figure 19). With the best relay group, the enantioselectivities were independent of the substituents on the C<sub>2</sub>-symmetric bis(oxazoline) ligands, again indicating that the chiral relay controlled the facial attack of the diene.

**Use of Achiral Additives without Chiral Conformations.** The use of additives to enhance catalyst performance is well documented. Additives can have a beneficial effect on catalytic activity and even the catalyst enantioselectivity. Although our understanding of the interactions of additives with catalysts is often rudimentary, it is logical that additives can often behave as ligands, coordinating to catalysts and changing the aggregation state of the catalyst and/or the metal geometry. The present review focuses on a subclass of additives, namely achiral and meso ligands that have chiral conformations. The use of achiral additives that do not extend the chiral environment of the catalyst has recently been reviewed by Vogl, Groger, and Shibasaki.<sup>113</sup> We will discuss here two examples that emphasize the potential utility of this method. A comparison will be made later of addition of achiral ligands without chiral conformation, ligands that become asymmetric in certain metal geometries, and ligands with chiral conformations.

One of the first and most striking examples of the impact of achiral ligands on an enantioselective process was reported by Kobayashi and co-workers.<sup>114,115</sup> They prepared a Lewis acid catalyst by reacting Yb(OTf)<sub>3</sub> with BINOL, followed by addition of 2 equiv of *meso*-(1,2,6)-trimethylpiperidine, to give a complex with the proposed structure **9** (Figure 20). The

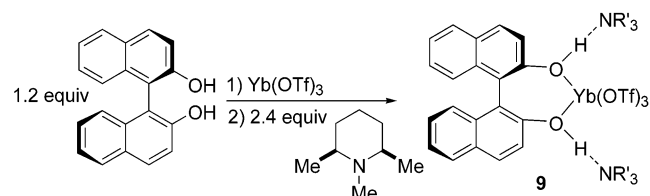


**Figure 20.** Preparation and proposed structure of chiral Yb(III) triflate Lewis acid.

resulting complexes were excellent catalysts for the asymmetric Diels–Alder reaction of 3-acyl-1,3-oxazolidin-2-ones with cyclopentadiene (Figure 21).

Careful investigation of the system revealed that aging the catalyst for different amounts of time resulted in a decay in the enantioselectivity of the catalyst. When aging took place in the presence of the substrate, however, the highest enantioselectivities were achieved.

Screening of achiral 1,3-dicarbonyl compounds that resembled the substrate revealed that not only were these achiral additives effective at stabilizing the catalyst, but they also impacted the enantiofacial selec-



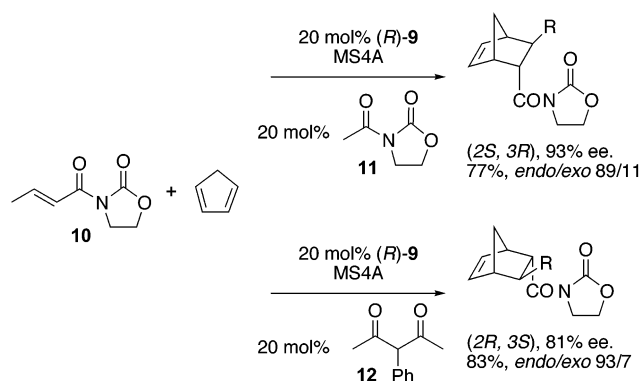


**Figure 21.** Asymmetric Diels–Alder reaction catalyzed by a Yb(III) BINOL-based catalyst.

tivity of the reaction. When catalyst **9** was treated with 3-acetyl-1,3-oxazolidin-2-one (**11**, Figure 21), the endo Diels–Alder adduct of **10** was obtained in 93% ee. Remarkably, using 3-phenylacetone (**12**) as an additive gave the endo adduct with the opposite absolute configuration in 81% ee. In both cases, the source of chirality was the same: (*R*)-BINOL.

An important attribute of achiral additives is that they enable the generation of new chiral catalysts without the need to modify the chiral ligand. This is particularly important when modification of the chiral ligand is not possible or practical. An illustration of this point is seen in the optimization of a palladium oxidation catalyst by Sigman and co-workers.

Palladium catalysts for the oxidative kinetic resolution of racemic alcohols were independently developed by the groups of Stoltz<sup>116</sup> and Sigman.<sup>117</sup> These catalysts employ sparteine as the chiral ligand, which is available from natural sources in only one enantiomeric form, although a recent paper containing a useful surrogate has appeared.<sup>118</sup> Sigman and co-workers have shown that the role of the sparteine is two-fold: to bind to the palladium center and to act as an exogenous base.<sup>119</sup> Sigman and co-workers have recently reported the oxidative kinetic resolution of 1-phenylethanol catalyzed by achiral palladium–carbene complexes using sparteine as the base (Figure 22).<sup>120</sup> They demonstrated that modification of

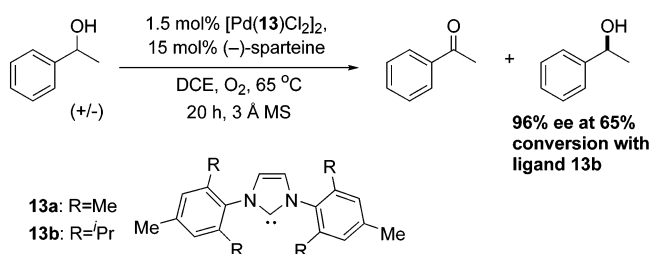


**Figure 22.** Oxidative kinetic resolution of 1-phenylethanol.

the achiral carbene ligand can have a profound effect on the relative rate of oxidation of the two enantiomeric alcohols, leading to an efficient kinetic resolution. Substitution of the achiral carbene **13b** for **13a** resulted in an increase in the relative rates of oxidation of the two enantiomers<sup>121</sup> from 6.1 to 11.6, allowing isolation of the alcohol starting material of 96% ee after 65% conversion.

These systems clearly indicate the potential of the use of achiral ligands in asymmetric catalysis. When the ultimate chiral promoter is not easily accessible, not susceptible to structural modifications through synthesis, or not available in both enantiomeric forms, the use of achiral additives allows the generation of new catalysts from the same chiral ligands.

## 2. The Use of Achiral Salen Ligands in Asymmetric Catalysis

As the results in the previous sections illustrate, the addition of achiral additives can have a beneficial impact on the enantioselectivity and activity of an asymmetric catalyst. It is unlikely that these achiral ligands, however, can greatly extend or amplify the chiral environment created by the enantiopure ligand or ligands. In contrast, Katsuki and co-workers<sup>39,122,123</sup> demonstrated, in groundbreaking investigations into the (salen)Mn-catalyzed asymmetric epoxidation reaction, that large, flexible achiral ligands with chiral conformations could efficiently convey asymmetry to a substrate in an asymmetric reaction. Jacobsen's<sup>124</sup> and Katsuki's<sup>125</sup> groups introduced the catalytic asymmetric epoxidation of unfunctionalized olefins in 1990 using chiral (salen\*)Mn complexes, and the reaction has since been studied in detail by these researchers, as well as others.<sup>126–128</sup>

At the time of Katsuki's initial results with achiral (salen)Mn complexes, investigations into the nature of the active species in the asymmetric epoxidation were being pursued experimentally and through calculations. Although the mechanism of transfer of asymmetry from the catalyst to the olefin remained unresolved at the time of this review, experimental evidence supports the intermediacy of a highly reactive Mn(V)–oxo complex.<sup>129,130</sup> It had been proposed that the salen ligands of such Mn(V)–oxo complexes existed in nonplanar, or stepped, conformations and that this nonplanar characteristic was an important element in the chiral environment of the catalyst (Figure 23).<sup>131,132</sup> Such a conformation had previously

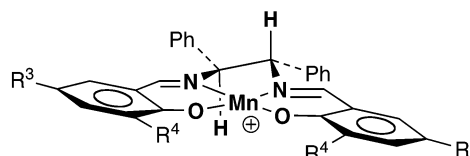


**Figure 23.** Stepped conformation of a chiral (salen)Mn complex proposed to be important in the transfer of asymmetry in the asymmetric epoxidation reaction.

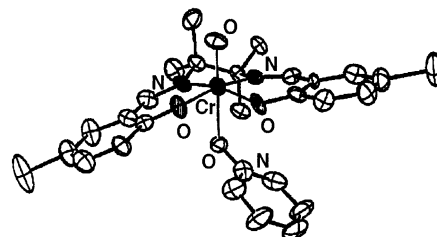


**Figure 24.** X-ray structure of [(salen)Cr(=O)L]<sup>+</sup> (L = pyridine *N*-oxide), showing the stepped conformation in the salen ring system.

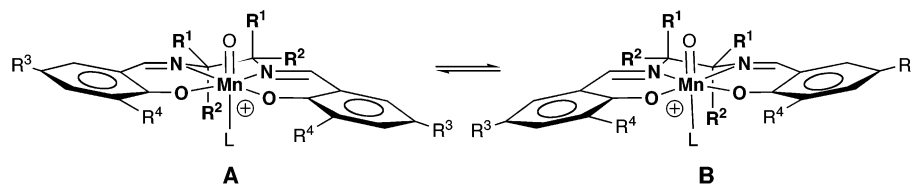


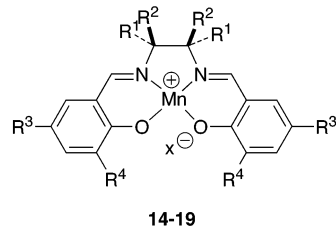
**Figure 25.** Chiral conformations of the (salen)Mn complexes.

been observed in the X-ray structure of the octahedral (L)(salen)Cr=O complex characterized by Kochi and co-workers (L = pyridine *N*-oxide, Figure 24).<sup>133</sup> In the (salen)Mn epoxidation system, the stepped conformation has been used in modeling the reaction of a (salen)Mn=O with olefins,<sup>131,132</sup> and it has been observed in some solid-state structures of (salen)-Mn(III) complexes, but not others.<sup>134</sup> The hypothesis of a stepped conformation in the active catalyst species led Katsuki's group to the idea that a (salen)-Mn complex with an *achiral* salen ligand could have chiral conformations and was crucial to the development of the concept that large, flexible achiral ligands could be used in asymmetric catalysis.

Also important to Katsuki's work was the realization that Lewis basic donor ligands, such as pyridine *N*-oxide, could increase the enantioselectivity of the (salen)Mn catalyst and extend the catalyst lifetimes in the asymmetric epoxidation reaction.<sup>135–137</sup> It is believed that the pyridine *N*-oxide ligand coordinates to the manganese, stabilizing the highly reactive Mn(V)-oxo intermediate, and that it remains bound during epoxide formation. This discovery, and the idea that (salen)Mn complexes with achiral ligands were chiral by virtue of a stepped conformation, set the stage for the use of achiral salen ligands in the asymmetric epoxidation.<sup>122,123</sup>

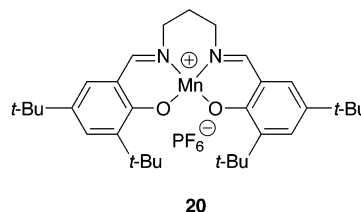
Katsuki envisioned that, in the case of an achiral (salen)Mn complex, the [(L)(salen)Mn=O]<sup>+</sup> intermediate, where L is a Lewis basic donor ligand, would exist as an equilibrium mixture of enantiomeric conformations under the conditions employed in the asymmetric epoxidation reaction (Figure 25). When L is an achiral ligand, the mixture of enantiomers formed is, of course, racemic. If, however, L is a chiral ligand, the manganese complexes **A** and **B** in Figure 25 are diastereomers. If the two diastereomeric forms of the [(L)(salen)Mn=O]<sup>+</sup> intermediate have significantly different energies, as a result of interactions between the achiral salen ligand and the chiral donor ligand L, the equilibrium is shifted to one side, and the (salen)Mn complex will exist predominantly in one of the chiral stepped conformations. As such, the salen ligand serves to amplify the chiral environment of the chiral ligand L and, in principle, can be used to transmit asymmetry in the epoxidation reaction. Of course, any detailed mechanistic study on such a system must also take into consideration that the rapidly interconverting diastereomeric catalysts will likely exhibit different reactivities (Curtin–Hammett principle<sup>138</sup>). Because such studies are rare, the reactivity of the diastereomeric catalysts will not be discussed, unless relevant data exist.

In his initial studies, Katsuki examined a series of achiral (salen)Mn complexes, **14–19**, and the



**14–19**

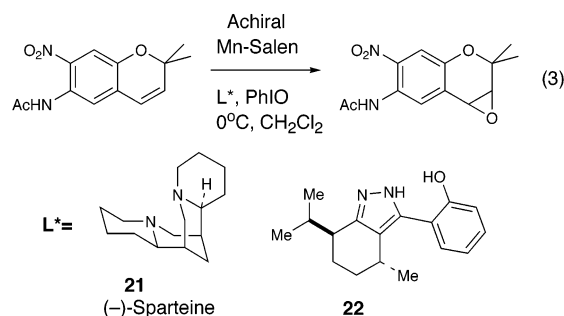
- 14:** R<sup>1</sup>=R<sup>2</sup>=R<sup>3</sup>=R<sup>4</sup>=H, X=PF<sub>6</sub>  
**15:** R<sup>1</sup>=R<sup>2</sup>=H, R<sup>3</sup>=R<sup>4</sup>=*t*-Bu, X=OAc  
**16:** R<sup>1</sup>=H, R<sup>2</sup>=(CH<sub>2</sub>)<sub>4</sub>, R<sup>3</sup>=R<sup>4</sup>=*t*-Bu, X=OAc  
**17:** R<sup>1</sup>=R<sup>2</sup>=Me, R<sup>3</sup>=R<sup>4</sup>=*t*-Bu, X=PF<sub>6</sub>  
**18:** R<sup>1</sup>=R<sup>2</sup>=Me, R<sup>3</sup>=R<sup>4</sup>=*t*-Bu, X=OAc  
**19:** R<sup>1</sup>=R<sup>2</sup>=Me, R<sup>3</sup>=OSi(*i*-Pr)<sub>3</sub>, R<sup>4</sup>=*t*-Bu, X=PF<sub>6</sub>



**20**

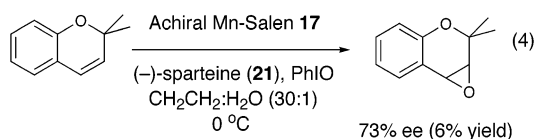
**Figure 26.** Achiral salen and salpene catalysts.

(salpene)Mn complex **20** (Figure 26) with a variety of enantiopure ligands (L = amines, alcohols, amino alcohols, diamines, or BINOL) for enantioselectivity in the asymmetric epoxidation reaction (eq 3). The

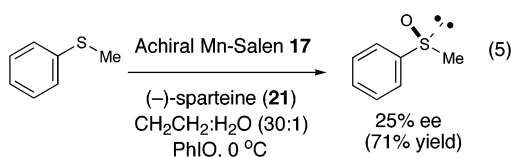


chromene derivative, 6-acetamido-7-nitro-2,2-dimethylchromene (eq 3), was employed as a test substrate, because it had been shown to give high ee's in the chiral (salen\*)Mn-catalyzed epoxidation reaction. Use of 2 mol % of the achiral manganese complex and 40 mol % of an optically active pyrazole donor ligand resulted in very low enantioselectivities, between 2 and 7%.<sup>123</sup> Testing of other donor ligands, however, led to increased enantioselectivities with 40 mol % of (–)-sparteine (**21**) or hydroxy pyrazole (**22**). Ee's as high as 60 and 52% were obtained using (–)-sparteine with complexes **17** and **19**, but the epoxide yields were a disappointing 11 and 28%, respectively. Attempts to optimize the reaction by adjusting the temperature or changing

solvents were unsuccessful. It was found, however, that adding water to the reaction improved enantioselectivity. In the search for a more suitable substrate, different 2,2-dimethylchromene derivatives and a variety of other olefins<sup>122</sup> were examined. Although enantioselectivities with chromene derivatives reached as high as 73% (eq 4), the epoxide yields remained below 20%. In contrast, the asymmetric epoxidation of 2,2-dimethylchromene derivatives with enantiopure (salen\*)Mn catalysts gave excellent enantioselectivities (>95%) and good yields (60–80%).<sup>139</sup> Thus, in comparison to the use of chiral (salen\*)Mn complexes, early systems exploring the use of achiral ligands did not illustrate the potential of these methods.



**Sulfide Oxidation Reactions.** The same catalyst system that was employed in the epoxidation reaction was also examined in the asymmetric sulfide oxidation reaction (eq 5).<sup>140</sup> Chiral (salen\*)Mn complexes are known to catalyze the oxidation of phenyl methyl sulfide with ee's up to 81% and yields over 90%.<sup>141</sup> Complex **17** (Figure 26) with (-)-sparteine and PhIO provided the sulfoxide with 25% ee and in 71% yield.<sup>122</sup> The sense of asymmetric induction in the sulfide oxidation reaction with **17** and (-)-sparteine, and the enantiofacial selectivity of the epoxidation reaction with the same catalyst, are consistent with the same stepped conformation of the reactive (salen)Mn-oxo catalyst.



**The Nature of the Active Species.** Investigations into the nature of the interaction between the sparteine and the achiral (salen)Mn complex have not been reported. Although experimental evidence indicates that dative ligands such as pyridine *N*-oxide coordinate to manganese in the epoxidation reaction, direct coordination of a tertiary nitrogen of sparteine was thought to be unlikely, due to the severe steric interactions between the sparteine and the (salen)Mn complex. To explain the asymmetric induction in the epoxidation and sulfide oxidation using achiral (salen)Mn complexes and the beneficial effect of water on the enantioselectivity in these reactions, Katsuki proposed that a water molecule, hydrogen bonded to the sparteine nitrogens, binds to the (salen)Mn complex as shown in Figure 27.<sup>122</sup>

**Use of Chiral *N*-Oxide Donor Ligands.** While the initial results from the Katsuki group discussed above were quite intriguing, a compelling argument for the potential uses of large, flexible achiral ligands in asymmetric catalysis was not made until 1999. In

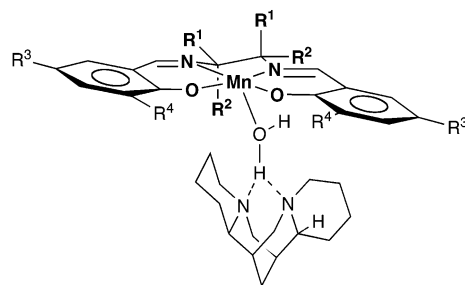
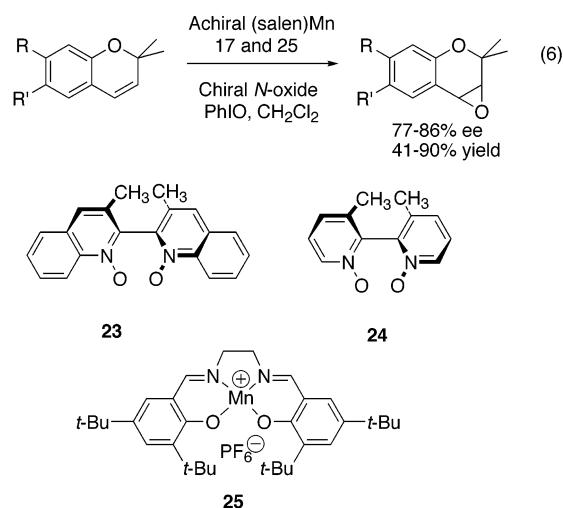


**Figure 27.** Proposed interaction between (-)-sparteine and the (salen)Mn complex via hydrogen bonding with a water molecule.

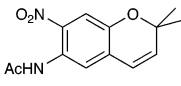
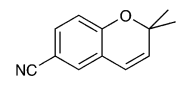
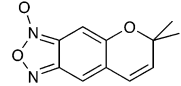
that year, Katsuki and co-workers reported the use of chiral *N*-oxide ligands in combination with achiral (salen)Mn complexes for asymmetric epoxidation.<sup>39</sup> This move was based on the fact that achiral *N*-oxide ligands had already been shown to improve the yield in asymmetric epoxidation reactions with chiral (salen\*)Mn complexes.<sup>135</sup> Atropisomeric *N,N*-dioxide ligands **23** and **24** were used with (salen)Mn complexes **17** (Figure 26) and **25** in eq 6. Employing



donor ligand **23** resulted in poor enantioselectivities, possibly due to low binding affinities between the bulky *N,N*-dioxide ligand and the (salen)Mn center. In sharp contrast, combination of **25** and *N,N*-dioxide ligand **24** resulted in formation of a very enantioselective catalyst, giving ee's between 77 and 83% and good yields (59–90%) with a series of 2,2-dimethylchromene derivatives, as illustrated in Table 1. The stronger binding of the smaller *N*-oxide-based ligand **24** allowed reduction of the mol % of the chiral donor ligand from 40 mol % required with sparteine to 5 mol % with **24** in the presence of 4 mol % (salen)Mn complex **25**, without substantial loss of enantioselectivity.

The results listed in Table 1 definitively showed, for the first time, that catalysts bearing large, flexible achiral ligands with chiral conformations could be used to efficiently transfer asymmetry to the substrate. An important aspect of the use of such achiral ligands in asymmetric catalysis that was not clearly demonstrated by the Katsuki study was that asym-

**Table 1. Asymmetric Epoxidation with (Salen)Mn 25 (4 mol %) and 24 (5 mol %)**

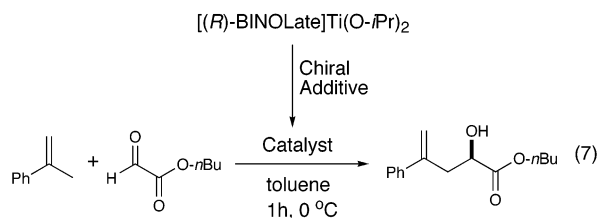
entry	substrate	yield (%)	% ee	config
1		90	83	3 <i>S</i> ,4 <i>S</i>
2		59	77	3 <i>S</i> ,4 <i>S</i>
3		60	78	3 <i>S</i> ,4 <i>S</i>

metric catalysts could be optimized by screening a series of achiral ligands.

### 3. Use of Achiral Biphenol-Based Ligands in Asymmetric Catalysis

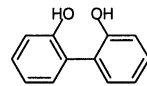
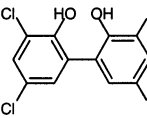
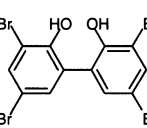
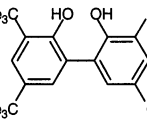
#### 3.1. Asymmetric Carbonyl–Ene Reaction

Initial results by Vallée and co-workers<sup>142</sup> provide a thought-provoking entry into the use of achiral biphenol ligands with chiral conformations. The reaction examined by these authors was the asymmetric carbonyl–ene reaction developed by Mikami and co-workers.<sup>143–145</sup> Mikami had shown that the reaction of a 1:1 mixture of (*R*)-BINOL and Ti(O-*i*-Pr)<sub>4</sub> in the presence of 4-Å molecular sieves generated a catalyst that promoted the asymmetric carbonyl–ene reaction illustrated in eq 7 with an enantioselectivity of 94.5% (Table 2, entry 1). Addition of a chiral activator, such as (*R*)-BINOL, resulted in an increase in the activity of the resultant catalyst by a factor of 26 and an increase in the enantioselectivity to 96.8% (Table 2, entry 2). A similar result was obtained on addition of chiral, configurationally stable biphenols. Interestingly, Mikami found that addition of (*S*)-BINOL to the catalyst formed from (*R*)-BINOL and Ti(O-*i*-Pr)<sub>4</sub> generated a new catalyst that promoted the asymmetric reaction with only slightly diminished enantioselectivity (86%, Table 2, entry 3). This result indicates that the *meso*-(BINOLate)<sub>2</sub>Ti is not the predominant species formed when the (*S*)-BINOL is added, because this complex would give racemic product. It also suggests that, on the time scale of the reaction, the (*R*)-BINOLate ligand bound to titanium does not exchange with free (*S*)-BINOL to an appreciable extent. Nonetheless, Mikami's observations clearly indicate that the initial [(*R*)-BINOLate]Ti species becomes a more active and enantioselective catalyst on addition of the second equivalent of (*R*)-BINOL. The nature of the interac-



tion of the [(*R*)-BINOLate]Ti complex with the added (*R*)-BINOL or the chiral biphenol remains to be identified. Vallée and co-workers reported that the catalyst derived from a 1:1 ratio of (*R*)-BINOL:Ti(O-*i*-Pr)<sub>4</sub> catalyzed the carbonyl–ene reaction of  $\alpha$ -methylstyrene with *n*-butyl glyoxylate with an enantioselectivity of 93.2% (Table 2, entry 4). In their hands, addition of 1 equiv of (*R*)-BINOL to the catalyst formed from (*R*)-BINOL and Ti(O-*i*-Pr)<sub>4</sub> also led to a more active catalyst, but a slight decrease in the enantioselectivity to 91.6% was reported (Table 2, entry 5). Vallée and co-workers then examined the effect of substituting an *achiral* biphenol for the second equivalent of (*R*)-BINOL in eq 8). Their

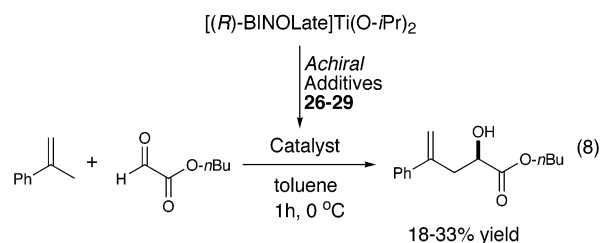
**Table 2. Carbonyl–Ene Reaction with [(*R*)-BINOLate]Ti Complex<sup>a</sup>**

entry	additive	ee
1	none	94.5
2	( <i>R</i> )-BINOL	96.8
3	( <i>S</i> )-BINOL	86.0
-----		
4	none	93.2
5	( <i>R</i> )-BINOL	91.6
6		95.4
7		96.7
8		96.3
9		97.3

<sup>a</sup> Entries 1–3 represent Mikami's results.<sup>143</sup> Entries 4–9 represent Vallée's results.<sup>142</sup>

tion of the [(*R*)-BINOLate]Ti complex with the added (*R*)-BINOL or the chiral biphenol remains to be identified.

Vallée and co-workers reported that the catalyst derived from a 1:1 ratio of (*R*)-BINOL:Ti(O-*i*-Pr)<sub>4</sub> catalyzed the carbonyl–ene reaction of  $\alpha$ -methylstyrene with *n*-butyl glyoxylate with an enantioselectivity of 93.2% (Table 2, entry 4). In their hands, addition of 1 equiv of (*R*)-BINOL to the catalyst formed from (*R*)-BINOL and Ti(O-*i*-Pr)<sub>4</sub> also led to a more active catalyst, but a slight decrease in the enantioselectivity to 91.6% was reported (Table 2, entry 5). Vallée and co-workers then examined the effect of substituting an *achiral* biphenol for the second equivalent of (*R*)-BINOL in eq 8). Their



hypothesis was that the interaction of the biphenol with the catalyst derived from (*R*)-BINOL would cause the achiral biphenol to preferentially adopt a chiral conformation. The chiral conformation could

then be used in the asymmetric carbonyl–ene reaction to increase the enantioselectivity of the catalyst.

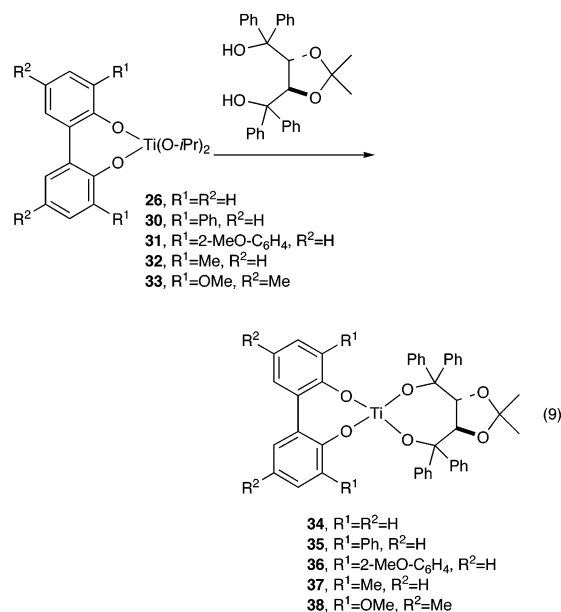
The results of their study of achiral biphenol ligands are illustrated in Table 2 (entries 4–9). Initially, the unsubstituted biphenol **26** was employed in the carbonyl–ene reaction as the achiral ligand in eq 8. The resulting catalyst provided product with greater enantioselectivity than when no activator was added, giving 95.4% ee, an increase of 2%, on addition of the biphenol (Table 2, entry 6). In the same fashion, tetrasubstituted biphenols **27**, **28**, and **29** also generated the product with enantioselectivities of 96.7, 96.3, and 97.3% respectively, which represented an increase in the product ee's of about 4% over the reaction without activator. The authors also reported that addition of achiral biphenols created catalysts that were more active than the [(*R*)-BINOLate]Ti catalyst in the absence of activator; however, the increased activity was not quantified. A complicating factor in interpreting these results is that Vallée reported low yields (18–33%) due to polymerization of the glyoxylate during the course of the reaction. When the reactions were run with ethyl glyoxylate, similar results were observed.

The origin of the increases in enantioselectivity on addition of the achiral biphenol ligands is not clear, nor is the manner in which the achiral ligands interact with the titanium center. On the basis of Mikami's results, it is unlikely that the catalyst has a structure of the type (BINOLate)(biphenolate)Ti. It is also surprising that achiral ligands such as **27** and **29**, which have ortho substituents that are very different in size, exhibit enantioselectivities within 2%. Although these results are quite interesting, more experiments will be necessary before concrete conclusions concerning the role of the achiral biphenol ligand can be drawn.

### 3.2. Asymmetric Addition of Methyl Groups to Aldehydes

In a related titanium system, Mikami and co-workers<sup>41</sup> prepared a series of complexes by reaction of (biphenoxide)Ti(O-*i*-Pr)<sub>2</sub> complexes (**26**, **30**–**33**) with (*R,R*)-TADDOL to provide new species with the proposed composition (biphenoxide)Ti(TADDOLate), as shown in eq 9.

These compounds were then used as catalysts (10 mol %) for the asymmetric transfer of methyl groups from MeTi(O-*i*-Pr)<sub>3</sub> to 3,5-bis(trifluoromethyl)benzaldehyde (**39**, eq 10). The authors found that the ee of the product alcohol (**40**) depended on the size of the 3,3' substituents (R<sup>1</sup>) on the biphenol ligand (Table 3). When R<sup>1</sup> = H, moderate enantioselectivity was observed (entry 1). Substitution of aryl groups at the R<sup>1</sup> position led to similar levels of enantioselectivity (entries 2 and 3). Use of the biphenol ligand **32** (R<sup>1</sup> = Me) resulted in an increase in the enantioselectivity to 88%. The most enantioselective catalyst, derived from biphenol **33** (R<sup>1</sup> = OMe and R<sup>2</sup> = Me), generated the product alcohol with enantioselectivity approaching 100% (entry 5). As emphasized by Mikami, these results could arise by formation of a single, highly enantioselective catalyst or by forma-



tion of two diastereomeric catalysts with very large differences in activity.<sup>146</sup> This study, which showed that variation of the achiral biphenol ligands resulted in a change in product ee of 35%, was one of the first examples demonstrating that the enantioselectivity of a catalyst could be optimized by screening achiral ligands with chiral binding modes.

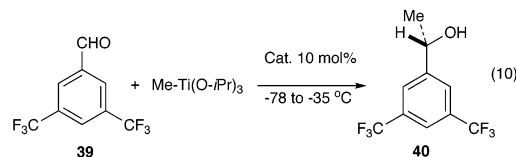


**Table 3. Enantioselectivities in Addition of Methyl Groups to Aldehyde **39** Catalyzed by (BINOLate)Ti(TADDOLate) Species (Eq 10)**

entry	achiral ligand	ee (%)
1		70
2		69
3		65
4		88
5		100

### 3.3. Asymmetric Baeyer–Villiger Oxidation

Bolm and Beckmann<sup>147</sup> demonstrated the use of achiral biphenol ligands in combination with enantiopure BINOL ligands in the asymmetric zirconium-mediated Baeyer–Villiger reaction. Initially, these researchers found that, by forming a chiral zirconium species in situ from Zr(O-*t*-Bu)<sub>4</sub> and 2 equiv of (*S*)-BINOL and using 1.5 equiv of *tert*-butyl hydroper-

oxide (TBHP) as an oxidant, they could effect the oxidation of bicyclooctanone *rac*-**41** to the corresponding lactones in 16% ee for regioisomer **42a** and 75% ee for regioisomer **42b** (Figure 28). Interestingly, they

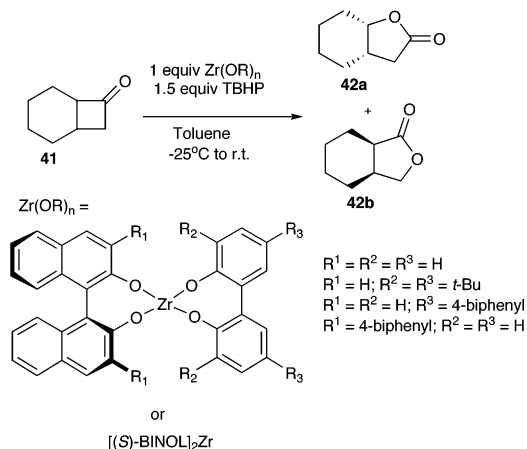


**Figure 28.** Asymmetric Baeyer–Villiger oxidation with chiral zirconium alkoxide complex.

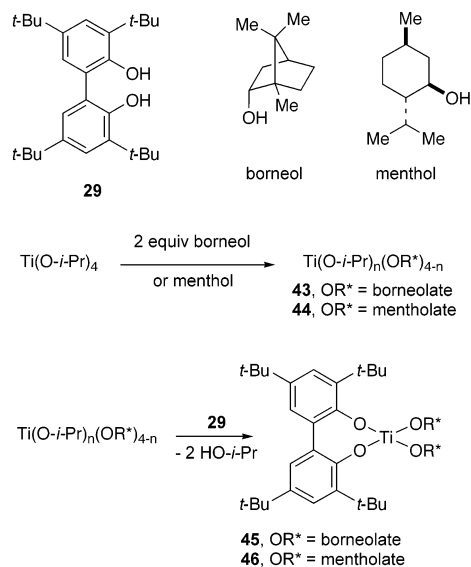
found that 1 equiv of BINOL could be replaced by the achiral 2,2'-biphenol ligand without a significant loss of enantioselectivity (12% ee for **42a** and 75% ee for **42b** in dichloromethane). The ratios of the regioisomers were similar in both cases (7.2:1 vs 5.8:1). Running the oxidation reaction in toluene improved the ee of the lactone products **42a** and **42b** to 16 and 84%, respectively, but further attempts to increase the enantioselectivity of the reaction and to make it catalytic were not successful.

Introduction of bulky *tert*-butyl groups at the 3, 3', 5, and 5' positions of the biphenol ligand led to a decrease in ee. The authors postulated that the decrease in enantioselectivity could be due to one of two factors: the unsubstituted biphenol might lead to a more favorable asymmetric cavity around the metal center, or a lower barrier to inversion in the unsubstituted biphenol might lead to faster selection between the diastereomeric complexes. The latter explanation was supported by the fact that changes in the length of time allowed for forming the [(*S*)-BINOL]Zr(biphenol) species before addition of the substrate led to changes in enantioselectivity, indicating that a time dependence for the concentrations of the active diastereomeric complexes exists. In addition, it was found that placing large biphenyl substituents on the 3 and 3' positions of the biphenol ligand decreased the enantioselectivity to 7% with the substrate 3-phenylcyclobutanone. Placing the same biphenyl groups on the 1 and 1' positions of the (*S*)-BINOL ligand, however, led to an increase in enantioselectivity relative to the unsubstituted [(*S*)-BINOL]Zr(biphenol) species (44% vs 31%). Bolm and Beckmann suggested that placing the extra steric bulk on BINOL, instead of the biphenol, allowed the achiral ligand to easily undergo inversion, such that the concentration of the more enantioselective zirconium species was higher, and the ee of the reaction increased.

The systems of Vallée,<sup>142</sup> Mikami,<sup>41</sup> and Bolm,<sup>147</sup> using achiral biphenol ligands and chiral bidentate

BINOL or TADDOL ligands, can be compared with recent solution and solid-state structural studies using biphenol ligand **29** (Scheme 1) and chiral

### Scheme 1. Synthesis of Diastereomeric 2,2'-biphenolate–Titanium Complexes



monodentate alkoxides.<sup>148</sup> Reaction of either borneol or menthol with titanium tetraisopropoxide gave a mixed alkoxide complex in each case (Scheme 1). Reaction of these intermediates with the biphenol **29** gave mixtures of diastereomers for the borneolate derivative **45** and the mentholate adduct **46**, after removal of the liberated 2-propanol. Analysis of the crude reaction mixtures by 500-MHz <sup>1</sup>H NMR spectroscopy indicated that both **45** and **46** were 1:1 mixtures of diastereomers, in which the bis(phenoxide) ligand had the *R* and *S* configuration. The four-coordinate diastereomers of **45** crystallized as a 1:1 mixture of diastereomers. Similarly, the five-coordinate acetonitrile adducts (biphenoxide)Ti(OR\*)<sub>2</sub>(NCMe), formed on crystallization of the borneolate and mentholate compounds **45** and **46** from acetonitrile, also resulted in 1:1 mixtures of diastereomers. In each of these three structures, both diastereomers were observed to cocrystallize and reside together in the same unit cell. From this study, it is not clear if the two pairs of diastereomers, **45** and **46**, are the thermodynamic products, which would indicate that the diastereomers have similar energies, or if they are the kinetic products, indicating, perhaps, that inversion of the biphenoxide stereochemistry does not occur under the reactions conditions in Scheme 1.<sup>148</sup>

### 4. Atropisomeric Biphenyl-Based Phosphines and Related Ligands in Asymmetric Catalysis

Several other important contributions highlighting the usefulness of ligands that have chiral conformations, yet are not configurationally stable at room temperature, have been based on the biphenyl and related backbones. Enantioselective reactions with 2,2'-bis(diarylphosphino)biphenyl derivatives (Figure 29) bound to late transition metals have attracted the most attention. Although the individual skew conformations of these BIPHEP (**47**, Ar = Ph)-derived

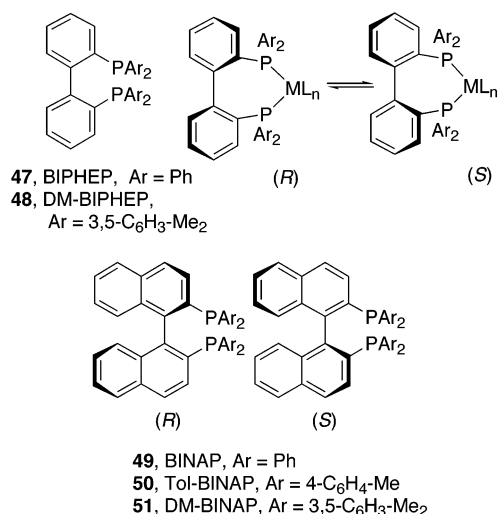


**Figure 29.** Configurationally dynamic 2,2'-bis(diarylphosphino)biphenyl derivatives and their enantiomeric complexes (above). Configurationally stable BINAP derivatives (below).

compounds are chiral, the barrier to racemization of the unbound parent ligand is 22 kcal/mol at 125 °C.<sup>149</sup> Such a barrier is not sufficiently high to allow resolution of the enantiomeric conformations at room temperature, and these ligands are considered to be configurationally dynamic. In general, disubstituted biphenyls are resolvable only if two large ortho substituents are present or with certain bridges between the 2 and 2' positions.<sup>150</sup> As illustrated by the constrained biphenyl derivatives in Figure 30, the

Z	$\Delta G^\ddagger$ (kcal/mol)
O	9
S	17
CH <sub>2</sub>	12
CH <sub>2</sub> CH <sub>2</sub>	24
C(CO <sub>2</sub> H) <sub>2</sub>	23

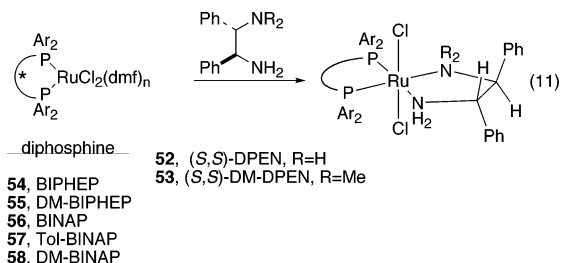
**Figure 30.** Barriers to racemization of various constrained biphenyl derivatives.

barrier to racemization of these compounds is strongly dependent on the nature of the tether.<sup>151–154</sup> Coordination of BIPHEP to a metal center forms a metalocycle, which, like the constrained biphenyl derivatives, will have a higher barrier to interconversion of the enantiomeric conformations, relative to the free ligand.

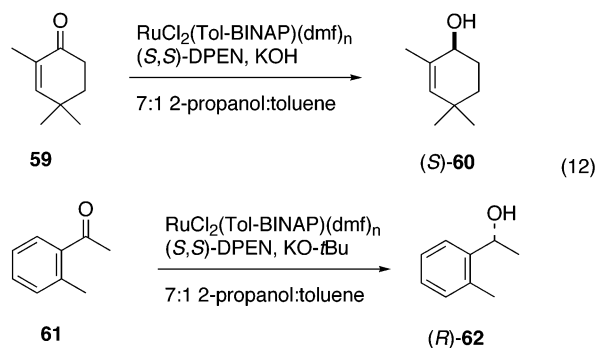
#### 4.1. Asymmetric Hydrogenation Reactions Using BIPHEP-Derived Ligands

The first report involving the use of BIPHEP derivatives in asymmetric catalysis was published by Noyori, Mikami, and co-workers.<sup>40</sup> The Noyori group has been a leader in development of new chiral hydrogenation catalysts, most of which have been based on the chelating diphosphine BINAP or its derivatives,<sup>1</sup> and in delineation of their reaction mechanisms.<sup>67,155</sup> Noyori, Mikami, and co-workers based their applications of BIPHEP derivatives in the asymmetric reduction of ketones<sup>40</sup> on their previous investigations into enantioselectivities and relative rates of diastereomeric catalysts.<sup>156</sup>

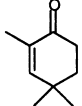
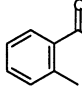
Catalyst precursors of the type RuCl<sub>2</sub>[(*S,S*)-BINAP] [(*S,S*)-DPEN] [(*S,S*)-1,2-diphenylethylenediamine, **52**], prepared as shown in eq 11, are activated with base and hydrogen to form highly enantioselective catalysts for the reduction of unfunctionalized ketones to alcohols.<sup>68,157–159</sup> In their studies with this catalyst system, Noyori and co-workers demonstrated that, when the configurations of the chiral diphosphine and chiral diamine were matched, a catalyst of remarkable efficiency was obtained.<sup>156</sup> Reaction of RuCl<sub>2</sub>[(*R*)-Tol-BINAP](dmf)<sub>n</sub>



(**57**) and (*S,S*)-DPEN (**52**) formed a precatalyst, RuCl<sub>2</sub>[(*R*)-Tol-BINAP][(*S,S*)-DPEN] (eq 11), that exhibited 96% enantioselectivity in the reduction of 2,4,4-trimethyl-2-cyclohexenone (**59**) to allylic alcohol (*S*)-**60** (eq 12, Table 4). The catalyst bearing the



**Table 4.** Enantioselective Reduction of Ketones with Diastereomeric (Tol-BINAP)RuCl<sub>2</sub>(DPEN) Catalysts (Eq 12)

substrate	Tol-BINAP config.	DPEN config.	product ee (config.)	relative rate
 59	<i>R</i>	<i>S,S</i>	96 ( <i>S</i> )	} 121 1
	<i>R</i>	<i>R,R</i>	26 ( <i>S</i> )	
	racemic	<i>S,S</i>	95 ( <i>S</i> )	
 61	<i>S</i>	<i>S,S</i>	97.5 ( <i>R</i> )	} 13 1
	<i>S</i>	<i>R,R</i>	8 ( <i>R</i> )	
	racemic	<i>S,S</i>	90( <i>R</i> )	

mismatched ligand set, (*R*)-Tol-BINAP (**50**) and (*R,R*)-DPEN (**52**), exhibited low efficiency and produced (*S*)-**60** in 26% ee (Table 4). The researchers then employed *rac*-Tol-BINAP and (*S,S*)-DPEN, which afforded a 1:1 mixture of diastereomeric precatalysts that promoted reduction of **59** to (*S*)-**60** (eq 12) with

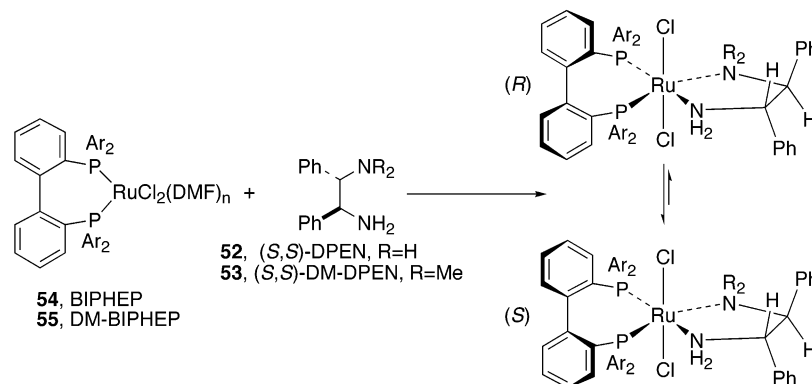


**Figure 31.** Reaction of  $(\text{BIPHEP})\text{RuCl}_2(\text{dmf})_n$  derivatives with  $(S,S)\text{-DPEN}$  to give mixtures of diastereomers.

**Table 5. Kinetic and Thermodynamic Diastereomeric Ratios from Reaction of  $(\text{BIPHEP})\text{RuCl}_2(\text{dmf})_n$  Derivatives with  $(S,S)\text{-DPEN}$  and  $(S,S)\text{-DM-DPEN}$**

	$\text{RuCl}_2(\text{diphosphine})(\text{dmf})_n$	diamine	$S/S,S:R/S,S$
kinetic	<b>55</b> , DM-BIPHEP	<b>52</b> , $(S,S)\text{-DPEN}$	1:1
thermodynamic			1:3
kinetic	<b>54</b> , BIPHEP	<b>52</b> , $(S,S)\text{-DPEN}$	1:1
thermodynamic			1:2
kinetic	<b>54</b> , BIPHEP	<b>53</b> , $(S,S)\text{-DM-DPEN}$	1:1
thermodynamic		$R = \text{Me}$	<1:> 20
kinetic	<b>55</b> , DM-BIPHEP	<b>53</b> , $(S,S)\text{-DM-DPEN}$	1:1
thermodynamic		$R = \text{Me}$	<1:> 20

an impressive 95% enantioselectivity. This result illustrates that diastereomeric catalysts not only have different enantioselectivities, but can also have very different turnover frequencies (TOFs). In this exceptional case, the faster diastereomer promoted the enantioselective reduction 121 times faster than the slower diastereomer! Such a surprisingly large rate difference emphasizes the fact that, when diastereomeric catalysts are employed together in an asymmetric reaction, the product ee is governed by the enantioselectivity of each of the diastereomeric catalysts and their relative rates.<sup>52,160–163</sup> It must also be borne in mind that *both enantioselectivities and TOFs are substrate dependent*, a fact that complicates reaction optimization in processes employing two diastereomeric catalysts in the same reaction vessel. An illustration of this point is the reduction of 2-methylacetophenone (**61**) in eq 12. Use of *rac*-Tol-BINAP and  $(S,S)\text{-DPEN}$  (**52**) afforded the reduction product,  $(R)\text{-62}$ , with 90% ee and in quantitative yield (Table 4). When enantiopure  $(S)\text{-Tol-BINAP}$  and  $(S,S)\text{-DPEN}$  were employed, the resulting catalyst rapidly reduced **61** to provide  $(R)\text{-62}$  of 97.5% ee. The other diastereomer, derived from  $(S)\text{-Tol-BINAP}$  and  $(R,R)\text{-DPEN}$  (which was the faster diastereomer with substrate **59** in eq 12), provided  $(R)\text{-62}$  of only 8% ee (Table 4). In this dual catalyst system with **61** (eq 12), the faster catalyst is 13 times faster than its diastereomer.<sup>156</sup>

Building on the exciting results above, Mikami, Noyori, and co-workers cleverly substituted the conformationally flexible diphosphine DM-BIPHEP (**48**, Figure 29) for the *rac*-Tol-BINAP ligand in the precatalyst  $(\text{Tol-BINAP})\text{RuCl}_2[(S,S)\text{-DPEN}]$ .<sup>40</sup> Upon combining the racemic precursor (DM-BIPHEP)- $\text{RuCl}_2(\text{dmf})_n$  (**55**) with  $(S,S)\text{-DPEN}$  (**52**), the two diastereomers were initially observed by NMR spec-

troscopy in a 1:1 ratio (Figure 31, Table 5). Over 3 h at room temperature, the  $S/S,S$  and  $R/S,S$  diastereomers were observed to slowly equilibrate to a 1:3 mixture. The asymmetric reduction of 1'-acetonaphthone was examined using catalysts composed of atropisomeric diphosphine ligands in combination with  $(S,S)\text{-DPEN}$ . The enantioselectivity was found to be dependent on the initial diastereomeric ratio of the precatalysts, as shown in Table 6. Use of an

**Table 6. Initial Ratios of Diastereomeric Catalysts (Figure 31) and Their Enantioselectivities in the Reduction of 1'-Acetonaphthone**

entry	diphosphine	$S/S,S:R/S,S$	$T$ (°C)	ee (%)
1	DM-BIPHEP	1:1	28	63
2	DM-BIPHEP	2:1	28	73
3	DM-BIPHEP	3:1	28	84
4	$(\pm)\text{-DM-BINAP}$	1:1	28	80
5	DM-BIPHEP	3:1	-35	92
6	$(\pm)\text{-DM-BINAP}$	1:1	-35	89

*initial* 1:1, 2:1, or 3:1 ratio of the diastereomeric precatalysts, generated as shown in Figure 31, resulted in enantioselectivities of 63, 73, and 84%, respectively, indicating that the major diastereomer is more enantioselective (Table 6, entries 1–3). It should be noted that the values in entries 1–3 are for the dichloride precatalysts. The proposed catalyst in the hydrogenation reactions is the dihydride complex.<sup>68,164,165</sup> The diastereomeric ratio of these species was not investigated.

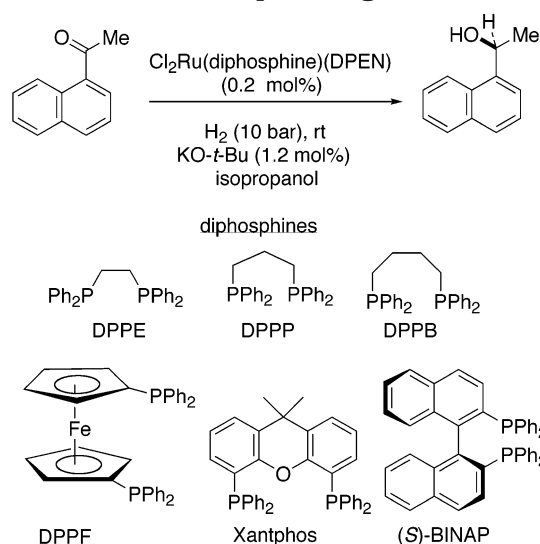
The advantages of using the conformationally flexible DM-BIPHEP ligand are evident on comparison of the enantioselectivities of the 3:1 mixture of diastereomers with use of racemic DM-BINAP in Table 6. The 1:1 mixture of diastereomers formed on combining  $(\pm)\text{-DM-BINAP}[\text{RuCl}_2(\text{dmf})_n]$  and  $(S,S)\text{-DPEN}$  was less enantioselective than the catalyst



mixture formed from DM-BIPHEP (entries 5 vs 6). These important studies set the stage for investigations into other enantioselective reactions using chelating diphosphines, such as BIPHEP, and studies to probe the interactions responsible for the relative populations of the observed diastereomers. An understanding of the factors that control both the kinetics and the thermodynamics of equilibration of the diastereomeric catalysts is crucial to developing catalysts based on the use of conformationally flexible ligands.

In a related system, Xiao and co-workers examined the effect of substituting achiral bidentate phosphines for the BINAP and BIPHEP ligands used in Table 6 and eq 12 for the asymmetric hydrogenation of 1-acetylnaphthone. The achiral diphosphines DPPE, DPPP, DPPB, DPPF, and Xantphos were used with (*R,R*)-DPEN and ruthenium(II), as shown in Scheme 2. It was envisioned that the chiral diamine would

### Scheme 2. Asymmetric Hydrogenation Using Various Bidentate Phosphine Ligands



bias the positions of the phosphine phenyl groups,<sup>70,71</sup> extending the asymmetric environment of the catalyst. As discussed in detail below, the cyclopentadienyl-bound phosphorus centers of the DPPF ligand can adopt a staggered conformation, giving rise to enantiomeric binding modes.<sup>167</sup> For the purpose of comparison, BINAP was also examined.<sup>40</sup> The catalysts were prepared in an analogous fashion to those of eq 11. The authors noted that the precatalysts were not characterized.<sup>166</sup>

The results of the study are compiled in Table 7, where it can be seen that the activity and enantioselectivity vary considerably with the nature of the diphosphine. The bite angles of the diphosphines are listed in Table 7 and show that there is little correlation between catalyst activity and the P–M–P bond angles. Diphosphines with alkyl backbones give similar enantioselectivities (entries 1–3), suggesting that the positioning of the *P*-aryl groups on these ruthenium–phosphines is similar. It appears that the chiral diamine is equally effective at inducing an asymmetric conformation into these ligands. DPPF

**Table 7. Results of Asymmetric Hydrogenation Reaction Illustrated in Scheme 2**

entry	diphosphine	convrsn (%) <sup>a</sup>	ee (%)	bite angle (deg)
1	DPPE	21	57	85
2	DPPP	76	56	91
3	DPPB	66	61	98
4	DPPF	93	65	96
5	Xantphos	>99	26	112
6	( <i>R</i> )-BINAP	>99	98	92
7	BIPHEP		84 <sup>b</sup>	

<sup>a</sup> Conversion after 3 h at 20 °C. <sup>b</sup> Reaction performed at 28 °C.

gives the most enantioselective catalyst of the achiral ligands examined in this study (entry 4). The enantioselectivity increases to 70% when the reaction is conducted at –20 °C. The catalyst formed from Xantphos is the least enantioselective, generating the aryl alcohol with only 27% enantioselectivity (entry 5). The rigid nature of Xantphos makes it difficult to induce asymmetry into the ruthenium–Xantphos metalocycle. It is notable, however, that this catalyst is the most efficient, showing high TOF, like the catalyst derived from BINAP. These results can be compared with those employing (*R*)-BINAP and BIPHEP (entries 6 and 7). Use of BINAP under identical conditions resulted in product formation with 98% ee and high activity. The catalyst formed from BIPHEP resulted in an enantioselectivity of 84%, although this reaction was performed under slightly different conditions.<sup>40</sup> The authors suggest that the difference in activity of the catalysts may be related to the basicity of the phosphine ligands.<sup>166</sup> The triaryl phosphines are less basic than the dialkyl aryl phosphines and lead to more efficient catalysts for the hydrogenation of carbonyl groups.

### 4.2. Asymmetric Diels–Alder and Carbonyl–Ene Reactions with BIPHEP-Derived Ligands

In the hydrogenation reactions above, the flexible BIPHEP derivatives formed an integral part of the chiral environment of the catalyst, when used in combination with an enantiopure ligand. Recent work by Gagné and co-workers has taken advantage of the barrier associated with atropisomerization in the (BIPHEP)Pt system<sup>168</sup> (the details of which are outlined below) to prepare an asymmetric catalyst, in which the only chiral ligand is the normally unresolvable BIPHEP locked in a chiral conformation.<sup>169</sup> As shown in Figure 32, reaction of [(*R*)-BIPHEP]Pt[(*S*)-BINOLate] (**63**) of high diastereopurity with HCl resulted in liberation of BINOL and generation of [(*R*)-BIPHEP]PtCl<sub>2</sub> (**64**). Likewise, reaction of the [(*R*)-BIPHEP]Pt[(*S*)-BINOLate] (**63**) with triflic acid gave [(*R*)-BIPHEP]Pt(OTf)<sub>2</sub> (**65**). To establish the enantiopurity of these compounds, samples of the bis(triflate) **65** were treated with (*S,S*)-DPEN (eq 13), and the diastereomeric excess of the resultant diamine complexes was determined by <sup>31</sup>P NMR analysis. A sample of [(*R*)-BIPHEP]Pt(OTf)<sub>2</sub> (**65**), determined to have an ee of 98%, was allowed to stand for 8 h at room temperature. It was then reacted with (*S,S*)-DPEN to give a 98:2 diastereo-

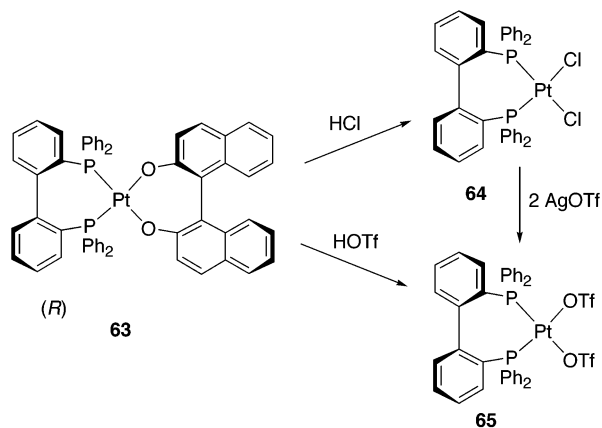
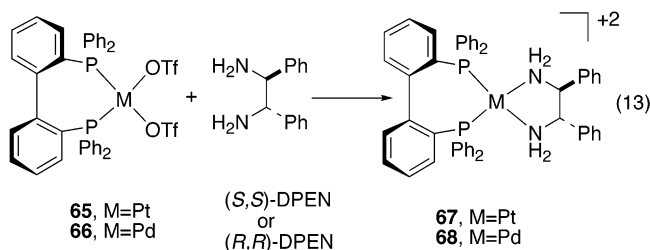
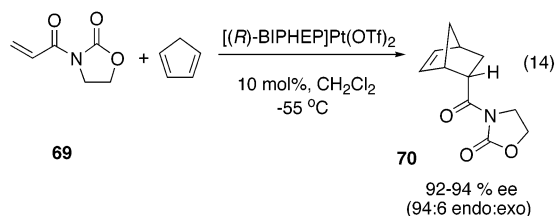


**Figure 32.** Protonation of **63** with acids to give (BIPHEP)-PtX<sub>2</sub> derivatives of high enantiopurity.

meric ratio of [BIPHEP]Pt[(*S,S*)-DPEN]<sup>2+</sup> (**67**), indicating that racemization in solution at room temperature was very slow.

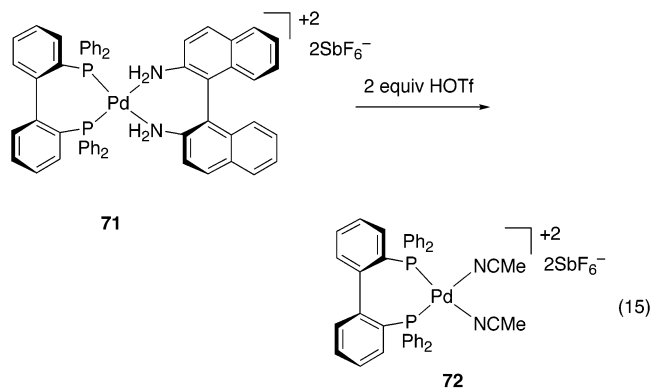


Having demonstrated that (BIPHEP)PdX<sub>2</sub> compounds were stable for several hours with respect to racemization at room temperature, Gagné and co-workers then tested the ability of these complexes to catalyze the asymmetric Diels–Alder and asymmetric carbonyl–ene reactions. The catalyst for these reactions was prepared either by direct treatment of the diastereopure [(*R*)-BIPHEP]Pt[(*S*)-BINOLate] with triflic acid or by reaction of [(*R*)-BIPHEP]PtCl<sub>2</sub> with AgOTf. Using this catalyst in eq 14 resulted in formation of the Diels–Alder adduct in 92–94% ee (94:6 endo/exo ratio). The enantiomeric excess of the platinum catalyst **65** did not deteriorate during the reaction, as determined by quenching the reaction at >90% conversion with (*S,S*)-DPEN (eq 13) and subsequent NMR analysis. The stereochemistry of the Diels–Alder adduct was consistent with that reported by Ghosh,<sup>170</sup> who used platinum complexes of [(*R*)-BINAP]Pt(OTf)<sub>2</sub> with the same substrates.



A parallel strategy was subsequently used by Mikami and co-workers in the resolution of (BIPHEP)-Pd dications that were employed in the hetero-Diels–Alder (HDA) reaction.<sup>171,172</sup> Reaction of [(*R*)-BIPHEP]-Pd[(*R*)-DABN]<sup>2+</sup> (**71**) with triflic acid at 0 °C in

acetonitrile resulted in formation of [(*R*)-BIPHEP]-Pd(NCMe)<sub>2</sub><sup>2+</sup> (**72**, eq 15). No loss of enantiopurity of



the [(*R*)-BIPHEP]Pd(NCMe)<sub>2</sub><sup>2+</sup> was reported after the removal of the 1,1'-binaphthyl-2,2'-diamine (DABN), as determined by NMR studies analogous to those of Gagné. The resolved Lewis acid catalyst [(*R*)-BIPHEP]Pd(NCMe)<sub>2</sub><sup>2+</sup> (**72**) was employed in the HDA reaction with glyoxylate, as illustrated in eq 16. Using 0.5 mol % of the catalyst provided product of 75% ee, albeit in low yield (11%). Increasing the catalyst loading to 2 mol % resulted in 82% enantioselectivity and 60% yield (Table 8, entries 1 and 2).

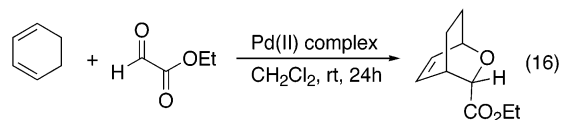
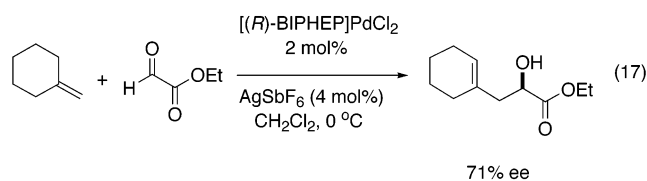


**Table 8.** Enantioselectivities of Pd(II) Catalysts in the HDA Reaction (Eq 16)

entry	ligands	mol %	yield (%)	ee (%) (config)
1	( <i>R</i> )-BIPHEP	0.5	11	75 (1 <i>R</i> ,3 <i>S</i> ,4 <i>S</i> )
2	( <i>R</i> )-BIPHEP	2	60	82 (1 <i>R</i> ,3 <i>S</i> ,4 <i>S</i> )
3	( <i>R</i> )-BIPHEP/( <i>R</i> )-DABN	0.5	62	94 (1 <i>R</i> ,3 <i>S</i> ,4 <i>S</i> )
4	( <i>R</i> )-BIPHEP/( <i>R</i> )-DABN	2	75	92 (1 <i>R</i> ,3 <i>S</i> ,4 <i>S</i> )
5	(±)-BINAP/( <i>R</i> )-DABN	2	61	7 (1 <i>R</i> ,3 <i>S</i> ,4 <i>S</i> )
6	(±)-BIPHEP/( <i>R</i> )-DABN	2	64	9 (1 <i>R</i> ,3 <i>S</i> ,4 <i>S</i> )

Interestingly, the authors found that use of the dual-ligand catalyst [(*R*)-BIPHEP]Pd[(*R*)-DABN]<sup>2+</sup> (**71**) resulted in a more efficient and enantioselective catalyst. Thus, even at 0.5 mol % catalyst loading, [(*R*)-BIPHEP]Pd[(*R*)-DABN]<sup>2+</sup> generated the product with an enantioselectivity of 94% (entry 3). Raising the catalyst loading gave a higher yield and similar enantioselectivity (entry 4). Both of the diastereomeric catalyst pairs, [(±)-BINAP]Pd[(*R*)-DABN]<sup>2+</sup> and [(±)-BIPHEP]Pd[(*R*)-DABN]<sup>2+</sup>, resulted in product with ee of less than 10% (Table 8, entries 5 and 6), indicating that the relative rates of the diastereomeric catalysts were similar in each case.<sup>171</sup> The platinum system used by Gagné<sup>169</sup> was also examined in the catalytic asymmetric carbonyl–ene reaction (eq 17).<sup>172,173</sup> The catalyst in this study was generated by addition of 2 equiv of AgSbF<sub>6</sub> to [(*R*)-BIPHEP]-PdCl<sub>2</sub> and exhibited an enantioselectivity of 71% with 99% conversion at room temperature. The combined results of these studies suggest that there are po-

tentially many uses for catalysts bearing resolved BIPHEP and related ligands in asymmetric catalysis.



### 4.3. Interconversion of Diastereomeric Catalysts and Catalyst Precursors Containing BIPHEP Derivatives

Following the initial report by Mikami and Noyori on the use of BIPHEP-derived ligands in the asymmetric hydrogenation reaction, the groups of Gagné<sup>169,174</sup> and Mikami<sup>171,172,175</sup> independently undertook studies to probe the interactions in diastereomeric metal complexes bearing stereochemically dynamic BIPHEP derivatives. Such studies are essential for understanding the factors that control the population of diastereomers and will enable more effective catalyst design. In the ruthenium system discussed previously, Mikami performed computational studies on the (BIPHEP)RuCl<sub>2</sub>(DPEN) system<sup>176</sup> and examined the effects of varying the size of substituents on the diphosphine and diamine ligands.<sup>171,172,175</sup> When the DM-BIPHEP ligand used in the asymmetric hydrogenation reactions in eq 12 was replaced with the parent BIPHEP ligand, the equilibrium ratio of the diastereomers dropped from 3:1 to 2:1 (Figure 31, Table 5). Augmentation of the substituents on the amino groups of the DPEN ligand was then examined as a strategy to increase the population of the major diastereomer. The unsymmetrical (*S,S*)-*N,N*-dimethyl-1,2-diphenylethylenediamine [(*S,S*)-DM-DPEN] (**53**, Figure 31) was added to [BIPHEP]RuCl<sub>2</sub>(dmf)<sub>*n*</sub> (**54**) and [DM-BIPHEP]RuCl<sub>2</sub>(dmf)<sub>*n*</sub> (**55**) to generate [BIPHEP]RuCl<sub>2</sub>[(*S,S*)-DM-DPEN] and [DM-BIPHEP]RuCl<sub>2</sub>[(*S,S*)-DM-DPEN], as shown in Figure 31 and Table 5. In both cases, the initial product was a 1:1 mixture of diastereomers. Heating these mixtures to 50 °C led to isomerization of the configurationally labile biphenylphosphine ligands and conversion to single diastereomers, as determined by <sup>1</sup>H NMR spectroscopy.

3,3'-Dimethyldiaminobinaphthyl (DM-DABN, **73**) was also examined for its ability to bias the configuration of the (BIPHEP)RuCl<sub>2</sub> fragment.<sup>177</sup> Reaction of *rac*-[BIPHEP]RuCl<sub>2</sub>(dmf)<sub>*n*</sub> with 1 equiv (*R*)-DM-DABN led to formation of only one of the diastereomeric adducts, [(*R*)-BIPHEP]RuCl<sub>2</sub>[(*R*)-DM-DABN], with the [(*S*)-(BIPHEP)]RuCl<sub>2</sub>(dmf)<sub>*n*</sub> and half of the (*R*)-DM-DABN remaining unreacted (Figure 33). Heating this mixture to 50 °C, however, provided [(*R*)-BIPHEP]RuCl<sub>2</sub>[(*R*)-DM-DABN] as a single diastereomer, possibly through epimerization of the [(*S*)-(BIPHEP)]RuCl<sub>2</sub>(dmf)<sub>*n*</sub>, followed by capture by the (*R*)-DM-DABN. As can be seen from these studies, ligands that extend further toward the BIPHEP group in the octahedral metal geometry are better able to bias the configuration of the BIPHEP ligand. The geometries of complexes [(*S*)-BIPHEP]RuCl<sub>2</sub>[(*S,S*)-DM-DPEN],<sup>175</sup> [(*S*)-DM-BIPHEP]RuCl<sub>2</sub>[(*S,S*)-

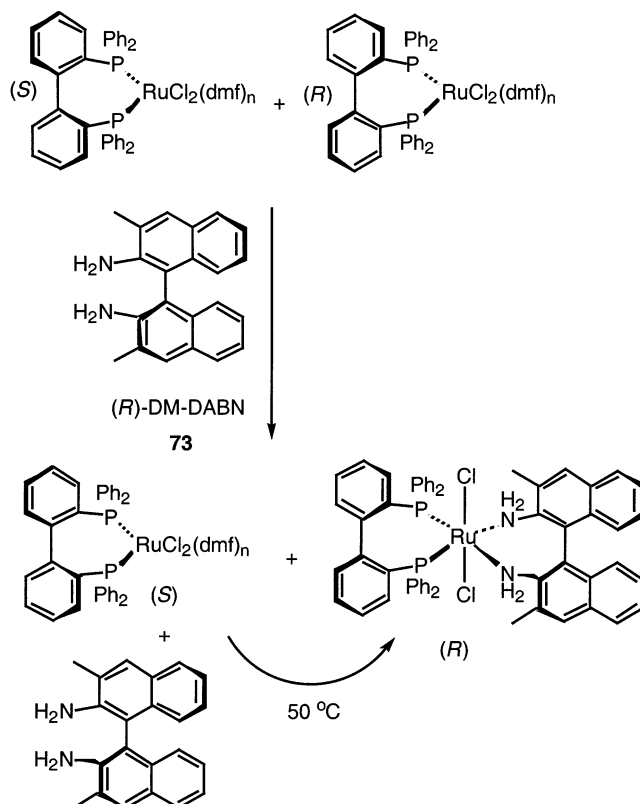


**Figure 33.** Reaction of (BIPHEP)RuCl<sub>2</sub>(dmf)<sub>*n*</sub> with (*R*)-DM-DABN and equilibration to afford a single diastereomer.

DM-DPEN],<sup>175</sup> and [(*R*)-BIPHEP]RuCl<sub>2</sub>[(*R*)-DM-DABN]<sup>171</sup> were elucidated by X-ray crystallography. An ORTEP diagram of one of these, [(*S*)-BIPHEP]RuCl<sub>2</sub>[(*S,S*)-DM-DPEN], is shown in Figure 34.

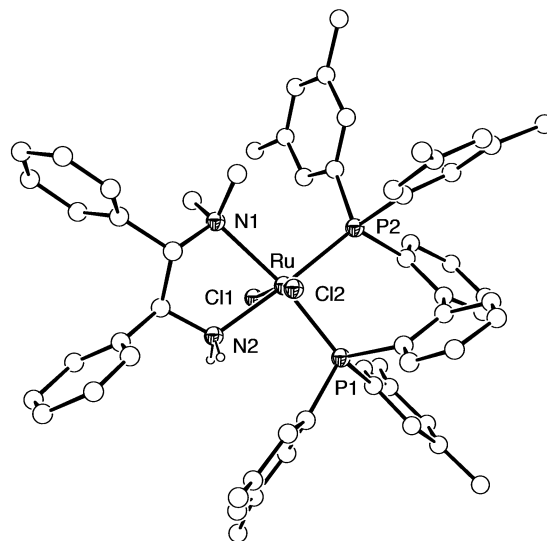


**Figure 34.** Structure of [(*S*)-BIPHEP]RuCl<sub>2</sub>[(*S,S*)-DM-DPEN] illustrating the pseudoequatorial positions of the *N*-methyl and *P*-phenyl rings.

In all three cases, the ruthenium centers are pseudooctahedral with trans chloride ligands, as was found in related (BINAP)Ru structures.<sup>159,178</sup> On the basis of the (BIPHEP)Ru structures and molecular modeling studies, Mikami and co-workers postulated that the increased diastereoselectivity in complexes

with the DM-DPEN ligands over the diastereoselectivity in complexes of the parent DPEN could be explained by the interaction of the pseudoaxial and pseudo-equatorial *N*-methyl groups of the DM-DPEN ligand with the phosphorus-bound aryl groups of the BIPHEP derivatives. In complexes of the BIPHEP ligand, as well as other chelating diphosphine ligands bearing the diphenylphosphino groups,<sup>159,174,178–180</sup> one pair of diastereotopic aryl rings is pseudo-equatorial and thrust forward as a result of the conformation of the diphosphametalocycle. In the more stable diastereomer, the protruding equatorial phenyl group and the equatorial *N*-methyl group are positioned above and below the plane defined by the nitrogen and phosphorus centers. In the less stable diastereomer, these two pseudo-equatorial groups are on the same face of the plane and in close proximity, resulting in a destabilization of the [(*R*)-BIPHEP]-RuCl<sub>2</sub>(*S,S*)-DM-DPEN] diastereomer (Figure 35). In

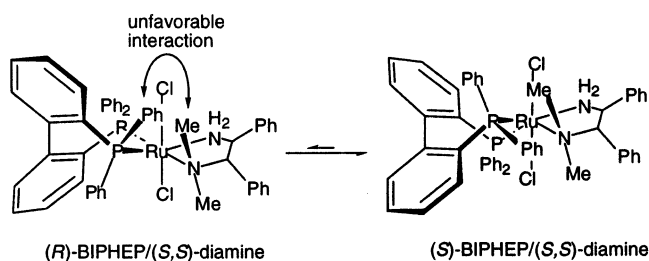
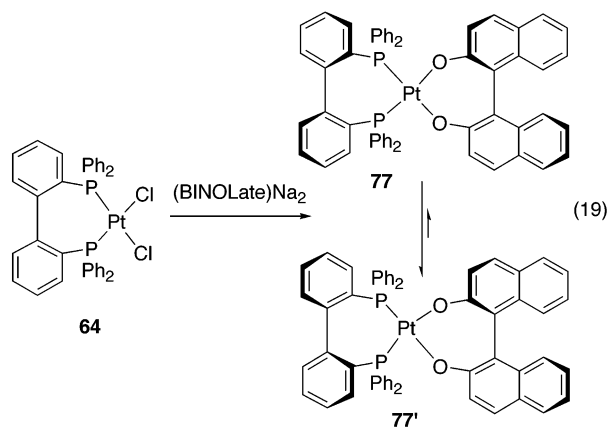
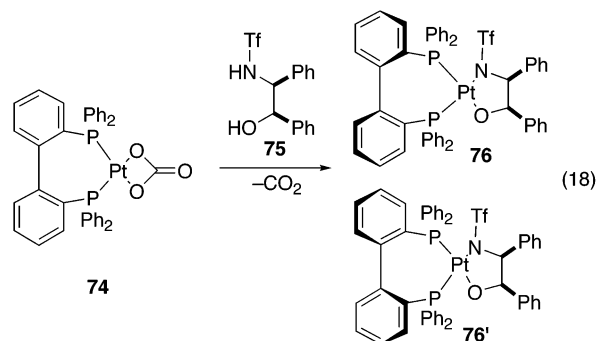


**Figure 35.** Diastereomers of [BIPHEP]RuCl<sub>2</sub>[(*S,S*)-diamine]. In the [(*R*)-BIPHEP]RuCl<sub>2</sub>[(*S,S*)-diamine], there is an interaction between the pseudo-equatorial P–Ph and N–Me that destabilizes this diastereomer. In the [(*S*)-BIPHEP]RuCl<sub>2</sub>[(*S,S*)-diamine] diastereomer, these groups are not directed toward each other (also see Figure 5).

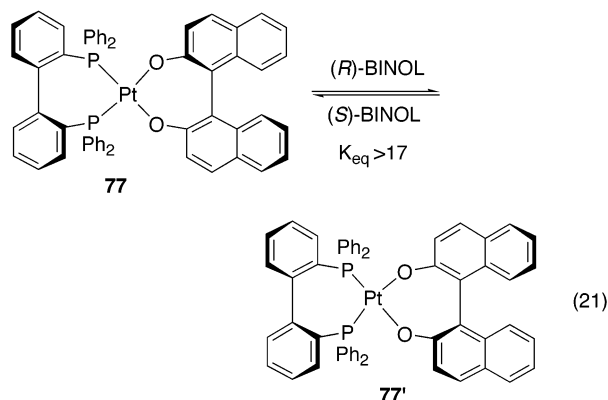
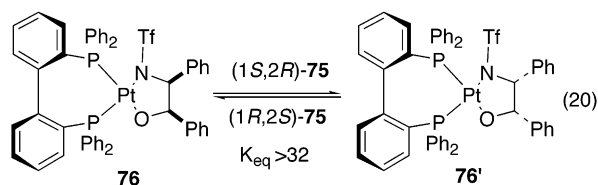
a similar manner, extension of the 3,3'-dimethyl groups in [(*S*)-BIPHEP]RuCl<sub>2</sub>[(*R*)-DM-DABN] will destabilize it over its diastereomer.

In a detailed study of the interconversion of BIPHEP configurations in diastereomeric (BIPHEP)-PtX<sub>2</sub> complexes, Gagné and co-workers found that high diastereomeric ratios can be obtained in this square planar platinum system.<sup>174</sup> Reaction of the racemic carbonate **74** with racemic hydroxy sulfonamide **75** gave a 1:1 mixture of diastereomers (eq 18). Likewise, reaction of the racemic (BIPHEP)PdCl<sub>2</sub> (**64**) with (BINOLate)Na<sub>2</sub> furnished a 1:1 kinetic ratio of the (BINOLate)Pt(BIPHEP) diastereomers **77** and **77'** (eq 19).

Two methods, exchange of the chiral ligands and thermal atropisomerization of the BIPHEP ligand, were employed to determine the thermodynamic populations of the diastereomeric complexes. Addition of a substoichiometric amount (0.2 equiv) of the racemic hydroxy sulfonamide *rac*-**75** to a solution of the racemic diastereomers *rac*-**76** and *rac*-**76'** at room temperature, conditions under which atropisomerization does not occur, resulted in slow exchange of the bound and free amino alcohol derivative, catalyzing equilibration of the diastereomers (eq 20). In this manner, the equilibrium constant between diastereomers *rac*-**76** and *rac*-**76'** was determined to be >32. In a similar fashion, the equilibrium constant between the BINOLate complexes *rac*-**77** and *rac*-**77'**



was measured, upon addition of *rac*-BINOL, to be >17 (eq 21). These studies demonstrate the powerful effect that chiral ligands can have on the diastereomeric excess involving configurationally dynamic ligands in square planar complexes.



Gagné's innovative use of ligand-exchange reactions to determine equilibrium constants should be of general utility.<sup>174</sup> It is particularly useful when the conditions that would lead to atropisomerization of the BIPHEP complex cause decomposition of one or both diastereomers. Such was the case with the minor diastereomer **76** (eq 20), which decomposed upon heating. This method is not applicable, however, to the synthesis of enantiopure thermodynamic

mixtures of diastereomers, which must be prepared by atropisomerization of the BIPHEP ligand. Thus, thermolysis of enantiopure diastereomers **77** and **77'** at 92–122 °C resulted in clean conversion to the equilibrium ratio of ~94:6 **77'/77**. Eyring analysis of the kinetic data measured over a 30 °C temperature range indicated that  $\Delta H^\ddagger$  was 27(2) kcal/mol and  $\Delta S^\ddagger$  was -5(5) eu. Determination of the equilibrium constants at a series of temperatures allowed van't Hoff analysis of the data, giving a  $\Delta H^\circ$  of -2.42(4) and a  $\Delta S^\circ$  of -0.6(10) eu.

To understand the molecular interactions that give rise to the strong thermodynamic preference between the sets of diastereomers **76** and **76'** and **77** and **77'**, the structures of **76'** and **77** were determined by X-ray crystallography. An ORTEP diagram of the thermodynamically more stable diastereomer, **76'**, is illustrated in Figure 36. The conformations and

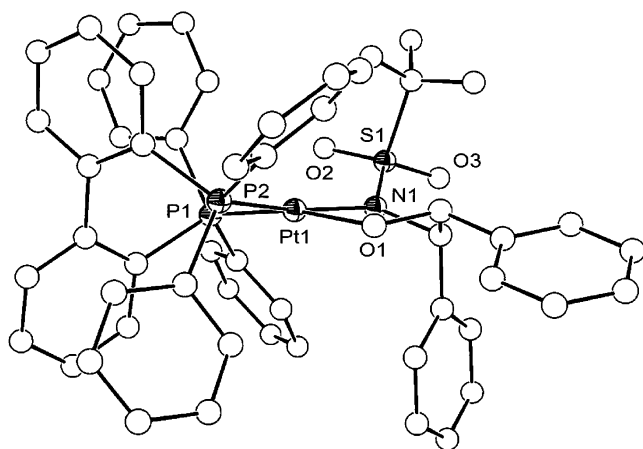


**Figure 36.** Structure of the more stable diastereomer, **76'**.

bonding of the triflamide and the BIPHEP ligands are similar to those found in complexes containing only one of these ligands.<sup>149,168,180</sup> In the square planar platinum complex **76'**, the cis phenyl groups of the amino alcohol-derived ligand occupy pseudoaxial and pseudoequatorial positions, forcing the bulky SO<sub>2</sub>CF<sub>3</sub> group to orient trans to the neighboring aryl group (Figure 36). It is the triflamide group that is closest to the BIPHEP ligand and believed to have the largest impact on the equilibrium constant of the diastereomeric complexes.<sup>174</sup> In the crystal structure of the major diastereomer, **76'**, one of the sulfonyl oxygens is directed toward a pseudoaxial phenyl of the BIPHEP. That pseudoaxial phenyl is oriented away from the metal and the sulfonyl oxygen. By analogy, in the less stable diastereomer, the pseudoequatorial *P*-phenyl is anticipated to be tilting forward, toward the triflamide sulfonyl oxygen, resulting in close contacts that destabilize this diastereomer. In the case of diastereomers **77** and **77'**, Gagné and co-workers were able to obtain crystals of the minor diastereomer (**77**) and determine its structure (Figure 37).<sup>174</sup> In this structure, the BIPHEP ligand is significantly distorted, to minimize interaction with the BINOLate 3,3'-hydrogens, which protrude toward the *P*-phenyl groups. In the more stable diastereomer, the 3,3'-hydrogens would point toward the pseudoaxial *P*-phenyl groups,

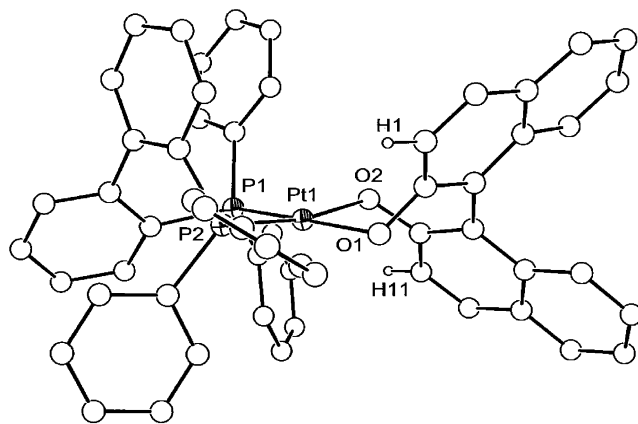


**Figure 37.** Structure of the less stable diastereomer, **77**.

which are oriented away from the metal center, thereby greatly reducing the steric interactions between the ligands.

In a similar vein, Mikami and co-workers examined the proficiency of diaminobinaphthyl derivatives in controlling the diastereomeric ratio when bound to the dicationic (BIPHEP)Pd<sup>2+</sup> center.<sup>171,172</sup> As in the ruthenium system above (Figure 33), reaction of (BIPHEP)Pd(NCCH<sub>3</sub>)<sub>2</sub><sup>2+</sup> (**78**) with [(*R*)-DM-DABN] resulted in formation of [(*R*)-BIPHEP]Pd[(*R*)-DM-DABN]<sup>2+</sup>, leaving the mismatched enantiomer, [(*S*)-BIPHEP]Pd(NCCH<sub>3</sub>)<sub>2</sub><sup>2+</sup>, unreacted (Figure 38). At-

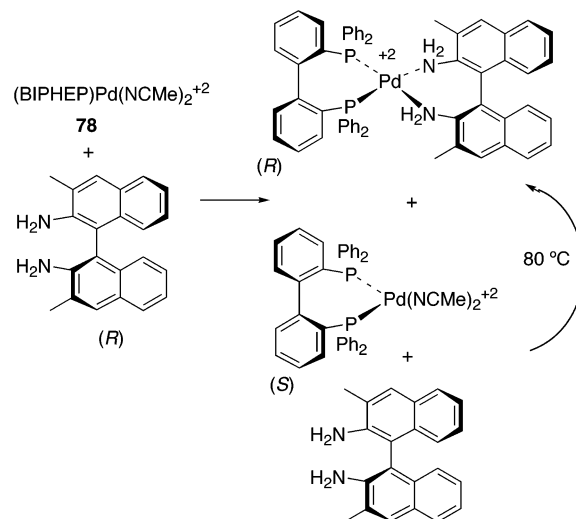


**Figure 38.** Reaction of (BIPHEP)Pd(NCMe)<sub>2</sub><sup>2+</sup> with (*R*)-DM-DABN and equilibration to afford a single diastereomer.

ropisomerization of [(*S*)-BIPHEP]Pd(NCCH<sub>3</sub>)<sub>2</sub><sup>2+</sup> was not observed at room temperature but readily took place when the reaction mixture was heated to 80 °C for 12 h, providing a single diastereomer.<sup>172</sup> Reaction of [(BIPHEP)Pd(NCCH<sub>3</sub>)<sub>2</sub>]<sup>2+</sup> with the less hindered parent diamine, DABN, showed analogous behavior.<sup>171</sup>

#### 4.4. Mechanistic Aspects of Atropisomerization of BIPHEP

Determination of the factors that affect the barrier to atropisomerization of catalysts bearing BIPHEP, and related ligands, is crucial to more effective

application of configurationally dynamic ligands in asymmetric catalysis. This is particularly relevant with BIPHEP derivatives because of their close structural similarity to BINAP, which has been shown to form numerous highly enantioselective catalysts with a broad range of metal centers. Parameters that are likely to impact the barrier to atropisomerization of BIPHEP include metal geometry, coordination number, electron count, metal–phosphorus bond distances, and steric and electronic properties of the ancillary ligands.<sup>181</sup> Theoretical studies on the mechanism of atropisomerization of the BIPHEP ligand in this system employing the ONIOM method (B3LYP:HF) suggested that the diastereomers *R/S,S* and *S/S,S* have similar energies, consistent with the 3:1 ratio observed experimentally (Figure 31, Table 5).<sup>40,176</sup> Reasonable mechanisms of atropisomerization of BIPHEP–metal adducts include a direct atropisomerization while the ligand remains chelated to the metal center (pathway a), or dissociation of one arm of the bidentate ligand followed by rotation about the biphenyl bond and recoordination to the metal (pathway b, Figure 39).

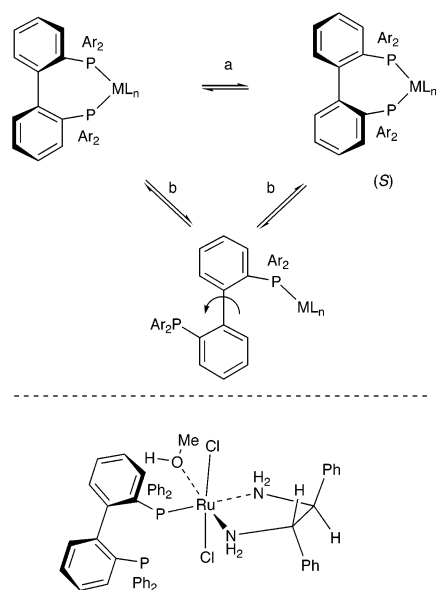


**Figure 39.** Mechanisms of atropisomerization: (a) direct atropisomerization, (b) dissociative mechanism (top). Below is the proposed transition-state structure.

Complete dissociation of the BIPHEP ligand had been investigated by conducting the atropisomerization in the presence of BINAP. No exchange of the BIPHEP and BINAP ligands was observed, indicating that complete loss of BIPHEP is unlikely.<sup>175</sup>

Rupture of an M–P bond has a high activation barrier<sup>182,183</sup> and leads to a coordinatively unsaturated metal center, while direct atropisomerization of the BIPHEP goes through a strained transition state. Unfortunately, it is not possible to kinetically distinguish these mechanisms. Therefore, mechanistic hypotheses must be formulated on the basis of computational studies and behavior in related systems.

In the hydrogenation catalyst of Noyori and Mikami, equilibration of the diastereomeric complexes (DM-BIPHEP)RuCl<sub>2</sub>[(*S,S*)-DPEN] was observed to

proceed over several hours at room temperature (Figure 31, Table 5).<sup>40</sup> On the basis of the known chemistry of Ru(II) complexes bearing phosphine ligands, it is likely that the interconversion of the diastereomers proceeds by dissociation of one of the phosphorus centers of the chelating ligand, followed by biphenyl rotation to invert the configuration of the ligand and recoordination (Figure 39, pathway b). It is known that the related (Ph<sub>3</sub>P)<sub>4</sub>RuCl<sub>2</sub> readily loses phosphine in solution to form considerable amounts of the unsaturated complex (Ph<sub>3</sub>P)<sub>3</sub>RuCl<sub>2</sub>.<sup>184,185</sup> Dissociation of one arm of chelating phosphines is less commonly observed but has been reported.<sup>186</sup> The computational studies by Yamanaka and Mikami suggest that the dissociative route (pathway b) is lower in energy than the concerted mechanism (pathway a).<sup>176</sup> The authors propose that the trigonal bipyramidal intermediate formed on dissociation of a phosphorus center is stabilized by coordination of methanol, further lowering the barrier.

Comparison of the barriers to atropisomerization in the ruthenium system outlined above with platinum complexes **77** and **77'** and palladium complexes (Figure 38) highlights how different metal–ligand sets can affect the barrier to isomerization. Atropisomerization of the platinum-bound BIPHEP in **77** and **77'** occurs at temperatures around 100 °C over the course of several hours.<sup>174</sup> The four-coordinate, 16-electron platinum complexes are stable square planar species and are known to undergo ligand exchange through associative mechanisms, although related Pd(II) complexes have also been shown to undergo loss of ligand to generate three-coordinate intermediates.<sup>187–193</sup>

Gagné and co-workers have taken advantage of the associative pathway by adding a donor ligand to accelerate atropisomerization of the BIPHEP–Pt center.<sup>174</sup> Heating a 1:1 ratio of platinum diastereomers **77** and **77'** in pyridine (Figure 40) to 40 °C for

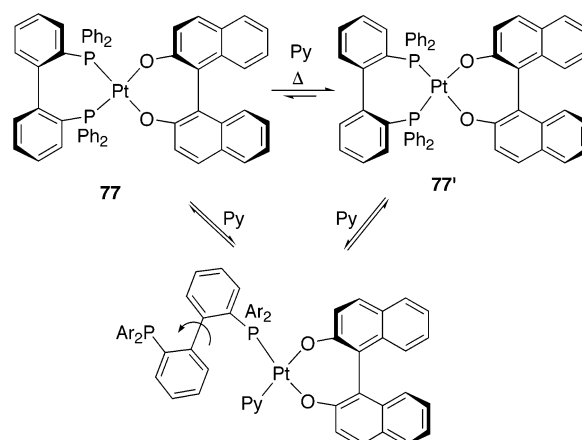


**Figure 40.** Mechanisms of atropisomerization: (a) direct atropisomerization requires 100 °C; (b) associative mechanism with pyridine (Py) requires 40 °C.

24 h resulted in equilibration to the thermodynamic mixture of >97:3 **77'**/**77**. Under these conditions, it is likely that the pyridine coordinates to the platinum to form a transient intermediate with one arm of the BIPHEP ligand dissociated (Figure 40). Once the BIPHEP ligand is bound to the platinum center in a

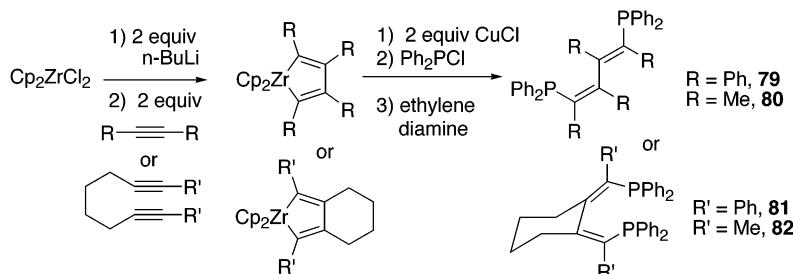


**Figure 41.** Synthesis of NUPHOS ligands.

monodentate fashion, atropisomerization of the ligand is facile. Reoordination with loss of pyridine regenerates the diastereomeric products. These conditions are considerably milder than those required for atropisomerization in the absence of pyridine (100 °C). On the basis of the mechanism of substitution of platinum complexes and the high temperature required to cause atropisomerization (in the absence of pyridine), it is not possible to confidently assign a mechanism for this process.

In the palladium system, atropisomerization occurs at a significantly lower temperature than that in the platinum and ruthenium systems (Figures 35 and 38). Direct comparison of these systems is complicated by the fact that the metals bear different ancillary ligands. It is known, however, that metal–ligand bond strength increases upon descending a column in the transition metals.<sup>194</sup> This is consistent with the observation that the palladium complex epimerizes more readily than the platinum complex if a dissociative mechanism is operative.

A possible cause for the marked difference in reaction rates for atropisomerization of ruthenium and platinum complexes is the coordination number. In the ruthenium complex, it is conceivable that the pseudoaxial *P*-phenyl substituents on the BIPHEP ligand interact with the apical chloride ligands, weakening the Ru–P bonds (ground-state destabilization<sup>182</sup>). This unfavorable interaction is reduced upon elongation of the Ru–P distance, as occurs in the transition state to phosphorus dissociation.

#### 4.5. A Potentially Useful New Class of Achiral Diphosphine Ligands (NUPHOS)

A new class of achiral chelating diphosphine ligands (NUPHOS, Figure 41) that form  $C_2$ -symmetric complexes on binding to metals has been reported by Doherty, Knight, and co-workers.<sup>195–197</sup> These phosphines are attractive, because a variety of substitution patterns can be prepared in one pot via a zirconocene-promoted reductive coupling of readily available alkynes and diynes with Negishi's reagent to generate a metallocyclopentadiene. This intermediate is then reacted with  $\text{CuCl}$  and  $\text{Ph}_2\text{P-CH}_2\text{-CH}_2\text{-PPh}_2$  to afford the NUPHOS derivatives in moderate to good yield after workup (Figure 41).

There are several striking similarities between BINAP, BIPHEP, and NUPHOS ligands. In all three cases, the diphenylphosphino groups are linked by a tether composed of four  $\text{sp}^2$ -hybridized carbons. They all form distorted square planar complexes with  $\text{PdCl}_2$  in which the seven-membered chelate pos-

sesses a distorted skew-boat conformation and a bite angle of  $92\text{--}93^\circ$ .<sup>180,195,198</sup> The conformation of the metallocycle causes the *P*-phenyl groups to adopt pseudoaxial and pseudoequatorial positions. The structure of (1,4- $\text{Ph}_2$ -2,3-cyclo- $\text{C}_6\text{H}_8$ -NUPHOS) $\text{PdCl}_2$  (**83**) is shown in Figure 42. The dihedral angle

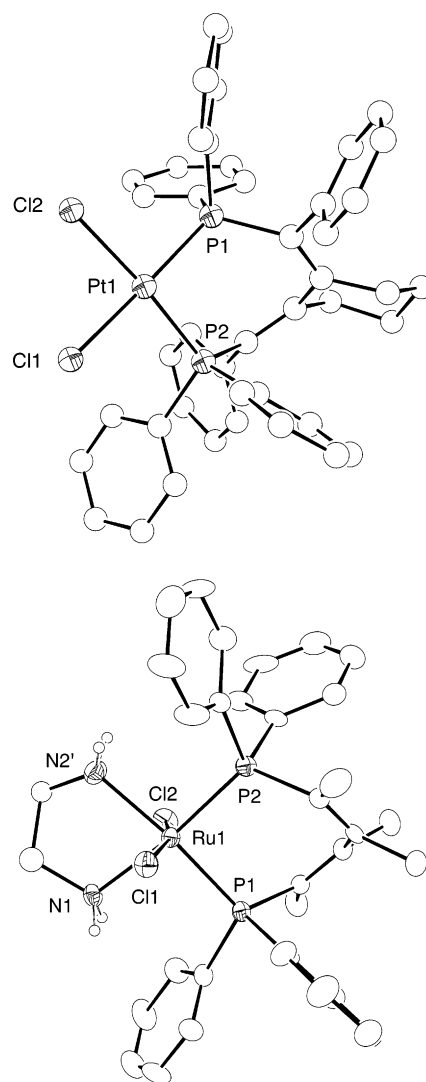
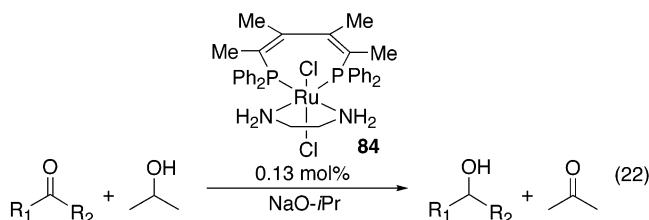


**Figure 42.** Structure of ligand 1,4- $\text{Ph}_2$ -2,3-cyclo- $\text{C}_6\text{H}_8$ -NUPHOS (**81**) in the complex (NUPHOS) $\text{PtCl}_2$  (**83**) (above) and structure of (1,2,3,4- $\text{Me}_4$ -NUPHOS) $\text{RuCl}_2$ (1,2-ethylenediamine) (**84**).

between the double bonds in the tether is  $47.7^\circ$ , which is on the low end of dihedral angles found in complexes with this class of ligands and those with BINAP ( $65\text{--}77^\circ$ ).<sup>196</sup> The barriers to atropisomerization of the metal complexes of NUPHOS have not

been reported, although the ligands exhibit  $C_2$  symmetry on the NMR time scale at room temperature. On the basis of the similarities in binding of NUPHOS ligand **80** (Figure 41) and BIPHEP to metals, we anticipate that the barriers to atropisomerization will be comparable. Given that a series of achiral NUPHOS ligands could be easily prepared, these ligands are attractive for further study in binding to chiral  $ML_n$  complexes.

The synthesis of (NUPHOS)RuCl<sub>2</sub>(diamine) complexes analogous to the (diphosphine)RuCl<sub>2</sub>(diamine) compounds of BINAP<sup>156</sup> and BIPHEP<sup>40</sup> phosphines previously discussed has been undertaken.<sup>197</sup> The chemistry is complicated by a higher propensity of NUPHOS **80** (Figure 41) to act as a six-electron donor, binding to the ruthenium through the two phosphine centers and one of the backbone double bonds of the NUPHOS ligand.<sup>197</sup> Nonetheless, a monomeric (1,2,3,4-Me<sub>4</sub>-NUPHOS)RuCl<sub>2</sub>(1,2-ethylenediamine) (**84**) has been prepared, isolated, and characterized crystallographically (Figure 42). This compound will efficiently catalyze the transfer hydrogenation of ketones under basic conditions (eq 22). Experiments using resolved diamines with NUPHOS derivatives to investigate the ability of the diamines to bias the stereochemistry of the NUPHOS ligand and influence the catalyst enantioselectivity in the asymmetric reduction of ketones will likely be forthcoming.



#### 4.6. Complexes of a Meso Cyclohexane-Based Diphosphine

An interesting and potentially useful type of meso diphosphine ligand that was explored by Knight, Doherty, and co-workers<sup>199</sup> is *cis*-1,2-bis(diphenylphosphinomethyl)cyclohexane (**85**, Figure 43). This ligand

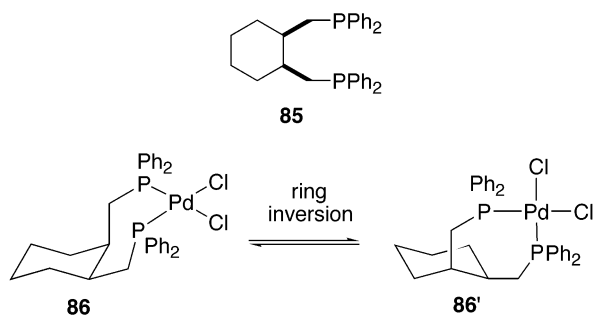


**Figure 43.** Interconversion of enantiomeric chair cyclohexane structures.

readily binds to palladium(II) to form the expected *cis* square planar complexes **86**. The variable-temperature <sup>31</sup>P{<sup>1</sup>H} NMR spectrum of the dichloride **86** at 328 K consisted of a broad singlet, suggesting that the phosphorus nuclei were equivalent on the time

scale of the experiment. Cooling the solution resulted in broadening of the signal into the baseline. Two new singlets appeared on further lowering the temperature, and at 213 K, two sharp, well-resolved singlets at 47.0 and 16.5 ppm were observed, indicating that interconversion of the phosphorus centers was slow on the NMR time scale. From the coalescence behavior between 278 and 283 K, the free energy of activation,  $\Delta G^\ddagger$ , was determined to be 11.5 kcal/mol. These data are consistent with ring inversion of the cyclohexane ring system, as illustrated in Figure 43.

An insightful study was also performed on the [*cis*-1,2-(diphenylphosphinomethyl)cyclohexane]Pd(Me)-Cl complex (**87**, Figure 44). The <sup>31</sup>P{<sup>1</sup>H} NMR spec-

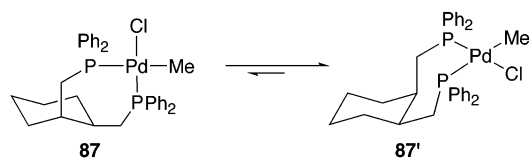


**Figure 44.** Interconversion of the diastereomers **87** and **87'**.

trum of this compound consists of two broad, featureless resonances at 45.0 and 12.1 ppm at room temperature (Figure 45). Variable-temperature NMR studies revealed that, at 213 K, two sets of doublets are observed in a 5.5:1 ratio. The doublets for the major diastereomer were found at 47.5 and 2.2 ppm ( $J_{PP} = 34.7$  Hz) and for the minor diastereomer at 25.4 and 22.1 ppm ( $J_{PP} = 36.0$  Hz). Line shape analysis gave  $\Delta G^\ddagger = 10.6$  kcal/mol. This process is proposed to result from interconversion of the diastereomers with the Pd-Me trans to the axial and equatorial diphenylphosphinomethyl groups through cyclohexane ring inversion.

The difference in energies of the diastereomeric complexes **87** and **87'** in this example is surprising, given the similarity of the two diastereomers. The origin of this effect was examined computationally. A difference of about 1 kcal/mol between two minimized structures was calculated, which translates to an equilibrium constant of 5 at room temperature. The most significant structural difference in the minimized structures is the P-Pd-Cl angle. In **87'** this angle is 88.5°, and in **87** it is 93.5°. The solid-state structure of the more stable diastereomer is illustrated in Figure 46. It is noteworthy that a small perturbation in the ligand environment can result in a significant shift in the equilibrium.

#### 4.7. Spontaneous Resolution of an Asymmetric Catalyst Bearing a Bis(phosphole) Ligand

A beautiful illustration of the application of stereochemically dynamic ligands to asymmetric catalysis was recently reported by Gouygou, Balavoine, and co-workers.<sup>200</sup> Their study employed the ligand 1,1'-diphenyl-3,3',4,4'-tetramethyl-2,2'-biphosphole (BIPHOS, **88**, Figure 47), which was originally synthesized by Mathey and co-workers.<sup>201,202</sup> This ligand uniquely has axial chirality in the bis(phosphole) and central chirality at the two phosphorus atoms, giving rise to three pairs of enantiomers (Figure 47).<sup>203</sup> The



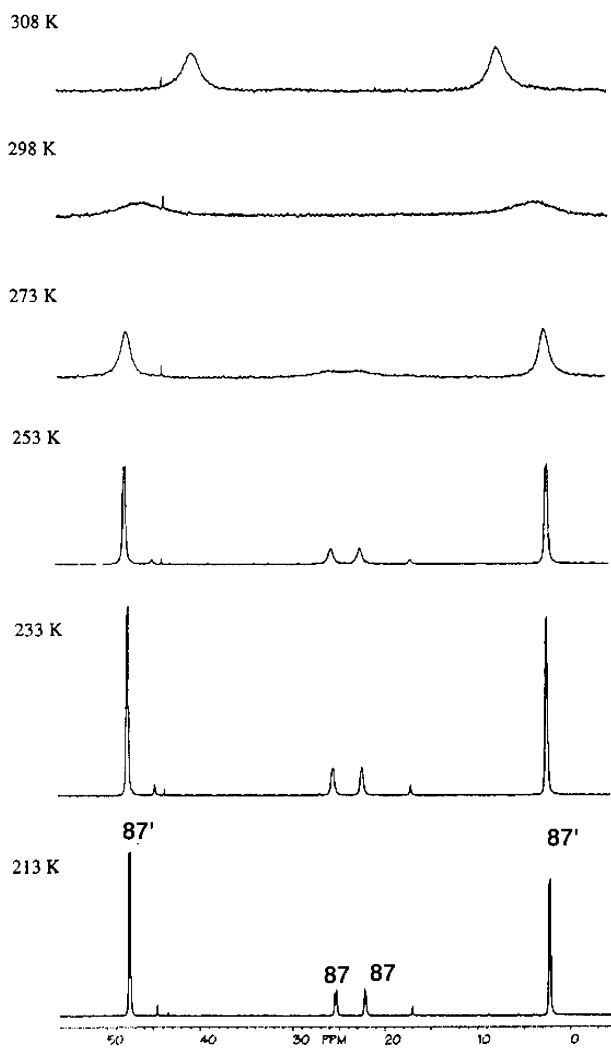


**Figure 45.** Variable-temperature  $^{31}\text{P}\{^1\text{H}\}$  NMR spectra of diastereomers **87** and **87'** (major)  $[cis-1,2-(\text{diphenylphosphinomethyl})\text{-cyclohexane}]\text{Pd}(\text{Me})\text{Cl}$ . Also see Figure 44.

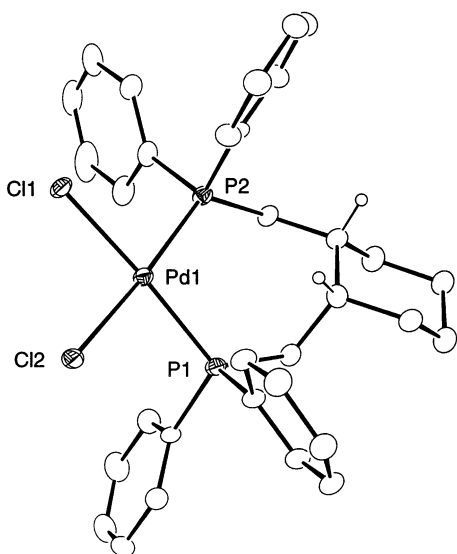
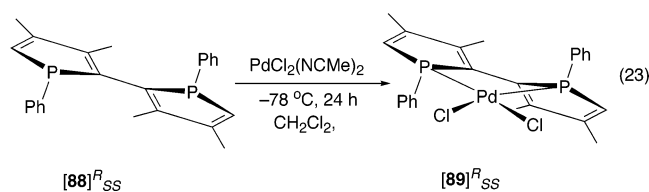


**Figure 46.** Solid-state structure of the  $[cis-1,2-(\text{diphenylphosphinomethyl})\text{-cyclohexane}]\text{Pd}(\text{Me})\text{Cl}$  complex (**87'**).

axial chirality in these compounds is denoted by a superscript and the configurations of the phosphorus atoms by subscripts. The chiral axis and the phos-

phorus centers of **88** invert readily, and interconversion of the stereoisomers is reported to occur at  $-60\text{ }^\circ\text{C}$ , albeit slowly. The inversion barrier of the pyramidal phosphorus centers was measured to be 16.5 kcal/mol.<sup>203</sup> The energy cost for pyramidal inversion in phospholes is reduced, relative to that in phosphines, as a result of the increase in aromatic character of the phosphole in the transition state.<sup>204</sup> The solution NMR spectra of the bis(phosphole) indicate that two diastereomers are present in a ratio of 88:12, and these have been identified as  $[\mathbf{88}]^{R_{SS}}$  and  $[\mathbf{88}]^{R_{SR}}$  (and their enantiomers).<sup>205</sup> BIPHOS **88** was found to crystallize as a conglomerate, meaning that only a single enantiomer of the ligand is present in each crystal.<sup>206</sup> Although the visual appearance of enantiomeric crystals of ligands are reported to be identical, large single crystals can be grown that weigh between 50 and 150 mg each, and these can be physically separated.

Analysis of the conformation of the BIPHOS ligand in Figure 47 suggests that only  $[\mathbf{88}]^{R_{SS}}$  and its enantiomer will bind to metals in a bidentate fashion. Complexes of  $(\pm)$ -BIPHOS with several metals have been characterized by X-ray crystallography.<sup>205</sup> These complexes are pseudo- $C_2$ -symmetric with the ligand stereochemistry of  $[\mathbf{88}]^{R_{SS}}$  and its enantiomer, as expected. The dihedral angles of the bis(phosphole) ligands bound to Ni, Pd, and Pt were 46.8, 50.6, and 53.8 $^\circ$ , respectively, which are similar to the dihedral angle of the free ligand in the solid state (46.6 $^\circ$ ).<sup>203,205</sup> A chiral, enantiopure palladium complex was synthesized by dissolving  $\text{Cl}_2\text{Pd}(\text{NCMe})_2$  and a single crystal of resolved  $[\mathbf{88}]^{R_{SS}}$  in dichloromethane at  $-78\text{ }^\circ\text{C}$ , at which temperature isomerization of BIPHOS is slow, to give  $[\mathbf{89}]^{S_{RR}}$  in 93% yield (eq 23). The



optical rotation of **89** was unchanged after 24 h at  $40\text{ }^\circ\text{C}$ , indicating that palladium locks the ligand in one of the skewed conformations. An X-ray diffraction study of  $[\mathbf{89}]^{S_{RR}}$  was performed, and an ORTEP diagram is shown in Figure 48.

The enantiopure palladium complex  $[\mathbf{89}]^{R_{SS}}$  was examined in the asymmetric allylic substitution reaction, as illustrated in eq 24.<sup>207</sup> Reaction of the classic test substrate, 1,3-diphenylprop-2-enyl acetate (**90**), with the sodium salt of dimethyl malonate proceeded efficiently at  $35\text{ }^\circ\text{C}$ , furnishing the diester product **91** in 84–93% yield with 80% ee. Switching enantiomers of the catalyst gave the opposite enantiomer of the product with the same enantioselectivity. Thus, use of the chiral bis(phosphole) ligand, after spontaneous resolution and complexation, proved to be as effective as use of well-known configurationally stable chiral ligands.<sup>208–211</sup>

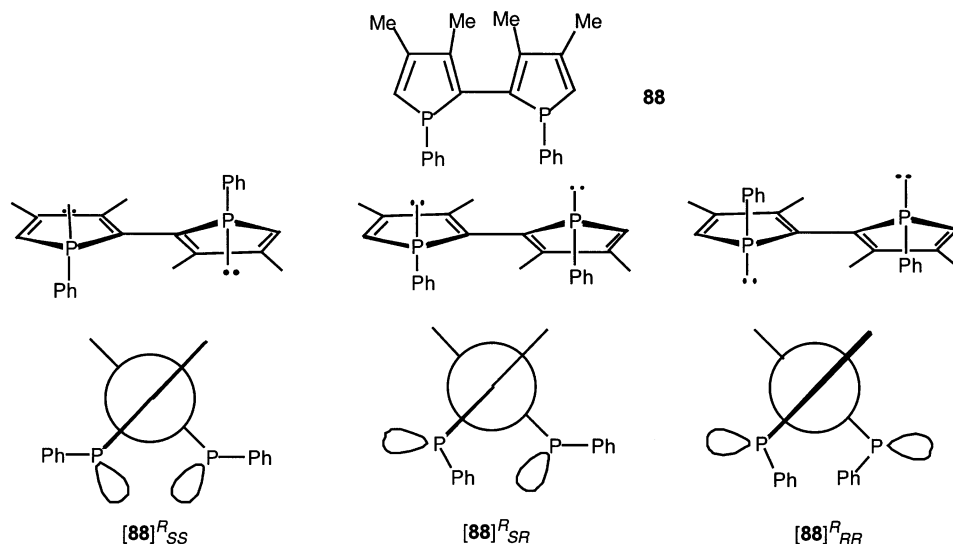


**Figure 47.** Isomers of **88**, with one enantiomer of each pair of bis(phosphole) ligands shown. A projection of each enantiomer along the axis of the C–C bis(phosphole) rings (below). The superscript denotes the axial chirality and the subscripts the configuration at phosphorus.

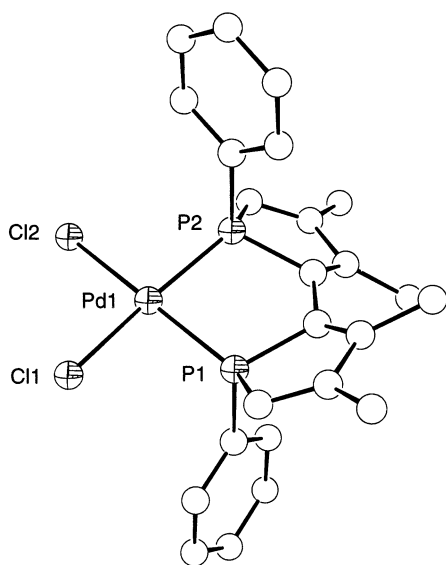
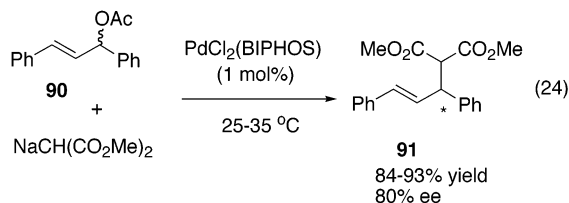


**Figure 48.** ORTEP drawing of  $[89]^{R_{SS}}$ , showing the pseudo- $C_2$  symmetry of the BIPHOS ligand.



#### 4.8. A Metallocene Catalyst with a Biphenyl Backbone

Various types of chiral metallocenes have been used successfully in asymmetric catalysis, with most of these compounds belonging to the *ansa*-metallocene class.<sup>212,213</sup> The majority of the *ansa*-metallocenes are planar-chiral with prochiral cyclopentadienyl rings, resulting from their substitution pattern, as exemplified by **92** (Figure 49). Racemic *ansa*-metallocenes are resolved using classical methods that employ the synthesis and separation of diaster-

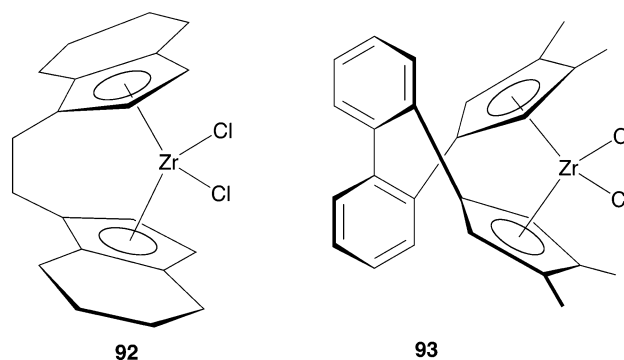


**Figure 49.** Chiral metallocene complexes.

eomeric derivatives. Other routes to resolved metallocene derivatives, such as through asymmetric synthesis, have generally proven to be difficult but have met with some success.<sup>214–217</sup> A new route to enantiopure metallocenes, based on a dynamic resolution, has recently been introduced by Brintzinger and co-workers.<sup>218</sup> Unlike the case with planar-chiral metallocenes, the chirality of these complexes resides solely in the biphenyl backbone of the bis(cyclopentadienyl) ligand system (Figure 49).<sup>217,219,220</sup>

Reaction of the racemic zirconium dimethyl derivative **94** (Figure 50) with (*R*)-BINOL yielded a diastereomeric mixture. Rather than the expected 1:1 ratio of diastereomers, a 2:1 ratio was formed, indicating that some interconversion of the diastereomers had taken place. Upon heating of the mixture of diastereomers at 100 °C for 2 days, equilibration proceeded to a single diastereomer in 99% yield (Figure 50).

Kinetic investigation into the mechanism of the interconversion revealed that it was first-order. The inversion of stereochemistry was accelerated by dioxygen gas or a catalytic amount of tetramethylpiperidine *N*-oxide (TEMPO). It is believed that the TEMPO facilitates cleavage of the Zr–cyclopentadienyl bond to give a radical intermediate that can rotate about the biphenyl bond and scramble the stereochemistry, as shown in Figure 51. Removal of

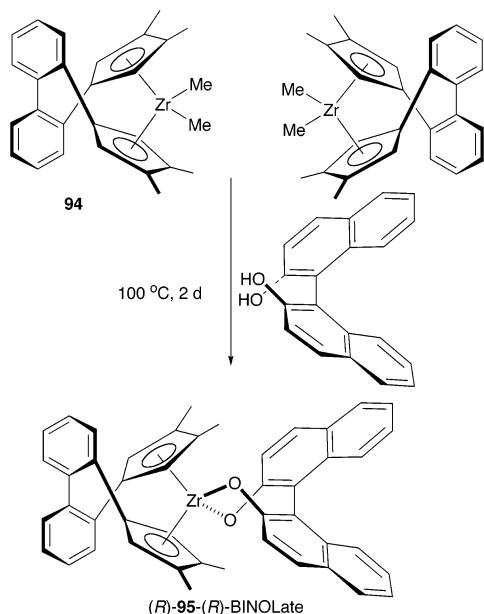


**Figure 50.** Resolution of *ansa*-metallocene **95**.

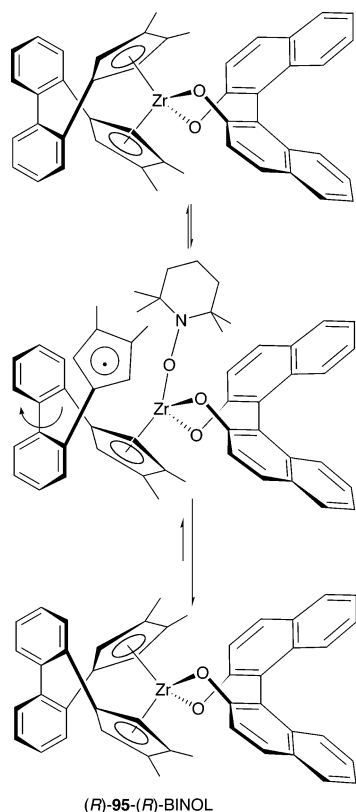


**Figure 51.** Mechanism of inversion of stereochemistry for *ansa*-metallocene **95**.

the BINOLate ligand from the zirconium complex **95** was accomplished by reaction with  $\text{AlMe}_3$  to give resolved **94**. The enantiopurity of the resolved dimethyl derivative **94** was determined to be 98% via its reaction with 2 equiv of (*R*)-1-phenyl-1-propanol to give the diastereomeric bis(alkoxide) complexes **96** (Figure 52).

Metalocene complexes have proven to be particularly efficient and enantioselective in the catalytic asymmetric hydrogenation of imines.<sup>221,222</sup> With this in mind, Brintzinger and co-workers tested their new

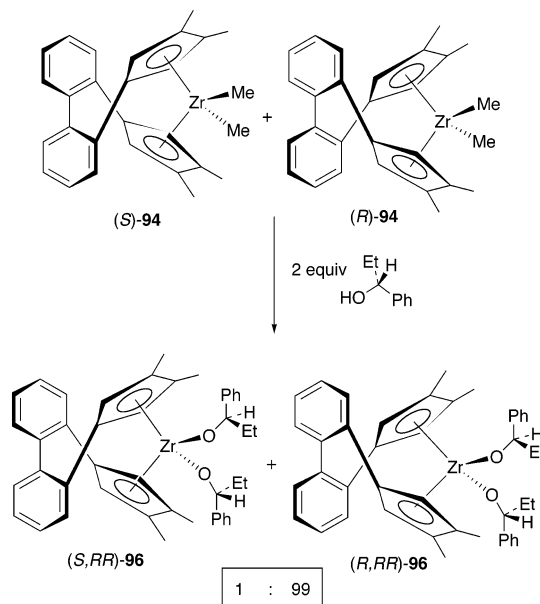


**Figure 52.** Formation of diastereomeric bis(alkoxide) complexes **96**.

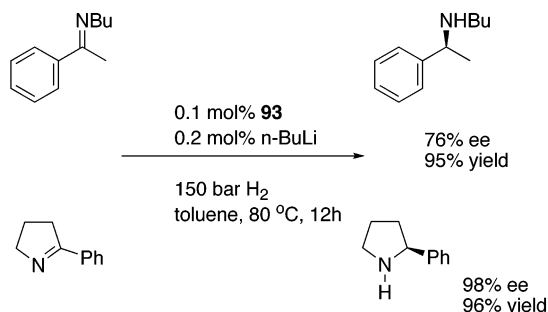


**Figure 53.** Asymmetric hydrogenation of imines with chiral metalocene derived from **93**.

*ansa*-metallocenes in this reaction. The catalyst was prepared from the dichloride **93** by reaction with 2 equiv of *n*-butyllithium. Imine hydrogenation was accomplished at 150 bar of  $\text{H}_2$  at 80 °C in toluene to provide good to excellent levels of enantioselectivity (Figure 53). The biphenyl *ansa*-metallocene catalyst could be used at catalyst loadings as low as 0.1 mol % in this process.<sup>218</sup>

#### 4.9. Use of Bis(diphenylphosphino)ferrocene and Related Ligands in Asymmetric Catalysis

Despite the great potential of the BIPHEP ligand in asymmetric catalysis, a serious drawback associated with this ligand system is the high barrier to atropisomerization when the ligand is chelated to metal centers. A consequence of this characteristic is that diastereomeric catalysts are formed, leading to unpredictable reactivity in catalytic asymmetric reactions.<sup>40</sup> Ligands with a lower barrier to interconversion in the metal–ligand adduct are, therefore, desirable. One such ligand is the commercially available bis(diphenylphosphino)ferrocene (DPPF, **97**, Scheme 3).<sup>167</sup> The X-ray structure of (DPPF)Pd-(DABN)<sup>2+</sup> is shown in Figure 54.<sup>42</sup> The cyclopentadienyl rings are staggered, with the torsional angles defined by the two P–C bonds of 34.86°, which is within the range commonly observed in metal complexes of the DPPF ligand.<sup>167</sup>

## Scheme 3. Conformations of DPPF Complexes

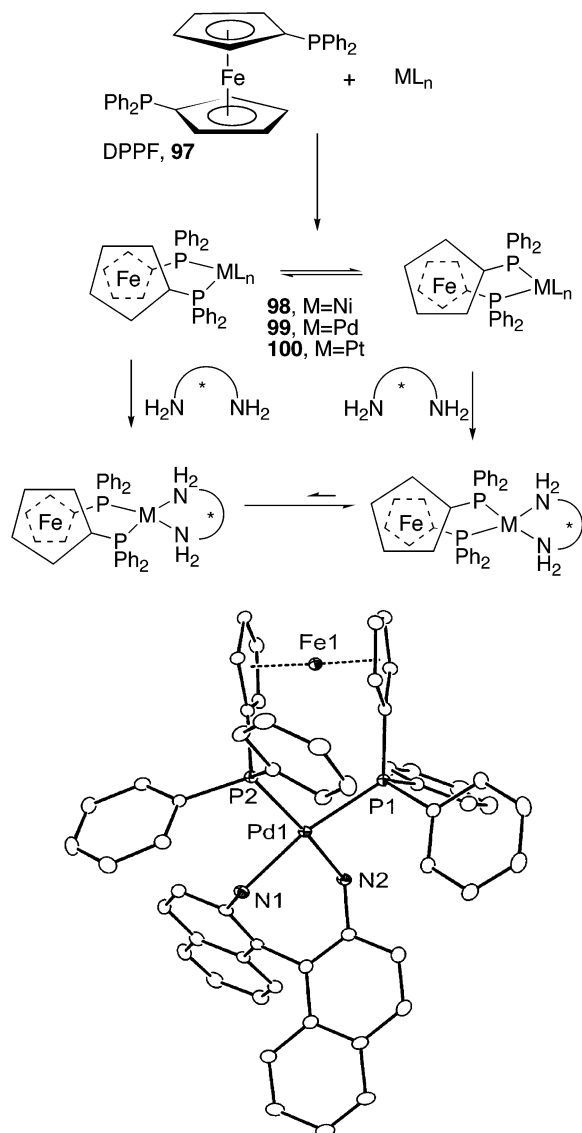
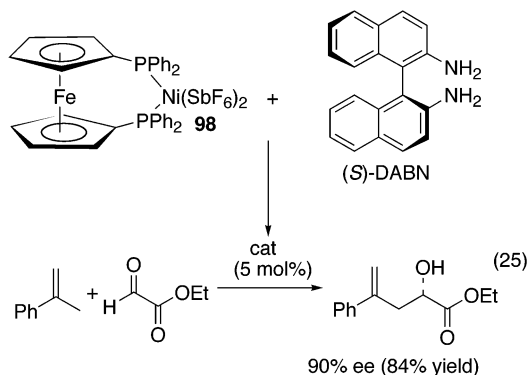


**Figure 54.** Structure of  $(\text{DPPF})\text{Pd}(\text{DABN})_2^{2+}$ .

It is known that the barrier to rotation of cyclopentadienyl groups in metallocene complexes is low when the cyclopentadienyl ligands are not substituted with bulky groups. Upon binding to metals, this ligand can adopt a conformation in which the cyclopentadienyl groups are staggered.<sup>223–226</sup> Mikami and Aikawa have used this property of the DPPF ligand to extend the chiral environment of Ni, Pd, and Pt catalysts in the asymmetric glyoxylate–ene reaction.<sup>42</sup>

Reactions of  $[(\text{DPPF})\text{M}(\text{NCMe})_2]^{2+}$  ( $\text{M} = \text{Ni}, \text{Pd}, \text{Pt}$ ) with DPEN (**52**), DM-DABN (**73**), and DABN were found to give a single diastereomer in each case, as depicted in Scheme 3. This observation indicates that the chiral ligands are effective at biasing the conformation of the ferrocene backbone and/or that inversion of the skewed conformations of the ferrocene backbone is rapid. Application of platinum and palladium complexes **99** and **100** (Scheme 3) in combination with DPEN, DABN, DM-DABN, and  $\text{H}_8$ -DABN in the asymmetric glyoxylate–ene reaction (eq 25) gave low enantioselectivities. In contrast, the nickel derivative **98** proved to be an excellent catalyst



for this process when combined with resolved DABN. The resulting catalyst gave 90% ee with  $\alpha$ -methylstyrene, as illustrated in eq 25. Comparison of the enantioselectivity of the (DPPF)Ni catalyst to related chelating bis(phosphines) in the reaction with methylene cyclohexane indicated that the catalyst derived from DPPF was the most enantioselective (Figure 55). It is tempting to hypothesize that the greater

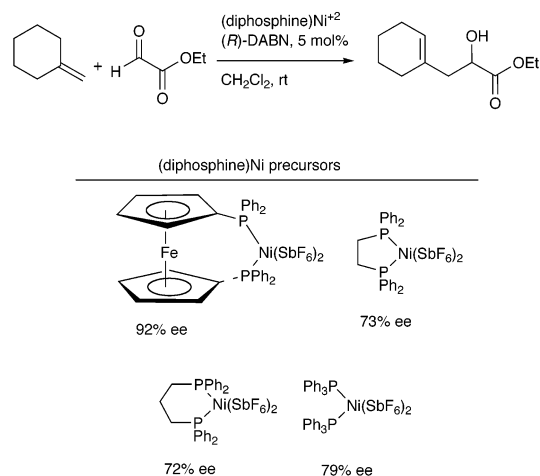


**Figure 55.** Effect of phosphine ligand on the enantioselectivity of Ni catalysts.

enantioselectivity of the (DPPF)Ni catalyst is due to the contribution of the chiral conformations of the DPPF ligand to the catalyst's chiral environment; however, other factors could be important. Nonetheless, this intriguing result warrants further investigation.

The bis(indenyl) analogue of bis(diphenylphosphino)ferrocene (DPPF) has recently been prepared and characterized.<sup>227</sup> This complex contains two planar-chiral units and, therefore, is formed as the rac and meso isomers. Many related planar-chiral ferrocene derivatives have been prepared for use in asymmetric catalysis.<sup>228</sup> This compound is unique in that, in the presence a donor solvent, such as THF, the initially formed mixture of rac and meso compounds undergoes isomerization to the rac derivative at room temperature (Figure 56).<sup>229</sup> The interconversion of the rac and meso compounds requires the iron center to migrate to the opposite face of the indenyl ligand. The activation parameters for isomerization of the meso derivative **102** to the rac compound **101** were determined to be  $\Delta H^\ddagger = 14$  kcal/mol and  $\Delta S^\ddagger = 35$  cal/molK. In THF, the rate was found to be  $1.59 \times$

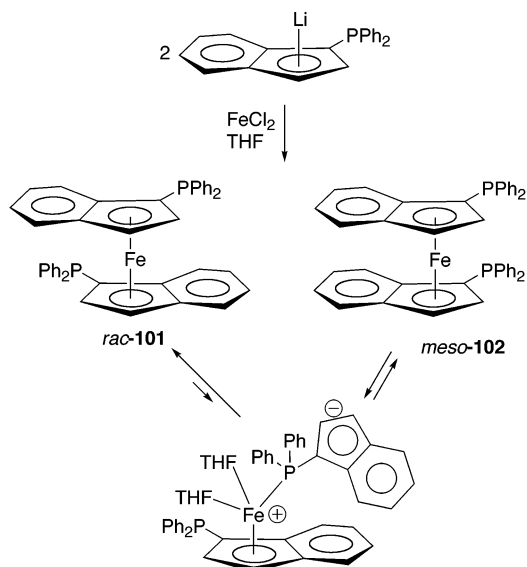


**Figure 56.** Synthesis and isomerization of bis(indenyl) analogue of DPPF.

$10^{-5}$ /s. This isomerization does not occur in chloroform. Both the *rac* and *meso* isomers can behave as chelating ligands, and complexes of both have been characterized structurally.<sup>227</sup> The structure of the *rac* ligand is shown bound to the  $\text{Mo}(\text{CO})_4$  group in Figure 57. The dynamic stereochemistry of these

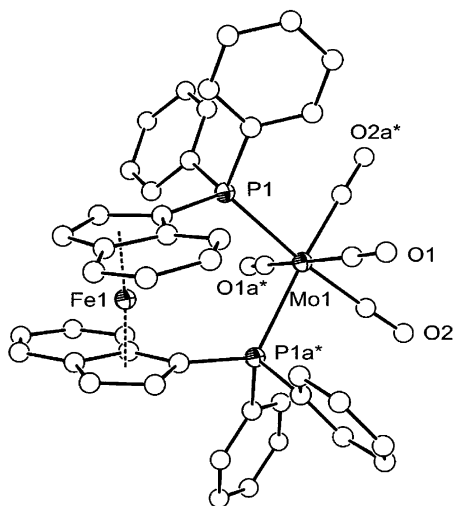


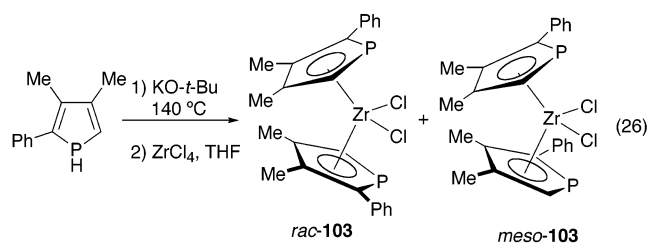
**Figure 57.** Structure of *rac*-**101** bound to the  $\text{Mo}(\text{CO})_4$  group.

complexes makes them potentially interesting in asymmetric catalysis.

#### 4.10. Dynamic Resolution of Bis(phospholyl)–Zr Complexes

Metallocene complexes in which both cyclopentadienyl rings are monosubstituted have chiral skewed conformations. When at least one cyclopentadienyl ring is disubstituted, the complex can be chiral, if the substituents on the cyclopentadienyl ring are inequivalent. Under these conditions, the compounds can, in principle, be resolved into the individual enantiomers. Such is the case with *ansa*-metallocene complexes, which have been extensively used in

asymmetric catalysis.<sup>212</sup> A less explored class of related catalysts that has recently attracted considerable interest is the heterometallocenes.<sup>230,231</sup> These compounds are prepared from readily available phospholes, as shown in eq 26. Reaction of the intermedi-

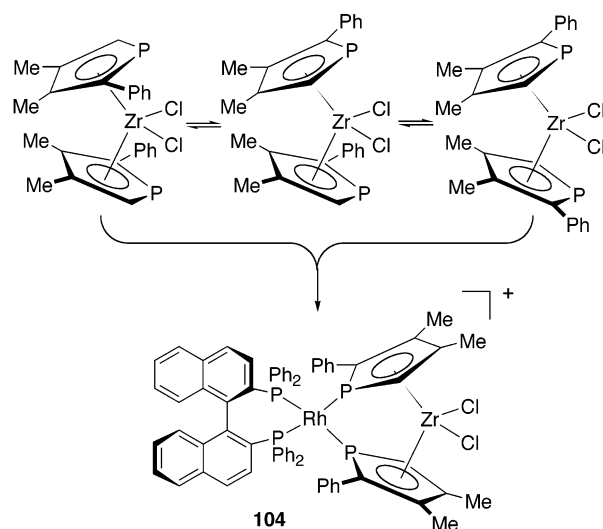


ate phospholide with  $\text{MCl}_4$  ( $\text{M} = \text{Zr}, \text{Hf}$ ) affords a mixture of the *rac*- and *meso*-bis(phospholyl)–metal complexes (**103**, eq 26). It has recently been shown that these diastereomers can readily interconvert, presumably through the intermediacy of a ring-slipped<sup>232</sup> intermediate.<sup>231,233</sup> In the case of the titanium analogue, the barrier to interconversion of the *rac* and *meso* metallocenes has been measured. The barrier was found to be  $\Delta G^\ddagger_{(298)} = 11.5$  kcal/mol, indicating that the isomerization takes place rapidly at room temperature. The equilibrium constant was determined to be 3.7 at  $-20$  °C, favoring the *rac* isomer.<sup>234</sup>

Bis(phospholyl)–metal complexes can behave as bidentate donors and chelate other metals.<sup>235,236</sup> A significant deterrent to the application of enantiopure bis(phospholyl) compounds as asymmetric ligands and catalysts is the resolution of these species. A novel approach to this challenging problem has been advanced by Hollis and co-workers<sup>233</sup> that takes advantage of the facile isomerization of the phospholyl group to accomplish a dynamic resolution of a bis(phospholyl) zirconium complex.

Reaction of the diastereomeric mixture of equilibrating bis(phospholyl)–zirconium complexes with  $[(R)\text{-BINAP}]\text{Rh}(\text{COD})\text{OTf}$ , as shown in Scheme 4, resulted in dynamic resolution of the bis(phospholyl)

#### Scheme 4. Dynamic Resolution of Bis(phospholyl)–Zr Complexes To Give a Single Diastereomer (104)



complex, as judged by the formation of a single diastereomer in the  $^{31}\text{P}$  NMR.

The solution NMR spectrum indicates that the complex is  $C_2$ -symmetric. To investigate the stereochemistry of the bis(phospholyl)–zirconium portion of the product, an X-ray crystallographic study was undertaken. The structure, illustrated in Figure 58,

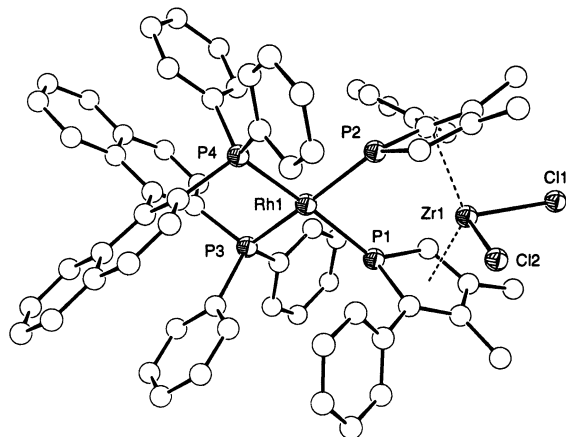


**Figure 58.** Structure of  $C_2$ -symmetric bis(phospholyl) complex **104**.

shows the phospholyl phenyl groups oriented away from the equatorial phenyl groups of the BINAP ligand.

In the Rh–Zr system of Hollis, either the rhodium or the zirconium could behave as the catalytically active metal center. Given the time-consuming synthesis of resolved *ansa*-metallocenes, this dynamic resolution process is very appealing and has significant potential.

## 5. Examination of the Barrier to Atropisomerization in Biphenyl-Based Diamines

### 5.1. 1,1'-Biphenyl-2,2'-diamine (DABP) Derivatives

Complexes of the diamine 1,1'-biphenyl-2,2'-diamine (DABP, **105**, Figure 59) and its derivatives

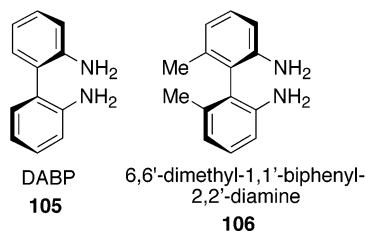


**Figure 59.** Structures of atropisomeric diamines.

have not yet, to our knowledge, been applied to asymmetric catalysis. Nonetheless, these atropisomeric ligands have attracted a significant amount of attention,<sup>237–248</sup> as they are the conformationally dynamic counterparts of the stereochemically fixed DABN and 6,6'-dimethyl-1,1'-biphenyl-2,2'-diamine (**106**, Figure 59), which have proven to be important chiral entities in asymmetric catalysis.<sup>3</sup> As such, we anticipate that DABP and its derivatives also have great potential in enantioselective catalysis.

In early reports with DABP, researchers claimed to have resolved all the diastereomers of the parent ligand bound to a chiral  $\text{Co}(\text{en})_2^{3+}$  group (en = ethylenediamine).<sup>237</sup> Subsequent reports, however, indicate that a single pair of enantiomers was observed, suggesting that the configuration of the DABP is dependent on the stereochemistry of the  $\text{Co}(\text{en})_2^{3+}$  center.<sup>242</sup> Supporting this idea is the fact that  $(\text{DABP})\text{Co}(\text{bipy})_2^{3+}$  was also obtained as a pair of enantiomers.<sup>242</sup> The platinum complex  $[(\text{DABP})\text{Pt}(\text{en})]^{2+}$  has been resolved and is stable to racemization at room temperature.<sup>238</sup> The high barrier to atropisomerization necessary for isolation of this complex is surprising, given that, in cases where DABP is bound to chiral metal–ligand combinations, only one diastereomer has been reported.<sup>242,244–246,248</sup>

The studies with DABP most relevant to this review have been done by Ashby and co-workers,<sup>247,248</sup> who recently showed that atropisomerization of bound DABP can be fast at room temperature. In the complex  $(\eta^6\text{-arene})\text{RuCl}(\text{DABP})^+$  (Figure 60), the half-

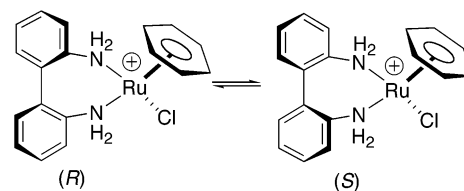


**Figure 60.** Atropisomerization of DABP bound to cationic ruthenium.

life of atropisomerization was about 250 ms at room temperature, as determined by spin-transfer NMR experiments.<sup>247</sup> On the basis of 2D-EXSY NMR spectroscopy,<sup>249</sup> it was found that the mechanism most consistent with the experimental data involves stereochemical inversion of the DABP ligand while chelated to the ruthenium center. The X-ray crystal structure of  $(\eta^6\text{-arene})\text{RuCl}(\text{DABP})^+$  was determined, and the dihedral angle between the aromatic rings in the DABP ligand was found to be  $60.4^\circ$  in the solid state. A similar dihedral angle was found in the structure of unbound DABP ( $59.8^\circ$ ) and was attributed to an intermolecular hydrogen bond.<sup>250</sup> The dihedral angles in complexes of DABP are similar to those found in the conformationally locked 6,6'-dimethyl-2,2'-diaminobiphenyl complexes.<sup>251</sup>

Octahedral compounds, such as  $\text{M}(\text{bipy})_3^{2+}$ , are chiral at the metal, as are  $\text{M}(\text{bipy})_2\text{L}_2$ , when the bipy ligands do not lie in the same plane.<sup>99</sup> Thus, in complexes of the type  $(\text{bipy})_2\text{Ru}(\text{DABP})^{2+}$ , two diastereomers are possible due to the chiral DABP skew conformations. Interestingly, only one diastereomer is observed in the solid state and in solution, suggesting that the chiral  $(\text{bipy})_2\text{Ru}^{2+}$  center effectively biases the configuration of the DABP ligand.<sup>248</sup> The structure of  $(\text{bipy})_2\text{Ru}(\text{DABP})^{2+}$  has also been determined, and the dihedral angle of the DABP ligand was found to be  $70^\circ$ .<sup>248</sup>

Efficient biasing of the DABP ligand was also observed in square planar systems. Reaction of *(trans*-1,2-diaminocyclohexane) $\text{PtCl}_2$  with DABP (Figure 61) was reported to give a single diastereomer (**107**), which was characterized crystallographical-

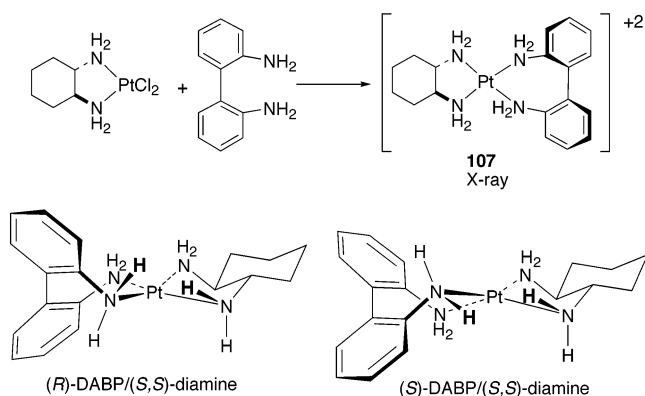


**Figure 61.** Reaction of (*S,S*)-diamine–platinum complex with DABP gave a single diastereomer (**107**) that was characterized crystallographically. In the (*R*)-DABP/(*S,S*)-diamine structure, there is a destabilizing interaction between the NH's of the diamines that is absent in the (*S*)-DABP/(*S,S*)-diamine diastereomer.

ly.<sup>245,246</sup> The diastereoselection is controlled by the interaction of the hydrogens on the diamine ligands. In the square planar platinum complex of (*S,S*)-*trans*-1,2-diaminocyclohexane with the (*S*)-DABP, the hydrogens on the opposing ligands are staggered. In the complex with (*S,S*)-*trans*-1,2-diaminocyclohexane and the (*R*)-DABP, however, eclipsing interactions between the N–H's of the ligands would have a destabilizing effect. The diastereomers are shown in Figure 61, with the hydrogens of interest in bold font. It is impressive that a seemingly subtle interaction can exhibit such a high degree of stereocontrol in complex **107**. Similar results were obtained with resolved 1,2-diaminopropane.<sup>245,246</sup>

As previously discussed, the DABN and DM-DPEN ligands have been shown to do an excellent job of biasing the conformation of the BIPHEP ligand in the complexes (BIPHEP)RuCl<sub>2</sub>(DM-DPEN) and [(BIPHEP)Pd(DABN)]<sup>2+</sup>.<sup>171,172</sup> Reversing the identity of the configurationally flexible and stereochemically fixed ligands, to give the currently unknown (BINAP)-RuCl<sub>2</sub>(DM-DABP) and [(BINAP)Pd(DABP)]<sup>2+</sup>, might lead to a strong thermodynamic preference for one diastereomer in each case. It would be interesting to compare the activity and enantioselectivity of these compounds to those of the analogues outlined above.

## 5.2. Atropisomeric Bisoquinolines and Bipyridines

Other potentially useful classes of stereochemically flexible ligands for asymmetric catalysis are bisoquinoline and 2,2'-bipyridyl derivatives that can bind to metals with skewed conformations. Racemization of bisoquinoline is rapid at room temperature and likely proceeds through the anti transition state (Figure 62). Coordination of the bisoquinoline ligand to a transition metal center favors atropisomerization by way of the syn transition state. In this situation, H8 and H8' must pass in close proximity to each other in the planar transition state.

Several complexes of the bisoquinoline ligand have now been synthesized and characterized by X-ray crystallography.<sup>252–257</sup> The crystal structure of one of these, in which the skewed conformation of the

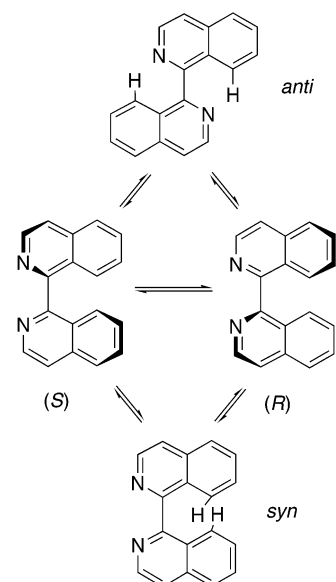


**Figure 62.** Isomerization of bisoquinoline system.

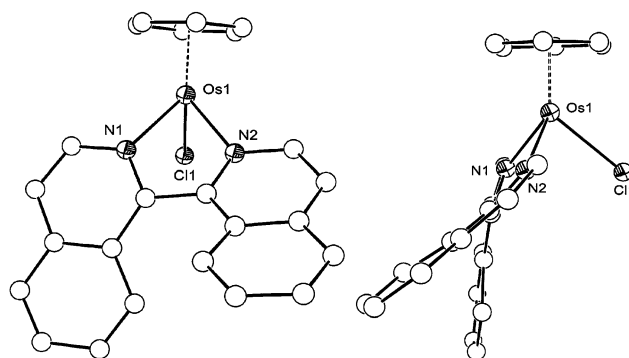


**Figure 63.** Two views of the structure of ( $\eta^6$ -arene)OsCl(bisoquinoline)<sup>+</sup> showing the chirality of the atropisomeric ligand.

bisoquinoline ligand can be seen, is shown in Figure 63. The dihedral angle is more acute than that found in complexes of BINOL and BINAP, with the N–C–C–N torsional angle of the bound bisoquinoline ligand ranging from 21 to 41°.

Complexes of the bisoquinoline ligand have been of considerable theoretical interest, and a number of detailed studies have been reported by Ashby regarding the mechanism of inversion of configuration of the bound ligand. In the ground state, the donor orbitals of the bisoquinoline nitrogens are “misdirected” with respect to the metal, meaning that they are not oriented directly toward the metal center.<sup>254,255</sup> These bonds have also been described as bent bonds, in analogy to the C–C bonds in cyclopropane.<sup>138</sup> In the planar transition state of atropisomerization in the bisoquinoline ligand, the N–C–C–N dihedral angle is 0°, and the nitrogen lone-pair orbitals are pointing directly toward the metal orbitals. The metal–nitrogen bonding is, therefore, strengthened in the transition state. Third-row metal compounds exhibit greater bond strengths compared to homologous second-row metal compounds. Therefore, the barrier to atropisomerization of the bisoquinoline is *decreased* in third-row metal complexes, relative to their second-row congeners, as

a result of the increased stabilization of the metal–ligand bonding in the transition state. The barriers to atropisomerization in biisoquinoline complexes have been determined to be below 20 kcal/mol and are dependent on the metal center and the nature of the ancillary ligands.<sup>256</sup> The biisoquinoline, therefore, undergoes stereochemical inversion rapidly at room temperature. This feature will decrease the likelihood of formation of diastereomeric catalysts resulting from a high kinetic barrier to diastereoisomerization, as found in the Noyori and Mikami system with BIPHEP.<sup>40</sup> An unknown factor with respect to use of the biisoquinoline ligand in combination with a chiral metal fragment is the extent to which it will contribute to the chiral environment of the catalyst, given the acute nature of the bound biisoquinoline torsional angle.

The 8,8'-dialkyl-1,1'-biisoquinolines (R = Me, Et, *i*-Pr, *t*-Bu) have been prepared and are known to racemize slowly at room temperature.<sup>258–260</sup> These ligands would be likely to have large dihedral angles, and chelation to metals may not be possible.

A more interesting class of substituted biisoquinoline ligands, from the perspective of asymmetric catalysis, is those bridged at the 7 and 7' positions, as shown in Figure 64.<sup>261</sup> The ease of racemization

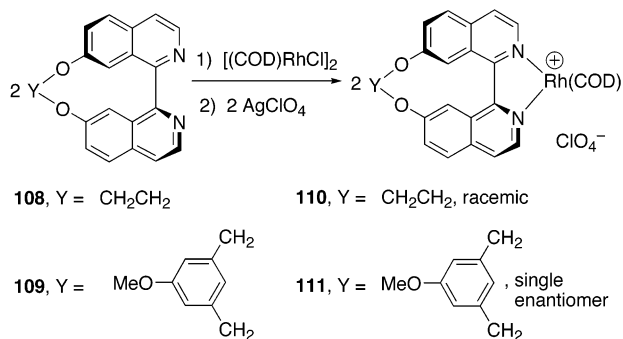


**Figure 64.** Reaction of 7,7'-bridged biisoquinoline ligands with [RhCl(COD)]<sub>2</sub>.

of these ligands is dependent on the nature of the bridge. With a simple ethylene linker (**108**), the half-life of racemization for the free ligand was 64 min at 78 °C ( $\Delta G^\ddagger = 26$  kcal/mol), while with the xylyl spacer (**109**), no racemization was observed at this temperature. Both ligands reacted when treated with [RhCl(COD)]<sub>2</sub> at room temperature followed by AgClO<sub>4</sub>. In the case of the ethylene-bridged derivative **108**, the adduct formed (**110**) was racemic. In contrast, the xylyl-bridged ligand **109** did not racemize on coordination. (Both complexes have been crystallographically characterized.<sup>261</sup>) Thus, coordination to rhodium dramatically decreases the barrier to atropisomerization in **108**, indicating that such compounds can readily serve as configurationally dynamic ligands in asymmetric catalysis.

Unlike the biisoquinoline ligands, most 2,2'-bipyridine ligands, and similar derivatives, form complexes in which the aromatic rings are coplanar, to maximize orbital overlap with the metal.<sup>262</sup> Despite the difficulty associated with the synthesis of enantiopure bipyridines, the use of such ligands in asymmetric catalysis has been reported.<sup>263–270</sup> The

asymmetry of these bipyridyl ligands is almost always due to stereogenic centers remote from the metal binding site;<sup>271,272</sup> however, some chiral bipyridine ligands with chiral axes have been reported.<sup>263,264,272–274</sup> Certain 3,3'-annulated 2,2'-bipyridines, biquinolines, and related derivatives,<sup>263,275–291</sup> as well as 3-substituted and 3,3'-disubstituted 2,2'-bipyridines,<sup>248,257,289,292–295</sup> have skewed conformations in the unbound and bound forms (Figure 65). The

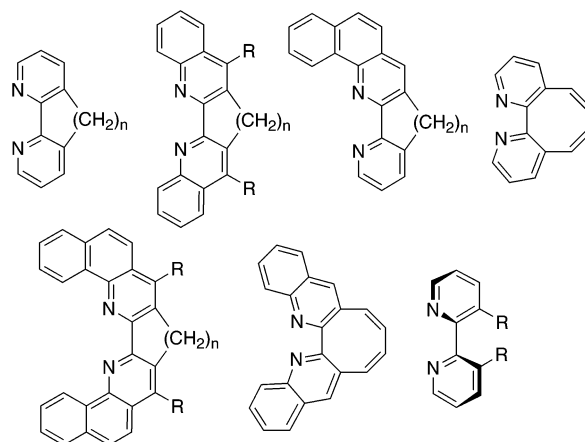


**Figure 65.** Structures of 3,3'-annulated 2,2'-bipyridines and derivatives with skewed conformations.

barrier to atropisomerization in the annulated derivatives is controlled by the length and substitution pattern of the tether. As shown in Figure 66, calcu-

n	N-C-C-N dihedral angle (°)	interconversion barrier (kcal/mol)
1	0	--
2	19	4.7
3	49	7.6
4	63	21.2

**Figure 66.** Dihedral angles and barriers to atropisomerization of 3,3'-annulated 2,2'-bipyridines.

lated N–C–C–N dihedral angles and barriers to atropisomerization vary considerably.<sup>296</sup> These estimates are in good agreement with experimentally determined values for related compounds.<sup>154,297–299</sup> The dihedral angles in the biquinoline derivatives are similar to those in the bipyridine ligands.<sup>277,289</sup> In the tetramethylene-bridged 2,2'-biquinoline<sup>277</sup> and 2,2'-bipyridine<sup>275</sup> compounds (Figure 65), the interconversion of the enantiomeric conformations is slow on the NMR time scale but sufficiently fast on the laboratory time scale to prevent resolution at room temperature. The large dihedral angle in the tetramethylene-bridged compounds minimizes eclipsing interactions between the hydrogens on the tether.

The ligands outlined in Figure 65 readily coordinate to transition metal complexes, and several complexes have been characterized by X-ray crystallography.<sup>263,278,280–282,285,287,289,290</sup> On coordination, these ligands retain their skewed conformations when the tether is three and four carbons long. In the X-ray crystal structures, a compression of the N–C–C–N dihedral angle is observed relative to that in the uncoordinated ligands. This results from opposing forces to minimize H–H eclipsing in the



tether and maximize the nitrogen lone-pair orbital overlap with the metal orbitals. It is also noteworthy that the C–C–C–C dihedral angle containing the biaryl axis is larger than the N–C–C–N dihedral angle. This is due to a distortion of the aromatic  $\pi$ -system originating from strain in the tethered ring. The difference between the C–C–C–C and N–C–C–N dihedral angles is greater in the coordinated ligand than in the free ligand.<sup>282</sup>

To highlight the potential of these atropisomeric ligands in asymmetric catalysis, some well-studied examples are discussed below. Elegant work has been reported in a series of studies by Rebek and co-workers regarding allosteric effects in organic chemistry.<sup>300</sup> In the bridged bipyridine ligand **112** (Figure 67), the *gem*-dimethyl groups are inequivalent in the

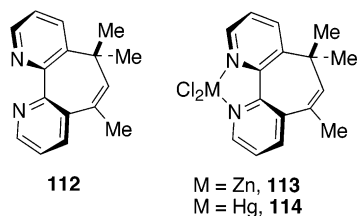


**Figure 67.** Bridged bipyridine ligand **112** and its metal complexes.

static structure but exchange on racemization. The *gem*-dimethyl groups appear as a broad singlet in the room-temperature <sup>1</sup>H NMR spectrum (90 MHz) and as two singlets at low temperature. From the coalescence temperature (2 °C), an atropisomerization barrier of 14.5 kcal/mol was calculated. Addition of ZnCl<sub>2</sub> or HgCl<sub>2</sub> to **112** to form **113** or **114**, respectively (Figure 67), resulted in a dramatic decrease in the barrier to atropisomerization to 10.5 kcal/mol. This represents a decrease in the barrier by about 4 kcal/mol or an increase in the rate of racemization by a factor of about 10<sup>3</sup> at room temperature.<sup>301</sup>

A more dramatic example of metal-accelerated racemization from the Rebek laboratories was demonstrated with a series of bipyridyl crown ethers (Figure 68). The barrier to racemization for com-

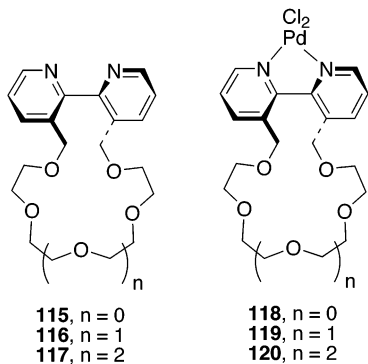


**Figure 68.** Rebek's bipyridyl crown ethers.

pounds **115**–**117** was calculated to be 25.7 kcal/mol by correlating variable-temperature <sup>1</sup>H NMR spectra between 50 and 227 °C with computer-simulated spectra. Upon addition of PdCl<sub>2</sub>, the resulting adducts **118**–**120** exhibited temperature-dependent behavior. At 50 °C, the benzylic protons were a singlet, while

at –50 °C, a coupled AB system was observed. Barriers to racemization of the palladium compounds were calculated from the coalescence temperatures to be between 13.9 and 14.6 kcal/mol. This decrease in  $\Delta G^\ddagger$  for racemization of at least 11 kcal/mol translates into a 10<sup>8</sup> increase in the rate of atropisomerization for the metal-bound ligand relative to the free ligand.

This remarkable increase in the rate of racemization is caused by several factors. The initial interaction of the ligand with palladium is weak, due to poor overlap of the nitrogen lone-pair orbitals with those of the metal. This hypothesis is supported by the ease of displacement of ligands **115**–**117** from palladium complexes **118**–**120** by *o*-phenanthroline and the ease of reaction of complexes **118**–**120** with a second equivalent of PdCl<sub>2</sub> to give the 2:1 complex (Figure 69).<sup>299,302</sup> Therefore, the increase in the Pd–N bond

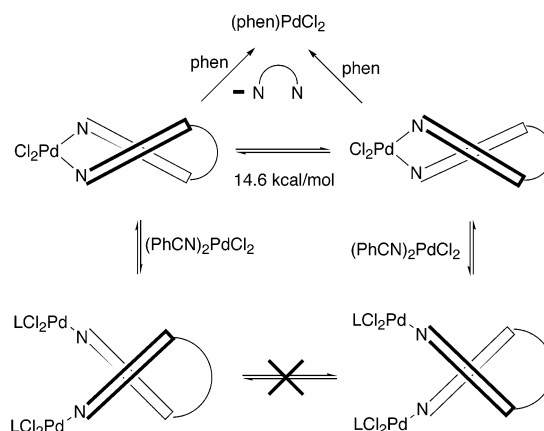


**Figure 69.** Reaction of compounds **118**–**120** with *o*-phenanthroline and additional palladium (L = NCPH).

strength in **118**–**120** on going from the ground state to the transition state, where the dihedral angle is 0°, is large. Additionally, it has been suggested that, in the process of racemization of biphenyl compounds, the 2 and 2' substituents must bend away from each other.<sup>303</sup> In the transition state, the metal may help the biphenyl nucleus undergo a slight in-plane distortion, such that the substituents are further separated and can more easily pass by each other.<sup>304,305</sup> An exaggerated illustration of this bending is shown in Figure 70.

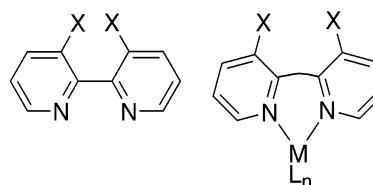


**Figure 70.** Exaggerated drawing showing how the in-plane bending can facilitate atropisomerization.

Crystallographic studies of one of the ligands and two of the complexes of the bipyridyl and biquinoline derivatives shown in Figure 71 have been reported.<sup>282</sup> The barrier to atropisomerization of the parent ligand **112** was determined to be 25 kcal/mol by CD spectroscopy of the resolved compound,<sup>284</sup> which is higher than that for analogues with saturated tethers.<sup>296</sup>

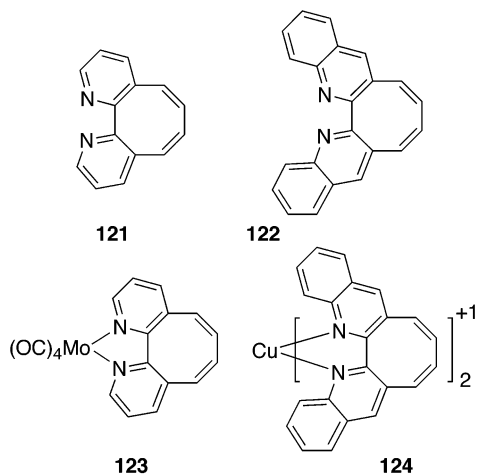


**Figure 71.** 3,3'-Annulated bipyridyl and biquinolyl ligands and their metal complexes.

Ligands **121** and **122** have been shown to form complexes with several metal centers, including Mo(0), W(0), Cu(I), Zn(II), Hg(II), and Pd(II).<sup>286</sup> Reaction of ligand **122** with copper(II) gave a reduced copper(I) complex,<sup>286</sup>  $\text{CuL}_2^+$  (**124**, Figure 71), while reaction of the bipyridine derivative **121** with  $\text{Mo}(\text{CO})_6$  gave the mono-ligated complex  $\text{LMo}(\text{CO})_4$  (**123**, Figure 71).<sup>263</sup> The unbound biquinoline ligand has N–C–C–N and C–C–C–C dihedral angles of 63° and 70°, respectively. In contrast, the N–C–C–N and C–C–C–C dihedral angles of the copper(I) complex were 38° and 53°, while those of the molybdenum complex were 31° and 53° respectively. The X-ray structure of ligand **121** bound to molybdenum is illustrated in Figure 72.<sup>282</sup>

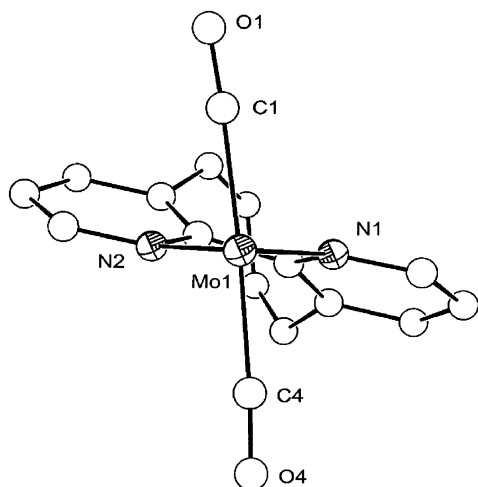


**Figure 72.** Structure of ligand **121** bound to the  $\text{Mo}(\text{CO})_4$  fragment. The two CO ligands trans to the nitrogens have been removed for clarity.

Although several excellent studies have been reported with the tetramethylene-bridged bipyridine and biquinoline derivatives, little quantitative data concerning the barriers to atropisomerization of the ligands or their complexes exists.<sup>272</sup> Nonetheless, circumstantial evidence suggests that atropisomerization occurs readily at room temperature. Reaction of a tetramethylene-bridged biquinoline ligand with  $\text{Pd}(\text{dba})_2$  and fumaronitrile gave a 57:43 mixture of

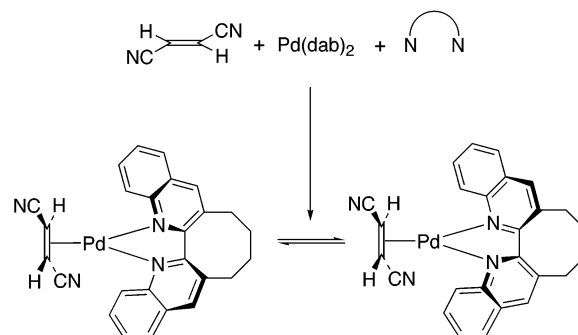


**Figure 73.** Equilibration of diastereomeric complexes via atropisomerization.

diastereomers (Figure 73). The diastereomers were recrystallized and the resulting crystals redissolved at 213 K. At this temperature, an 80:20 mixture of diastereomers was observed. Once the sample was warmed to room temperature, the mixture equilibrated to the 57:43 ratio. Magnetization-transfer experiments found an activation barrier to atropisomerization of 17.6 kcal/mol at 330 K.<sup>289</sup>

Indirect evidence for facial atropisomerization of tetramethylene-bridged bipyridine was also found upon reaction of racemic  $(\text{bipy})_2\text{RuCl}_2$  with **125** to give **126** (Figure 74).<sup>280</sup> Although two pairs of dia-

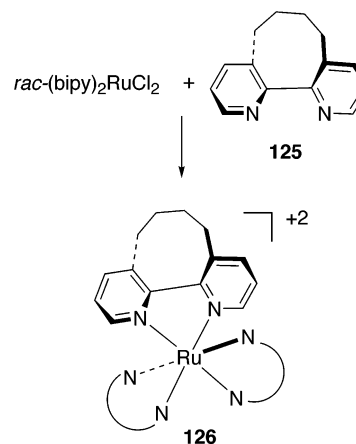


**Figure 74.** Reaction of  $(\text{bipy})_2\text{RuCl}_2$  with **125** affords a single diastereomer of the ligand adduct, **126**.

stereomers are possible, only one was observed. The diastereoselection in this reaction is thought to be thermodynamic, arising from equilibration of the possible diastereomers. It is also notable that the  $(\text{bipy})_2\text{Ru}^{2+}$  core effectively biases the skewed conformation of the ligand.

### 5.3. 2,2'-Bis(2-imidazole)biphenyl Ligands

Imidazole-based ligands are known to bind tightly to a number of metal centers in different oxidation states.<sup>306</sup> Combination of the imidazole binding ability with the axial chirality of the biphenyl backbone results in ligands having skewed conformations and low barriers to atropisomerization in the metal-bound state (Figure 75).<sup>307–309</sup> Such 2,2'-bis(2-imidazole)-biphenyl ligands, which were developed by Knapp, Schugar, and co-workers, are akin to the chiral bis-(oxazoline)biphenyl ligands, **129** and **130**, that have been successfully used in catalytic asymmetric cy-

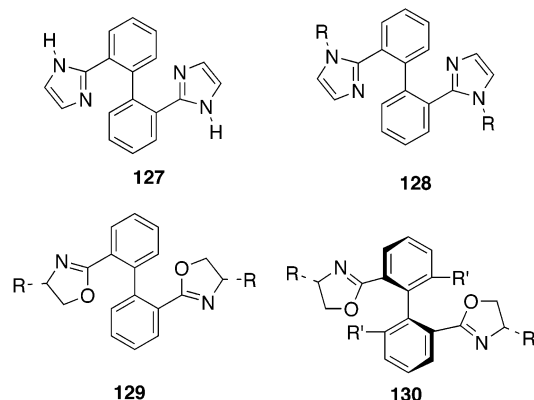


**Figure 75.** Structures of bis(2-imidazole) and bis(oxazoline) ligands.

clopropanation<sup>310</sup> and asymmetric Wacker-type reactions.<sup>311</sup> Both of these types of ligands form nine-membered metallocycles on coordination.<sup>311</sup> The bis(2-imidazole)biphenyl ligand **127** forms  $C_2$ -symmetric  $ML_2$  adducts with Co(II), Ni(II), Cu(I), Cu(II), and Zn(II), which have been characterized by X-ray crystallography.<sup>307,309</sup> The structure of one of these  $L_2M$  derivatives (**131**) is shown in Figure 76. Both classes

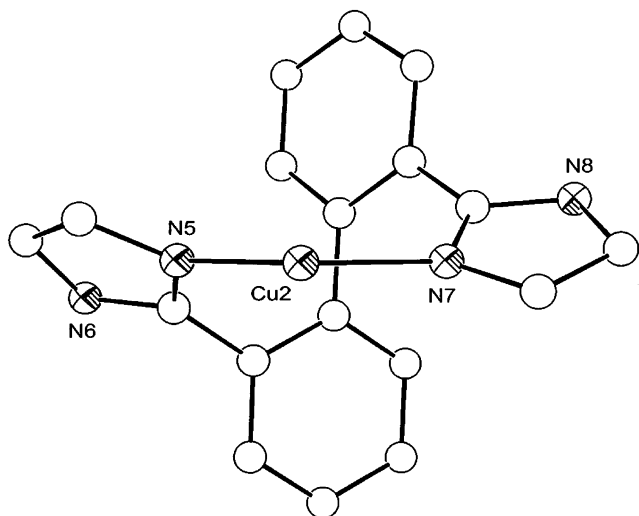


**Figure 76.** Structure of bis(2-imidazole)biphenyl  $ML_2^+$  complex (**131**) illustrating the asymmetry in the chelating ligand. One of the ligands has been removed for clarity.

of the related biphenyl bis(oxazoline) ligands, those with stereochemically fixed chiral axes<sup>311–313</sup> (**130**, Figure 75) and those with stereochemically dynamic axes having only two ortho substituents (**129**, Figure 75),<sup>310,314</sup> have been reported. The advantage of the stereochemically dynamic derivatives is that the biphenyl backbone does not need to be resolved (nor can it be resolved at room temperature). The drawback is that, in some cases, the coordination of such ligands to achiral metal centers gives rise to diastereomeric complexes with different configurations about the chiral axis.<sup>310</sup> The biphenyl bis(2-imidazole) ligands **127** and **128** cannot be resolved and can form only enantiomeric complexes on binding to an achiral metal center. These ligands can also be easily modified. The *N,N*-dimethyl analogue **128** ( $R = \text{Me}$ ) was readily prepared in 87% yield from **127**. Modification

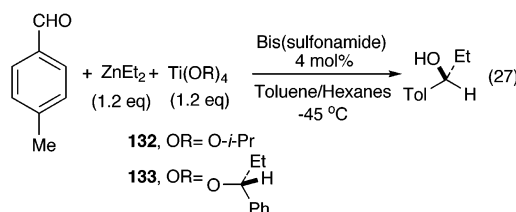
of the imidazole ring has also been accomplished by a directed ortho-lithiation/electrophile quench sequence.<sup>315</sup> Given the attributes of the biphenyl bis(2-imidazole) ligands, we believe that they merit investigation in catalytic asymmetric reactions.

## 6. Catalyst Optimization with Achiral and Meso Ligands Having Chiral Conformations

### 6.1. Achiral and Meso Bis(sulfonamide) Ligands with Chiral Titanium Alkoxides

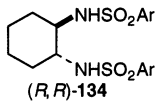
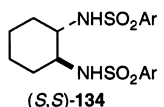
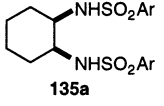
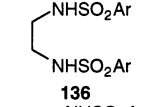
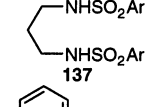
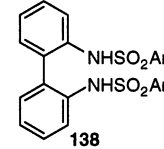
The use of achiral and meso ligands with chiral conformations to extend the chiral environment of asymmetric catalysts was illustrated by the impressive initial results of Katsuki<sup>39</sup> and Noyori and Mikami.<sup>40</sup> The stage was then set for an important advance in this area, namely the demonstration that asymmetric catalysts could be optimized through the synthesis and screening of *achiral and meso ligands with chiral conformations*, rather than by screening enantiopure ligands. Katsuki's early efforts in this direction, using achiral salen ligands with a wide variety of enantioenriched ligands, were not conclusive due to low enantioselectivities, low yields, or both.<sup>122,123</sup>

The first demonstration that large, conformationally flexible achiral and meso ligands could be used in the optimization of asymmetric catalysts was reported by Balsells and Walsh,<sup>44</sup> using the asymmetric addition of alkyl groups to aldehydes as a test system. This reaction, which employs dialkylzinc reagents as the source of alkyl groups, a stoichiometric amount of titanium tetraisopropoxide, and a catalytic quantity of a bis(sulfonamide) ligand (eq 27), was introduced by Takahashi and co-workers,<sup>78,79</sup> and the scope was expanded by the Knochel group.<sup>316,317</sup> It is believed to involve the intermediacy of bis(sulfonamido)Ti(*O-i*-Pr)<sub>2</sub> complexes,<sup>78,79,81</sup> which were subsequently synthesized and characterized by X-ray diffraction.<sup>82</sup> These complexes were also determined to be competent catalysts for the asymmetric reaction.



Initially, a series of experiments was performed to determine the effect of varying the alkoxide ligands on the enantioselectivity of the catalyst. For these reactions, resolved *trans*-bis(sulfonamide) ligands that gave catalysts of moderate enantioselectivity (Table 9, entries 1–3) were employed so that it could be determined if perturbations to the system resulted in an increase or decrease in the enantioselectivity of the catalyst. Use of ligand (*R,R*)-**134** in eq 27 with titanium tetraisopropoxide (**132**) and 4-methylbenzaldehyde provided the corresponding secondary alcohol with 79% ee. Substitution of the chiral alkoxide complex Ti(OR\*)<sub>4</sub> (**133**) (prepared with (*S*)-1-phenyl-1-propanol of >98% ee) for titanium tetra-

**Table 9. Results of Screening Bis(sulfonamide) Ligands in Eq 27<sup>a</sup>**

entry	Ti(OR) <sub>4</sub> R=	ligand	SO <sub>2</sub> Ar Ar=	ee (config)
1	- <i>i</i> -Pr	 ( <i>R,R</i> )- <b>134</b>	2,4-C <sub>6</sub> H <sub>3</sub> -Me <sub>2</sub>	79 ( <i>S</i> )
2	( <i>S</i> )-CHPhEt	( <i>R,R</i> )- <b>134</b>	2,4-C <sub>6</sub> H <sub>3</sub> -Me <sub>2</sub>	84 ( <i>S</i> )
3	( <i>S</i> )-CHPhEt	 ( <i>S,S</i> )- <b>134</b>	2,4-C <sub>6</sub> H <sub>3</sub> -Me <sub>2</sub>	81 ( <i>R</i> )
4	( <i>S</i> )-CHPhEt	 <b>135a</b>	4-C <sub>6</sub> H <sub>4</sub> -CMe <sub>3</sub>	84 ( <i>R</i> )
5	( <i>S</i> )-CHPhEt	<b>135b</b>	4-C <sub>6</sub> H <sub>4</sub> -OMe	78 ( <i>R</i> )
6	( <i>S</i> )-CHPhEt	<b>135c</b> (4 mol%)	2,4-C <sub>6</sub> H <sub>3</sub> -Me <sub>2</sub>	4 ( <i>S</i> )
7	( <i>S</i> )-CHPhEt	<b>135c</b> (10 mol%)	2,4-C <sub>6</sub> H <sub>3</sub> -Me <sub>2</sub>	32 ( <i>R</i> )
8	( <i>S</i> )-CHPhEt	<b>135d</b>	1-Naphthyl	20 ( <i>S</i> )
9	( <i>S</i> )-CHPhEt	<b>135e</b>	2,4,6-C <sub>6</sub> H <sub>3</sub> -Me <sub>3</sub>	37 ( <i>S</i> )
10	( <i>S</i> )-CHPhEt	 <b>136</b>	4-C <sub>6</sub> H <sub>4</sub> -CMe <sub>3</sub>	22 ( <i>R</i> )
11	( <i>S</i> )-CHPhEt	 <b>137</b>	4-C <sub>6</sub> H <sub>4</sub> -CMe <sub>3</sub>	2 ( <i>R</i> )
12	( <i>S</i> )-CHPhEt	 <b>138</b>	4-C <sub>6</sub> H <sub>4</sub> -CMe <sub>3</sub>	19 ( <i>R</i> )

<sup>a</sup> 4 mol % ligand was used, unless noted.

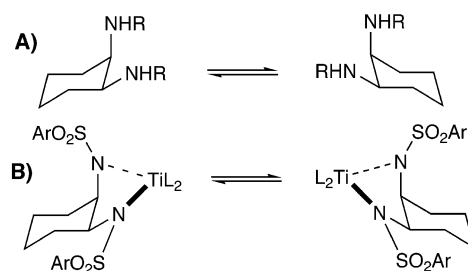
isopropoxide in this reaction led to a slight increase in the enantioselectivity of the catalyst (84% ee, Table 9, entry 2). When the experiment was conducted with the same configuration of the chiral alkoxide complex and the opposite enantiomer of the chiral ligand, (*S,S*)-**134**, the product was generated with an ee of 81%, but the opposite enantiomer of the product predominated. This result demonstrates that it is the *trans*-bis(sulfonamide) that controls the transmission of asymmetry from the catalyst to the substrate. Given that the magnitudes of the enantioselectivities of the diastereomeric catalysts formed from the chiral alkoxide complex (*S*)-Ti(OR\*)<sub>4</sub> and ligands (*R,R*)-**134** and (*S,S*)-**134** are so similar, it is clear that the influence of the chiral alkoxides on the transfer of asymmetry is insignificant.

The asymmetric addition reaction in eq 27 is an example of ligand-accelerated catalysis,<sup>318</sup> which has important implications for the interpretation of the results that follow. The asymmetric addition of alkyl groups to aldehydes, like many other reactions in asymmetric catalysis, has a background reaction,<sup>60</sup> which is a reaction that takes place in the presence of the catalyst, but without its participation. A series of experiments was conducted to examine the background rate in this process. At -45 °C, in the absence of both the titanium alkoxide complexes and the bis(sulfonamide) ligands, the reaction of diethylzinc with

aldehydes is extremely slow. In the presence of the Lewis acidic titanium alkoxides, however, the rate increases such that, in the absence of the bis(sulfonamide) ligand, titanium tetraisopropoxide promotes ethyl addition to aldehydes to give the racemic alcohol product, and the chiral alkoxide complex (*S*)-**133** produces product with an ee of 42% (*S*). In this case, the reaction was 12% complete after 1 h at -45 °C. Thus, for catalysts with low TOF, the background reaction can have a significant impact on the product ee.

A series of achiral and meso bis(sulfonamide) ligands (4 mol %) were then examined in the asymmetric addition reaction with chiral alkoxide complex (*S*)-**133**. When the reaction was conducted with bis(sulfonamide) ligands derived from *cis*-1,2-diaminocyclohexane, the product ee was dependent on the size of the aryl substituent on the sulfur. When Ar was 4-*tert*-butylbenzene (**135a**) or 4-methoxybenzene (**135b**), the (*R*)-configuration of the product alcohol was obtained in 84 and 78% ee, respectively. Thus, by addition of the meso bis(sulfonamide) ligand **135a**, a change in the product ee of 120% was observed with respect to the background reaction [42% ee of the (*S*)-enantiomer]. It was found that increasing the size of the aryl substituents on the ligand sulfonyl groups resulted in a decrease in the enantioselectivity of the catalysts (Table 9, entries 6–9). Use of other diamine backbones also resulted in decreases in the enantioselectivity of the catalyst (Table 9, entries 10–12). It is not clear whether ligands that form catalysts that generate product of low ee are not very enantioselective or if they catalyze the reaction at rates similar to that of the background reaction.

In the chair structures of *meso*-diaminocyclohexane, the static conformations are enantiomers which interconvert readily through ring inversion (Scheme 5). Coordination of bis(sulfonamide) ligands based on

**Scheme 5<sup>a</sup>**

<sup>a</sup> (A) The enantiomers of *cis*-1,2-diaminocyclohexane interconvert through ring inversion. (B) Likewise, when L is achiral, the two enantiomers interconvert in a similar fashion; however, if L is chiral, the two structures are diastereomeric and have different energies. (Sulfonyl coordination not shown.)

this meso diamine backbone to a metal center bearing a chiral ligand or ligands renders the two chair conformations diastereomeric. Additionally, once the *cis*-bis(sulfonamide) ligand is bound to titanium, the sulfonyl oxygens become inequivalent. It has been shown, in the case of the *trans*-bis(sulfonamide) ligands, that the sulfonyl oxygens coordinate to titanium in the bis(sulfonamido)Ti(O-*i*-Pr)<sub>2</sub> complexes in the solid state (Figure 9).<sup>82</sup> Additionally, solution reactivity studies indicate that the *trans* disposition

of the sulfur-bound aryl groups is important in the transition state for the asymmetric addition reaction.<sup>319</sup> Further studies are necessary to determine if coordination of the sulfonyl oxygens is germane with the *cis*-bis(sulfonamido)Ti complexes.

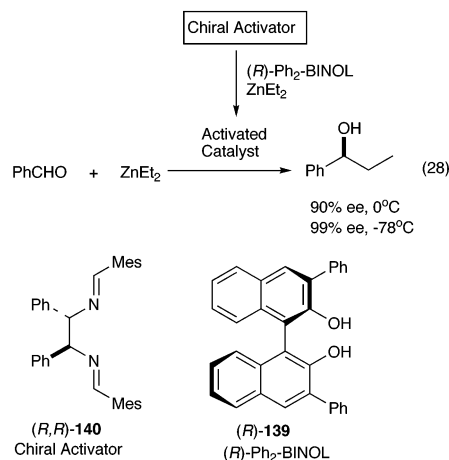
This report clearly demonstrates that asymmetric catalysts can be optimized by modification of achiral and meso ligands with chiral conformations. As exemplified by the results in Table 9, a single chiral alkoxide ligand can be used to generate a series of catalysts. It is easy to envision how this concept could be applied to high-throughput screening methods with a series of chiral ligands and a variety of achiral and meso ligands. It is also impressive that the chiral alkoxide, derived from 1-phenyl-1-propanol, which has not previously been found useful in asymmetric catalysis, can effectively bias the conformation of the meso bis(sulfonamide) ligand such that it preferentially adopts a chiral conformation and efficiently transmits the stereochemical information to a substrate.

Although this report represents a milestone in the use of achiral ligands in asymmetric catalysis, the system is not ideal in that the chiral alkoxide complex is used stoichiometrically, and the reaction mechanism is complicated by an alkoxide-exchange process.<sup>320</sup> The alkoxide ligands of the chiral titanium alkoxide complex used in this study are almost identical to the alkoxide produced in the asymmetric addition of an ethyl group to the substrate, 4-methylbenzaldehyde. This choice of alkoxide ligands was made in order to minimize the impact of an autoinduction process, that is, the evolution of the catalyst by incorporation of the product alkoxide.<sup>321–323</sup> As has previously been demonstrated, alkoxide-exchange reactions in bis(sulfonamido)titanium complexes are facile.<sup>324</sup> To reduce the additional complexities that arise when the alkoxide product becomes incorporated into the catalyst, enantioselectivities were determined by sampling reactions at low conversion.

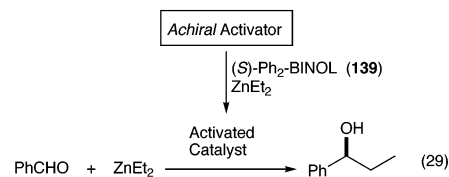
## 6.2. Achiral and Meso Diamine and Diimine Ligands with Zinc(BINOLate)

The next generation of reactions used to illustrate the power of catalyst optimization with achiral and meso ligands employed catalytic quantities of all ligands and was not complicated by an alkoxide-exchange process. This detailed investigation by the Walsh group<sup>46</sup> was based on an intriguing report by Mikami and co-workers in a study of the "chiral activation" strategy<sup>43</sup> in the asymmetric addition of alkyl groups to aldehydes using a zinc-based catalyst.<sup>29,325</sup> Mikami and co-workers found that the catalyst generated from 3,3'-diphenyl BINOL ( $\text{Ph}_2\text{-BINOL}$ , **139**, eq 28) and diethylzinc was slow and exhibited low enantioselectivity. In contrast, when this same catalyst was treated with an enantiopure diimine ligand, the new activated catalyst exhibited a high degree of ligand acceleration.<sup>318</sup> The researchers then optimized the catalyst enantioselectivity by varying the enantiopure diimine ligand. They found that the optimal diimine ligand for this reaction was a stilbene diamine derivative, **140** (eq 28), which, in combination with  $\text{Ph}_2\text{-BINOL}$ , generated a catalyst

that produced 1-phenyl-1-propanol in 90% ee at 0 °C and 99% ee at -78 °C. Mikami's catalyst optimization process illustrates the strength of the chiral activation strategy to maximize catalyst efficiency and enantioselectivity by generation of many catalysts in a modular fashion. A disadvantage of this method is that it requires two enantiopure ligands for each catalyst, and therefore, more effort is needed in the synthesis and resolution of the ligands.



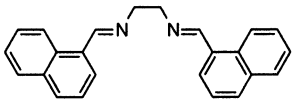
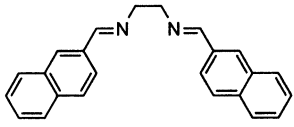
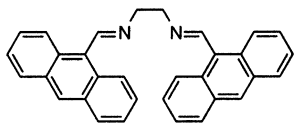
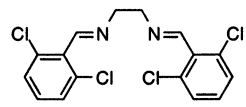
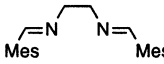
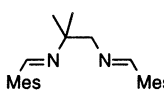
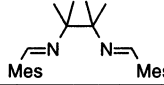
A more advanced strategy than chiral activation would be *achiral* activation (eq 29), whereby an achiral or meso ligand with chiral conformations would be added to a metal complex bearing an enantiopure ligand. This approach to catalyst optimization would be more efficient, because many catalysts could be generated from each enantiopure ligand through combination with a series of achiral and meso ligands. Since many more achiral and meso ligands and ligand precursors are commercially available than their enantiopure counterparts, catalysts with a wider variety of shapes can be synthesized. Furthermore, the cost of achiral and meso compounds is typically a small fraction of the cost of related enantiopure compounds.



**Achiral and Meso Ligand Categories.** The ligands that were examined in these studies were classified as follows: (1) achiral diimine ligands that do not generate additional chirality on binding to tetrahedral metals, (2) diimine ligands with meso backbones that have chiral conformations, (3) achiral diimine ligands with backbones that become axially chiral on coordination to metal centers, (4) achiral diamine ligands that do not form stereocenters on coordination to metal centers, (5) achiral diamine ligands that form stereocenters on coordination to metal centers, and (6) achiral diamine ligands with pendant groups that have axially chiral conformations.

**Reactions with Only  $\text{Ph}_2\text{-BINOL}$ .** Under typical reaction conditions, using 10 mol % (*S*)- $\text{Ph}_2\text{-BINOL}$

**Table 10. Results of Screening Achiral Diimine Activators 141a–g with (*S*)-Ph<sub>2</sub>-BINOL (139) in Eq 29<sup>a</sup>**

entry	ligand	ee at 0°C (config)	ee at -45°C (config)
1	No achiral activator	44 ( <i>S</i> )	--
2	<b>141a</b> 	52 ( <i>S</i> )	--
3	<b>141b</b> 	49 ( <i>S</i> )	--
4	<b>141c</b> 	30 ( <i>R</i> )	--
5	<b>141d</b> 	66 ( <i>R</i> )	74 ( <i>R</i> )
6	<b>141e</b> 	75 ( <i>R</i> )	87 ( <i>R</i> )
7	<b>141f</b> 	76 ( <i>R</i> )	78 ( <i>R</i> )
8	<b>141g</b> 	74 ( <i>R</i> )	77 ( <i>R</i> )

<sup>a</sup> Reaction employed 10 mol % Ph<sub>2</sub>-BINOL, 10 mol % diimine ligand, and 300 mol % diethylzinc.

and no additional ligands, benzaldehyde was slowly converted to (*S*)-1-phenyl-1-propanol of 44% ee (eq 29, Table 10, entry 1). After 28 h, the reaction was only 83% complete. Throughout this study, both the Ph<sub>2</sub>-BINOL and achiral or meso ligands were used at 10 mol % loading, and 3 equiv of diethylzinc was employed with respect to substrate.

### 6.2.1. Simple Achiral Diimine Ligands

Mikami and co-workers had successfully used enantiopure diimine ligands in their optimization of the (Ph<sub>2</sub>-BINOLate)Zn catalysts (eq 28). Therefore, achiral diimines prepared from commercially available diamines and aromatic aldehydes were a logical starting point. In screening these simple diimine ligands with a single chiral ligand, product ee's spanning almost 140% were recorded [52% ee (*S*) with **141a** to 87% ee (*R*) with **141e**, Table 10]. As seen in Table 10, ligands derived from 1,2-diaminoethane and less bulky aldehydes gave catalysts that exhibited moderate enantioselectivities, with the (*S*)-enantiomer of the product predominating (entries 2 and 3). Surprisingly, with ligands prepared from larger aromatic aldehydes, the opposite enantiomer of the product formed with moderate to good enantioselectivity (Table 10, entries 4–6). Diimines derived from 2,4,6-trimethylbenzaldehyde gave catalysts with enantioselectivities of 74–76% at 0 °C and as high as 87% at -45 °C (entries 6–8). As detailed

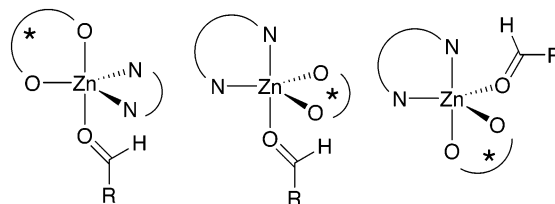


**Figure 77.** Diastereomeric coordination geometries of (Ph<sub>2</sub>-BINOLate)Zn(diimine) bonded to the substrate aldehyde.

in later sections, simple achiral ligands can bind in an asymmetric fashion in certain metal geometries.<sup>45,99</sup> Figure 77 illustrates three possible diastereomeric trigonal bipyramidal compounds in which the coordination sites occupied by the aldehyde and ligands are different. One explanation for the wide variation in product ee's is that the disposition of the ligands and substrate about the zinc center is strongly dependent on the sterics and bite angle of the achiral diimine ligand. These results underscore the significant impact that simple achiral ligands can exert on the enantioselectivity of asymmetric catalysis.

### 6.2.2. Diimine Ligands with Meso Backbones

Meso diimine ligands derived from *cis*-1,2-diaminocyclohexane and (1*R*,2*S*)-1,2-diamino-1,2-diphenylethane were also examined in the asymmetric addition reaction (Table 11). As previously discussed (Scheme 5), the two static chair conformations of the *cis*-1,2-diaminocyclohexane-based ligands are enantiomers that interconvert by cyclohexane ring inversion (Table 11, entries 1–5). When diimines derived from (1*R*,2*S*)-1,2-diamino-1,2-diphenylethane bind to a metal, the two conformations of the resultant metallocycle are enantiomeric, because the metallocycle will pucker to avoid eclipsing the phenyl groups. In the coordination sphere of the (Ph<sub>2</sub>-BINOLate)Zn moiety, the enantiomeric conformations of the metallocycle become diastereomeric (Figure 78). If the diimine ligand in (Ph<sub>2</sub>-BINOLate)Zn(diimine) preferentially adopts one of the diastereomeric conformations, the meso diimine can extend the chiral environment of the catalyst.

Use of catalysts formed from the meso ligands illustrated in Table 11 showed an enantioselectivity profile that paralleled those in Table 10. The bulkier the aryl groups of the diimines, the greater the enantioselectivity of the resultant zinc complexes. Catalysts incorporating diimines derived from 2,4,6-trimethylbenzaldehyde were the most enantioselective, regardless of the structure of the ligand backbone. (Compare entries 6–8 of Table 10 with entries 5 and 7 of Table 11.) In contrast to the meso bis(sulfonamide) ligands used in the titanium chemistry (Table 9),<sup>44</sup> the meso backbone of the ligands in Table 11 had no additional influence on the enantioselectivity of the resultant catalyst when compared with their simple ethylene diimine counterparts in Table 10.

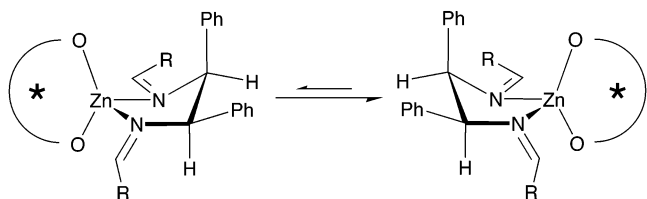
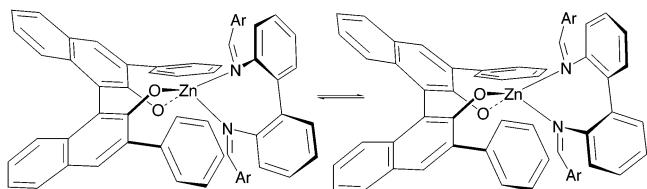
### 6.2.3. Diimine Ligands with Atropisomeric Biphenyl Backbones

The next class of diimine ligands was based on the 2,2'-diaminobiphenyl backbone. Binding of these axi-

**Table 11. Results of Screening Meso Diimines **142a–g** with (*S*)-Ph<sub>2</sub>-BINOL (**139**) in Eq 29<sup>a</sup>**

entry	ligand	ee at 0°C (config)	ee at -45°C (config)
1	<b>142a</b> 	20 ( <i>S</i> )	--
2	<b>142b</b> 	3 ( <i>R</i> )	--
3	<b>142c</b> 	66 ( <i>R</i> )	--
4	<b>142d</b> 	74 ( <i>R</i> )	71 ( <i>R</i> )
5	<b>142e</b> 	75 ( <i>R</i> )	60 ( <i>R</i> )
6	<b>142f</b> 	39 ( <i>R</i> )	--
7	<b>142g</b> 	73 ( <i>R</i> )	86 ( <i>R</i> )

<sup>a</sup> Reaction employed 10 mol % Ph<sub>2</sub>-BINOL, 10 mol % diimine ligand, and 300 mol % diethylzinc.

**Figure 78.** Diastereomeric conformations of (Ph<sub>2</sub>-BINOLate)Zn(diimine) derived from ligands **142f** and **142g**.**Figure 79.** Diastereomeric conformations of (Ph<sub>2</sub>-BINOLate)Zn(diimine) derived from ligands **143a–f**.

ally chiral ligands raises the barrier to interconversion of their atropisomeric conformations and extends the chiral environment of the catalyst (Figure 79). Use of ligands **143a–f** (Table 12) in combination with

**Table 12. Results of Screening Achiral Diimine Activators Derived from 2,2'-Diaminobiphenyl **143a–f** with (*S*)-Ph<sub>2</sub>-BINOL (**139**) in Eq 29<sup>a</sup>**

entry	ligand	ee at 0°C (config)	ee at -45°C (config)
1	<b>143a</b> 	38 ( <i>S</i> )	--
2	<b>143b</b> 	27 ( <i>S</i> )	--
3	<b>143c</b> 	38 ( <i>S</i> )	--
4	<b>143d</b> 	25 ( <i>R</i> )	--
5	<b>143e</b> 	54 ( <i>R</i> )	--
6	<b>143f</b> 	89 ( <i>R</i> )	96 <sup>b</sup> ( <i>R</i> )

<sup>a</sup> Reaction employed 10 mol % Ph<sub>2</sub>-BINOL, 10 mol % diimine ligand, and 300 mol % diethylzinc. <sup>b</sup> The catalyst formed from ligand **143f** was not completely soluble at -45 °C.

(*S*)-Ph<sub>2</sub>-BINOL in eq 29 resulted in a broad range of enantioselectivities from 38% ee (*S*) to 89% ee (*R*) at 0 °C. Ligand **143f** resulted in formation of the most enantioselective catalyst reported, generating the product in 89% ee at 0 °C and 96% ee at -45 °C (Table 12).

Despite the notable difference in the ligand backbones between the entries in Tables 9–11, trends in the enantioselectivities of the resultant catalysts were observed. For example, with the exception of **142b** (Table 11), the 1- and 2-naphthyl derivatives gave the (*S*)-enantiomer, and the anthracene, 2,6-dichlorobenzene, and 2,4,6-trimethylbenzene derivatives gave the (*R*)-enantiomer of the product. It is interesting that ligands derived from 2,4,6-trimethylbenzaldehyde formed the most enantioselective catalysts, regardless of the nature of the ligand backbone (Tables 9–11). The data in Tables 9–11 imply that the *N*-aryl groups are very important in determining the enantioselectivity of the catalyst. It is possible that the (Ph<sub>2</sub>-BINOLate)Zn sets the position of the mesityl groups and, therefore, minor changes in the diimine backbone (Table 10, **141e–g**

and Table 11, **142e** and **142g**) have little influence on the enantioselectivity of the catalyst. In sum, examination of diimine ligands in eq 29 resulted in enantioselectivities from 96% (*R*) to 52% (*S*).

#### 6.2.4. Simple Achiral Diamine Ligands

It was also found that diamines exerted substantial ligand acceleration in eq 29 (Tables 13 and 14). The

**Table 13. Results of Screening Diamines 144a–d with (S)-Ph<sub>2</sub>-BINOL (139) in Eq 29<sup>a</sup>**

entry	ligand	ee at 0°C (config)	ee at -45°C (config)
1	<b>144a</b> 	47 ( <i>S</i> )	--
2	<b>144b</b> 	64 ( <i>S</i> )	--
3	<b>144c</b> 	36 ( <i>R</i> )	72 ( <i>R</i> )
4	<b>144d</b> 	4 ( <i>S</i> )	75 ( <i>R</i> )

<sup>a</sup> Reaction employed 10 mol % Ph<sub>2</sub>-BINOL, 10 mol % diamine ligand, and 300 mol % diethylzinc.

**Table 14. Results of Screening Diamines 145a–d with (S)-Ph<sub>2</sub>-BINOL in Eq 29<sup>a</sup>**

entry	ligand	ee at 0°C (config)	ee at -20°C (config)
1	<b>145a</b> 	47 ( <i>S</i> )	--
2	<b>145b</b> 	73 ( <i>S</i> )	76 ( <i>S</i> )
3	<b>145c</b> 	30 ( <i>R</i> )	--
4	<b>145d</b> 	48 ( <i>S</i> )	--

<sup>a</sup> Reaction employed 10 mol % Ph<sub>2</sub>-BINOL, 10 mol % diamine ligand, and 300 mol % diethylzinc.

simple achiral ligands in Table 13 were available from commercial sources. It was determined that the product ee was very sensitive to the size of the *N*-alkyl groups and the length of the diamine backbone. While ethylenediamine and TMEDA resulted in slight increases in the ee's relative to that obtained with Ph<sub>2</sub>-BINOL alone (Table 13, entries 1 and 2), *N,N,N,N*-tetraethylethylenediamine (**144c**) gave the opposite enantiomer with 36% ee of the (*R*)-product at 0 °C and 72% ee at -45 °C. Similarly, *N,N,N,N*-tetramethyl-1,3-propanediamine (**144d**) gave 4% of the (*S*)-enantiomer at 0 °C and 75% ee of the (*R*)-enantiomer at -45 °C. A conceivable explanation for the large difference in enantioselectivity generated with **144b** and **144d** could be that the ligands bind to different coordination sites on the metal (Figure 77). Although it is not clear why some catalysts show large changes in enantioselectivity with decreasing temperature and others do not, it is possible that, at lower temperatures, certain ligand conformations or catalyst geometries are less accessible. If the most active form of the catalyst involves a higher energy

conformation of the ligand, the product ee might show more complex behavior with changes in temperature.

#### 6.2.5. Diamine Ligands That Form Stereogenic Centers on Binding to Metals

The next class of diamine ligands examined forms stereocenters at nitrogen on coordination of the nitrogen lone pairs to zinc.<sup>99,150</sup> It is anticipated that this coordination is reversible, allowing scrambling of the stereochemistry at nitrogen through a three-coordinate zinc species.<sup>326–328</sup> It was envisioned that the *C*<sub>2</sub>-symmetric (Ph<sub>2</sub>-BINOLate)Zn would favor binding of the diamine in a *C*<sub>2</sub>-symmetric fashion. The chiral nitrogens would then impact the enantiofacial selectivity in the C–C bond-forming process. Biasing of the nitrogens in a chiral diamine ligand bound to zinc has been observed previously (Figure 13).<sup>98</sup>

Examination of secondary diamines **145a–d** (Table 14) in eq 29 generated product ee's of 30% (*R*) to 76% (*S*), and the diamine *N,N*-di-*tert*-butylethylenediamine (**145b**) gave the highest ee for the (*S*)-product in the study (73% ee at 0 °C and 76% ee at -20 °C). The proposed catalyst for this process, (Ph<sub>2</sub>-BINOLate)Zn(diamine), was characterized by X-ray crystallography, and the ORTEP diagram in Figure 80

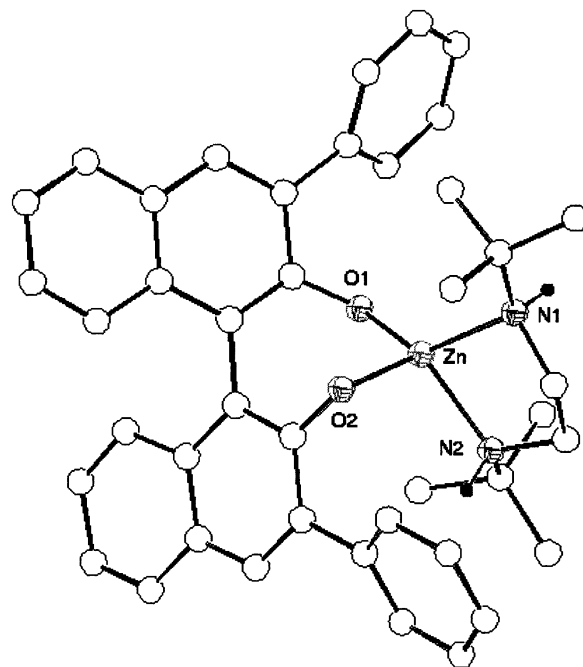


**Figure 80.** Structure of (Ph<sub>2</sub>-BINOLate)Zn(diamine) with ligand **145b**.

illustrates the tetrahedral zinc. In this structure, the diamine nitrogens have the expected (*R,R*)-configurations.

#### 6.2.6. Diamine Ligands with Pendant Atropisomeric Substituents

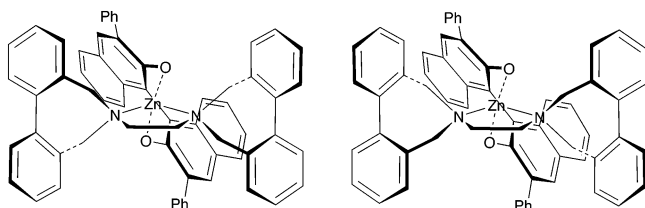
Diamines with biphenyl substituents were also examined in eq 29 (Table 15). Inversion of the configuration of the biphenyl moiety is anticipated to have a low barrier.<sup>105,150,153,247,329</sup> Interaction of the stereochemical dynamic biphenyl groups with the (Ph<sub>2</sub>-BINOLate)Zn center should influence the bi-



**Table 15. Results of Screening Achiral Diamines 146a–d with (*S*)-Ph<sub>2</sub>-BINOL in Eq 29<sup>a</sup>**

entry	ligand	ee at 0°C, -45°C, -78°C (config)		
1	<b>146a</b> 	71 ( <i>R</i> )	87	90
2	<b>146b</b> 	75 ( <i>R</i> )	87	92
3	<b>146c</b> 	83 ( <i>R</i> )	92	94
4	<b>146d</b> 	45 ( <i>S</i> )	--	--

<sup>a</sup> Reaction employed 10 mol % Ph<sub>2</sub>-BINOL, 10 mol % diamine ligand, and 300 mol % diethylzinc.

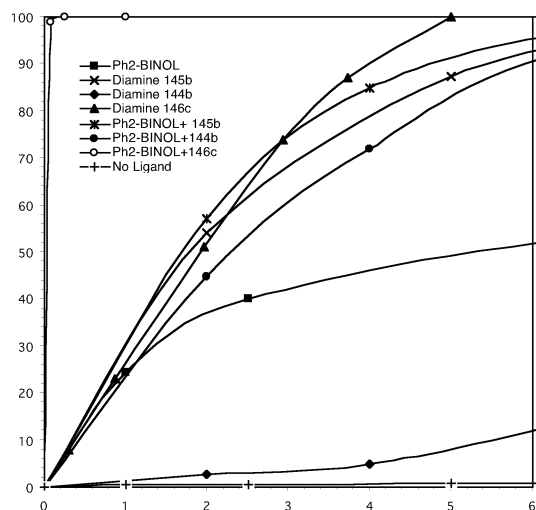
**Figure 81.** Diastereomeric conformations of (Ph<sub>2</sub>-BINOLate)Zn(diamine) derived from ligand **146a**.

phenyl stereochemistry and extend the chiral environment of the resulting catalyst (Figure 81).

Catalysts derived from atropisomeric ligands **146a,b** formed product of the (*R*)-configuration in 71% ee and 75% ee, respectively, at 0 °C (Table 15, entries 1 and 2) and gave 90 and 92% ee at -78 °C. In contrast, the TMEDA-based catalyst generated the opposite enantiomer in 64% ee at 0 °C (Table 13, entry 2). Ligand **146c**, with the *cis*-1,2-diaminocyclohexane backbone, generated one of the most enantioselective catalysts in this study. At 0, -45, and -78 °C, (*R*)-1-phenyl-1-propanol was generated in 83, 92, and 94% ee, respectively.

### 6.2.7. Impact of Achiral and Meso Ligands on Catalyst Efficiency

Experiments were performed to determine the effect of the achiral and meso ligands on the catalyst efficiency. The reaction of diethylzinc with benzaldehyde in the absence of other ligands is 1% complete after 8 h at 0 °C. Addition of Ph<sub>2</sub>-BINOL resulted in

**Figure 82.** Conversion vs time for ligands **144b**, **145b**, and **146c** with and without Ph<sub>2</sub>-BINOL.

an increase in the rate of the reaction, to give just under 25% conversion after 2 h (Figure 82). Combination of diamine (10 mol %), diethylzinc, and benzaldehyde (without Ph<sub>2</sub>-BINOL) also resulted in an increase in the rate of the addition reaction. Under 3% conversion was detected after 2 h using ligand **144b**, diethylzinc, and aldehyde. Greater conversions were observed for **145b** (54%) and **146c** (51%) in the same time. When the diamine **144b** was combined with Ph<sub>2</sub>-BINOL, the reaction was 46% complete after 2 h, which was slightly faster than that with Ph<sub>2</sub>-BINOL alone. Likewise, the catalyst formed from **145b** and Ph<sub>2</sub>-BINOL showed moderate conversion (57%) after 2 h. Surprisingly, combination of Ph<sub>2</sub>-BINOL with **146c** resulted in a remarkable acceleration in the reaction rate. The reaction was complete in 5 min at 0 °C (Figure 82, open circles), and the product was generated with high enantioselectivity (Table 15, entry 3). Use of diimines and Ph<sub>2</sub>-BINOL also resulted in significant ligand acceleration.<sup>46</sup>

The most efficient (Ph<sub>2</sub>-BINOLate)Zn(diamine) and (Ph<sub>2</sub>-BINOLate)Zn(diimine) catalysts studied in this work are markedly faster than catalysts formed from amino alcohol ligands.<sup>60</sup> This may be due to the fact that the amino alcohol-based catalysts have dimeric resting states and, therefore, the concentration of the active, three-coordinate zinc catalyst is low.

Optimization of asymmetric catalysts has traditionally been performed by the synthesis and screening of chiral ligands.<sup>2</sup> The resolution of such chiral ligands, or their components, can be an arduous and time-consuming task that severely limits the production of new catalysts. The results outlined above demonstrate that catalyst enantioselectivity and activity can be optimized by modification of achiral and meso ligands. The *most enantioselective catalysts in this study* were derived from achiral and meso ligands that have chiral conformations and can amplify or extend the chiral environment of the catalyst. Thus, using a single configuration of a resolved ligand and a series of carefully chosen achiral and meso ligands, a remarkable range of enantioselectivities was observed [76% (*S*) to 96% (*R*)].

In a related study, Muñoz-Muñiz and Juaristi<sup>330</sup> reported an increase in enantioselectivity upon addition of an achiral bis(sulfonamide) ligand in the asymmetric addition of diethylzinc to benzaldehyde with a series of chiral nitrogen- and oxygen-based ligands (Figure 83, Table 16). Using 5 mol % of the

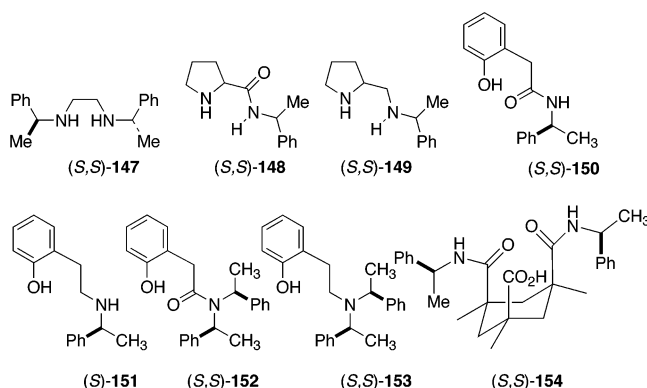


**Figure 83.** Ligands **147–154** employed in the asymmetric addition of ethyl groups to benzaldehyde (Table 16).

**Table 16. Results of Screening Ligands 147–154 in the Absence and in the Presence of Achiral Ligand 155**

entry	ligand	ee (%) (config)	chiral ligand + achiral ligand	ee (%) (config)	$\Delta$ ee
1	<b>147</b>	29 ( <i>R</i> )	<b>147</b> + <b>155</b>	35 ( <i>R</i> )	6
2	<b>148</b>	42 ( <i>S</i> )	<b>148</b> + <b>155</b>	61 ( <i>S</i> )	19
3	<b>149</b>	65 ( <i>R</i> )	<b>149</b> + <b>155</b>	79 ( <i>R</i> )	14
4	<b>150</b>	27 ( <i>S</i> )	<b>150</b> + <b>155</b>	40 ( <i>S</i> )	13
5	<b>151</b>	58 ( <i>R</i> )	<b>151</b> + <b>155</b>	71 ( <i>R</i> )	13
6	<b>152</b>	45 ( <i>S</i> )	<b>152</b> + <b>155</b>	59 ( <i>S</i> )	14
7	<b>153</b>	66 ( <i>R</i> )	<b>153</b> + <b>155</b>	79 ( <i>R</i> )	13
8	<b>154</b>	14 ( <i>S</i> )	<b>154</b> + <b>155</b>	23 ( <i>S</i> )	7

ligands **147–154**, they observed enantioselectivities between 14 and 65%. Addition of the achiral bis(sulfonamide) **155** in combination with the ligands **147–154** resulted in an increase in the enantioselectivity in each case (Table 16). The increase in enantioselectivity on addition of the achiral ligand ranged from 6 to 19 percentage points. Using the combination of chiral ligands and achiral **155** gave enantioselectivities as high as 79%.<sup>330</sup>

### 6.3. Geometry-Induced Ligand Asymmetry

A conceptually novel approach to the use of achiral ligands in asymmetric catalysis centers on achiral ligands that are symmetric in certain metal coordination geometries but can become asymmetric when the metal binds an additional ligand.<sup>45</sup> The achiral ligand in the chiral binding mode can play an

integral, or even dominant, role in the transmission of asymmetry to the substrate.

This approach, studied by Walsh and co-workers using achiral substituted 2,2'-methylene-bis(phenol) ligands (MBP-H<sub>2</sub>, **156**, Figure 84), should be ap-

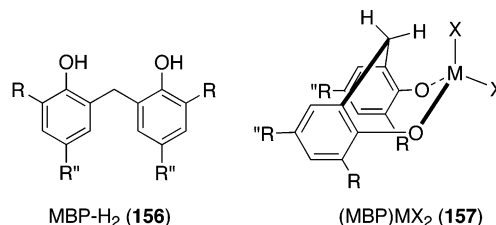


**Figure 84.** Free MBP-H<sub>2</sub> ligand **156** and achiral tetrahedral (MBP)TiX<sub>2</sub> complex **157**.

licable to optimization of a variety of asymmetric catalysts. These ligands had been studied with group IV metals<sup>331–336</sup> and found to adopt boat-type conformations in solution and in the solid state. Tetracoordinate (MBP)TiCl<sub>2</sub> (**157**, X = Cl, Figure 84) is an achiral complex that contains a plane of symmetry. Upon this complex binding dative ligands such as THF, to give (MBP)TiCl<sub>2</sub>(THF), the MBP oxygens occupy apical and equatorial positions in the adduct and are, therefore, inequivalent (Figure 85).<sup>334</sup> The

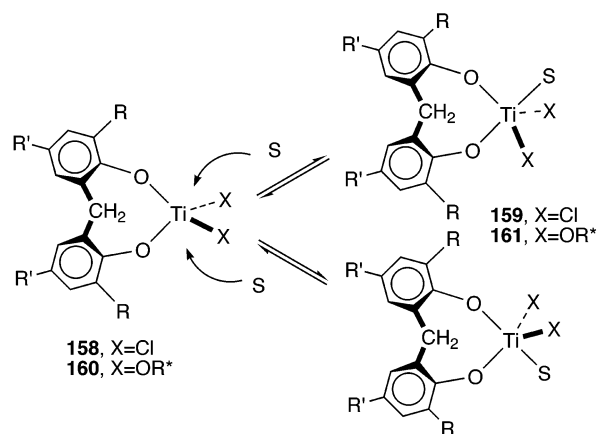


**Figure 85.** When X = Cl and S = THF, coordination of THF leads to two enantiomeric five-coordinate titanium centers (**159**). When X = OR\* and S = aldehyde substrate, the five-coordinate titanium complexes (**161**) are diastereomers.

inequivalence of the MBP oxygens in (MBP)TiCl<sub>2</sub>(THF) causes the (MBP)Ti metalocycle to be asymmetric, and (MBP)TiCl<sub>2</sub>(THF) exists as enantiomers, as observed in the crystal structure of this compound reported by Okuda.<sup>334</sup> Similar geometries have been observed with other five-coordinate group IV complexes of this ligand.<sup>332,337</sup>

It was noted that, when one oxygen was axial and the other was equatorial, the THF molecule in the five-coordinate complex was in an asymmetric environment, due to the metal geometry and the asymmetric (MBP)Ti metalocycle. If the THF were instead a prochiral substrate, attack on this coordinated substrate would occur enantioselectively. Proof of concept was demonstrated by Walsh and co-workers in the context of the asymmetric transfer of alkyl groups to aldehydes from diethylzinc.<sup>60,338</sup> This reac-

tion is particularly suitable because of its highly ordered, yet sensitive, transition state.<sup>37,53–55,60,339</sup> In the presence of the resolved alkoxide complex, (*S*)-Ti(OR\*)<sub>4</sub> [OR\* = (*S*)-OCHEt(*p*-Tol)], without any other ligands added, the asymmetric addition resulted in formation of the (*S*)-alcohol with 39% ee (eq 30 and Table 17, entry 11).

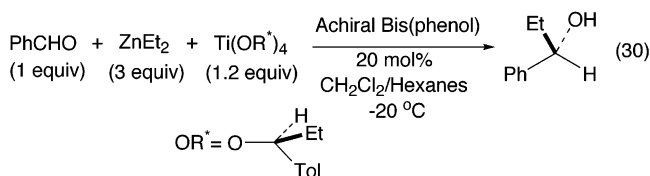


**Table 17. 2,2'-Methylenebis(phenol) Derivatives 156a–j (MBP-H<sub>2</sub>) Used in the Asymmetric Addition of Alkyl Groups to Aldehydes**

entry	ligand	R	R'	R''	ee % (config)
1	156a	H	H	H	1 ( <i>S</i> )
2	156b	H	H	Cl	9 ( <i>R</i> )
3	156c	Cl	Cl	Cl	24 ( <i>S</i> )
4	156d	Me	H	Me	16 ( <i>S</i> )
5	156e	Ph	H	H	36 ( <i>S</i> )
6	156f	<i>t</i> -Bu	H	<i>t</i> -Bu	68 ( <i>S</i> )
7	156g	<i>t</i> -Bu	H	Me	79 ( <i>S</i> )
8	156h	<i>t</i> -Bu	H	H	73 ( <i>S</i> )
9	156i	Adamantyl	H	Me	83 ( <i>S</i> )
10	156j				28 ( <i>S</i> )
11	NO MBP-H <sub>2</sub> Ligand added				39 ( <i>S</i> )

A series of substituted MBP-H<sub>2</sub> ligands (20 mol %) was combined with Ti(OR\*)<sub>4</sub> in the asymmetric addition to aldehydes (eq 30). To avoid complications arising from autoinduction, the ee's in Table 17 were measured at low conversion. Examination of the data in Table 17 indicates that the achiral MBP-H<sub>2</sub> ligands can have a significant impact on the ee of the product [9% (*R*) to 83% (*S*)]. MBP-H<sub>2</sub> ligands with small R substituents gave lower enantioselectivities (entries 1–5). When the volume of the R groups was increased to *t*-Bu, the enantioselectivities rose markedly (entries 6–8). The enantioselectivity rose with **156i** (R = adamantyl) and Ti(OR\*)<sub>4</sub> (entry 9, 83% at 20 mol % and 87% stoichiometrically) is approaching that of BINOL and Ti(O-*i*-Pr)<sub>4</sub><sup>340–342</sup> (89% ee).

A model was advanced to explain the wide variance of the enantioselectivities. The four-coordinate bis-(alkoxide) complex **160** (Figure 85) exists as a single enantiomer. Coordination of the substrate (S) potentially leads to six trigonal bipyramidal isomers (Figure 86).

In compounds **A–C**, the MBP ligand is bound through apical and equatorial positions, as in the structures of (MBP)TiCl<sub>2</sub>(THF),<sup>334</sup> (MBP)Zr(BH<sub>4</sub>)<sub>2</sub>-THF,<sup>332,333</sup> and (MBP)Ti(OTf)(η<sup>2</sup>-2-C<sub>6</sub>H<sub>4</sub>-CH<sub>2</sub>NMe<sub>2</sub>).<sup>337</sup>

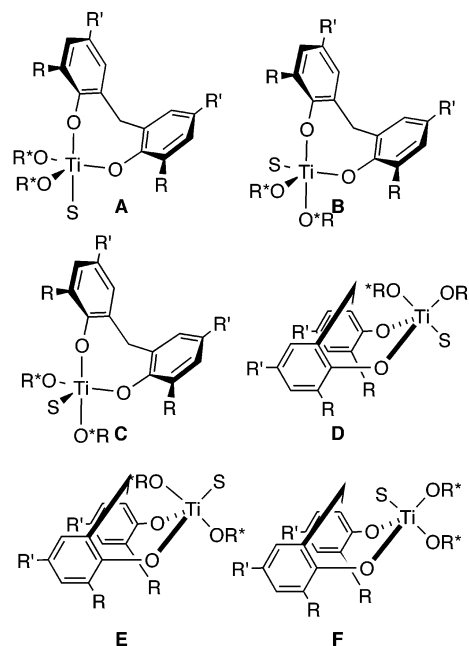


**Figure 86.** Possible geometries of substrate adducts. Diastereomers which are generated by inversion of the MBP ligand are not shown.

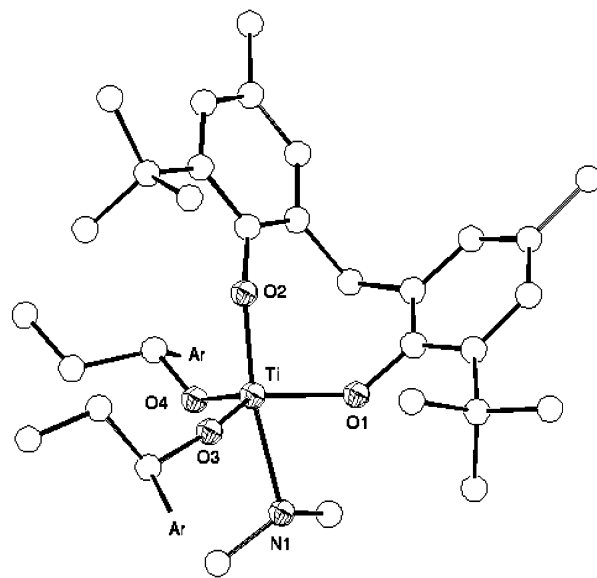


**Figure 87.** Structure of (MBP)Ti(OR\*)<sub>2</sub>(NMe<sub>2</sub>H) (**162**) illustrating the asymmetric binding of the MBP ligand. [OR\* = (*S*)-OCHEt(4-C<sub>6</sub>H<sub>4</sub>-Cl)]

The structure of (MBP)Ti(OR\*)<sub>2</sub>(NMe<sub>2</sub>H) [**162**, OR\* = (*S*)-OCHEt(4-C<sub>6</sub>H<sub>4</sub>-Cl)] was reported (Figure 87), and the asymmetric environment created by the MBP ligand is evident from this structure. The HNMe<sub>2</sub> acts as a substrate analogue and is trans to the axial MBP phenoxide oxygen in the distorted trigonal bipyramidal geometry.

In geometries **D–F**, the MBP ligand is roughly symmetric with respect to the substrate, and the asymmetry would be transferred from just one (**D**, **F**) or two (**E**) proximal chiral alkoxide ligands. In geometries **A–C**, the MBP ligand is asymmetric with respect to the substrate position. Due to the large impact of the MBP ligand on the ee of the product [from 9% ee (*R*) to 83% ee (*S*)], it was proposed that

the MBP ligand is directly involved in formation of the chiral environment and the transmission of asymmetry to the substrate. Based on Okuda's structure (**159**, Figure 85) and the structure of (MBP)Ti(OR\*)<sub>2</sub>(NMe<sub>2</sub>H) (**162**, illustrated in Figure 87), geometry **A** was favored. It must be noted, however, that it is often very difficult to deduce the metal geometry of a complex in the transition state. Crystal structures provide information on how the ligands bind to metals and what is the preferred geometry in these ground-state complexes.

Substrate coordination can temporarily increase the number of stereocenters in a catalyst.<sup>99,100</sup> In this (MBP)Ti system, it is proposed that a change in metal geometry from tetrahedral to trigonal bipyramidal on coordination of a substrate can induce asymmetry in the (MBP)Ti metalocycle. Once in an asymmetric geometry, the (MBP)Ti moiety can participate in, or even control, the relay of asymmetry to the aldehyde substrate. On the basis of this work, the authors proposed that catalysts with achiral ligands that become asymmetric when the catalyst binds the substrate would be particularly effective in the optimization of asymmetric catalysts.

## 7. Concluding Remarks

In this review, we have presented examples of how large, flexible achiral and meso ligands can be used in the optimization of asymmetric catalysts. Although this approach to catalyst development is in its infancy, successful results have been obtained with a variety of catalyst types in several different classes of reactions. It is, therefore, clear that catalyst optimization through the modification of achiral and meso ligands represents a viable approach. The benefits of catalyst optimization with achiral and meso ligands are that many different catalysts can be prepared with a single chiral ligand and a series of achiral ligands and that achiral ligands are, in general, more economical and less labor intensive to prepare than enantiopure chiral ligands.

This review also highlights a number of achiral and meso ligands that could potentially be employed in the optimization of enantioselective catalysts. These ligands have chiral conformations when bound to transition metals and in many cases are stereochemically dynamic. Through interaction of these ligands with chiral ligands, the chiral environment of the catalyst can be extended.

Not all catalysts can be optimized by using achiral and meso ligands. In general, the catalyst must have a chiral ligand and an achiral or meso ligand coordinated during the asymmetric bond-forming step. There are, however, many reactions that do meet these criteria. Given the ingenuity and resourcefulness of chemists, we predict that an increasing number of catalysts will be optimized using these techniques.

## 8. Acknowledgments

We thank the National Institutes of Health (NIGMS 058101) for supporting this work. We are grateful to Dr. Patrick J. Carroll for generating the X-ray

structural diagrams from data in the Cambridge Crystallographic Data Centre and Alice Chen for finding, copying, and entering the references into EndNote.

## 9. References

- (1) Noyori, R. *Asymmetric Catalysis in Organic Synthesis*; Wiley: New York, 1994.
- (2) Jacobsen, E. N.; Pfaltz, A.; Yamamoto, H., Eds. *Comprehensive Asymmetric Catalysis*; Springer: Berlin, 1999; Vols. 1–3.
- (3) Ojima, I., Ed. *Catalytic Asymmetric Synthesis*, 2nd ed.; Wiley-VCH: New York, 2000.
- (4) Angelaud, R.; Matsumoto, Y.; Korenaga, T.; Kudo, K.; Senda, M.; Mikami, K. *Chirality* **2000**, *12*, 544–547.
- (5) Bromidge, S.; Wilson, P.; Whiting, A. *Tetrahedron Lett.* **1998**, *39*, 8905–8908.
- (6) Brouwer, A. J.; van der Linden, H. J.; Liskamp, R. M. J. *J. Org. Chem.* **2000**, *65*, 1750–1757.
- (7) Buck, R. T.; Coe, D. M.; Drysdale, M. J.; Moody, C. J.; Pearson, N. D. *Tetrahedron Lett.* **1998**, *39*, 7181–7184.
- (8) Copeland, G. T.; Miller, S. J. *J. Am. Chem. Soc.* **2001**, *123*, 6496–6502.
- (9) Degrado, S. J.; Mizutani, H.; Hoveyda, A. H. *J. Am. Chem. Soc.* **2001**, *123*, 755–756.
- (10) Duursma, A.; Minnaard, A. J.; Feringa, B. L. *Tetrahedron* **2002**, *58*, 5773–5778.
- (11) Evans, M. A.; Morken, J. P. *J. Am. Chem. Soc.* **2002**, *124*, 9020–9021.
- (12) Gilbertson, S. R.; Chang, C.-W. T. *J. Chem. Soc., Chem. Commun.* **1997**, 975–976.
- (13) Guo, J.; Wu, J.; Siuzdak, G.; Finn, M. G. *Angew. Chem., Int. Ed.* **1999**, *38*, 1755–1758.
- (14) Janes, L. E.; Kazlauskas, R. J. *J. Org. Chem.* **1997**, *62*, 4560–4561.
- (15) Kagan, H. B. *J. Organomet. Chem.* **1998**, *567*, 3–6.
- (16) Korbel, G. A.; Lalic, G.; Shair, M. D. *J. Am. Chem. Soc.* **2001**, *123*, 361–362.
- (17) Krueger, C.; Kuntz, K.; Dzierba, C.; Wirschn, W.; Gleason, J.; Snapper, M.; Hoveyda, A. *J. Am. Chem. Soc.* **1999**, *121*, 4284–4285.
- (18) Long, J.; Ding, K. *Angew. Chem., Int. Ed.* **2001**, 544–547.
- (19) Luchaco-Cullis, C. A.; Mizutani, H.; Murphy, K. E.; Hoveyda, A. H. *Angew. Chem., Int. Ed.* **2001**, *40*, 1456–1460.
- (20) Moreau, C.; Frost, C. G.; Murrer, B. *Tetrahedron Lett.* **1999**, *40*, 5617–5620.
- (21) Moyesherman, D.; Welch, M. B.; Reibenspies, J.; Burgess, K. *J. Chem. Soc., Chem. Commun.* **1998**, 2377–2378.
- (22) Reetz, M. T.; Becker, M. H.; Klein, H.-W.; Stockigt, D. *Angew. Chem., Int. Ed.* **1999**, *38*, 1758–1761.
- (23) Sawada, M.; Yamaoka, H.; Takai, Y.; Kawai, Y.; Yamada, H.; Azuma, T.; Fujioka, T.; Tanaka, T. *J. Chem. Soc., Chem. Commun.* **1998**, 1569–1570.
- (24) Sawada, M.; Yamaoka, H.; Takai, Y.; Kawai, Y.; Yamada, H.; Azuma, T.; Fujioka, T.; Tanaka, T. *Int. J. Mass Spectrosc.* **1999**, *193*, 123–130.
- (25) Sigman, M. S.; Vachal, P.; Jacobsen, E. N. *Angew. Chem., Int. Ed.* **2000**, *39*, 1279–1281.
- (26) Taran, F.; Gauchet, C.; Mohar, B.; Meunier, S.; Valleix, A.; Renard, P. Y.; Creminon, C.; Grassi, J.; Wagner, A.; Mioskowski, C. *Angew. Chem., Int. Ed.* **2002**, *41*, 124–127.
- (27) Taylor, S. J.; Morken, J. P. *J. Am. Chem. Soc.* **1999**, *121*, 12202–12203.
- (28) Welch, C. J.; Pollard, S. D.; Mathre, D. J.; Reider, P. J. *Org. Lett.* **2001**, *3*, 95–98.
- (29) Ding, K.; Ishii, A.; Mikami, K. *Angew. Chem., Int. Ed.* **1999**, *38*, 497–501.
- (30) Lipkowitz, K. B.; Scheffzick, S. *Chirality* **2002**, *14*, 677–682.
- (31) Gao, D.; Scheffzick, S.; Lipkowitz, K. B. *J. Am. Chem. Soc.* **1999**, *121*, 9481–9482.
- (32) Lipkowitz, K. B.; Scheffzick, S.; Avnir, D. *J. Am. Chem. Soc.* **2001**, *123*, 6710–6711.
- (33) Lipkowitz, K. B.; D'Hue, C. A.; Sakamoto, T.; Stack, J. N. *J. Am. Chem. Soc.* **2002**, *124*, 14255–14267.
- (34) Kozlowski, M. C.; Waters, S. P.; Skudlarek, J. W.; Evans, C. A. *Org. Lett.* **2002**, *4*, 4391–4393.
- (35) Kozlowski, M. C.; Panda, M. *J. Mol. Graphics Model.* **2002**, *20*, 399–409.
- (36) Panda, M.; Phuan, P.-W.; Kozlowski, M. C. *J. Org. Chem.* **2003**, *68*, 564–571.
- (37) Vidal-Ferran, A.; Moyano, A.; Pericas, M. A.; Riera, A. *Tetrahedron Lett.* **1997**, *38*, 8773–8776.
- (38) Seyden-Penne, J. *Chiral Auxiliaries and Ligands in Asymmetric Synthesis*; John Wiley and Sons: New York, 1995.
- (39) Miura, K.; Katsuki, T. *Synlett* **1999**, 783–785.

- (40) Mikami, K.; Korenaga, T.; Terada, M.; Ohkuma, T.; Pham, T.; Noyori, R. *Angew. Chem., Int. Ed.* **1999**, *38*, 495–497.
- (41) Ueki, M.; Matsumoto, Y.; Jordy, J. J.; Mikami, K. *Synlett* **2001**, 1889–1892.
- (42) Mikami, K.; Aikawa, K. *Org. Lett.* **2002**, *4*, 99–101.
- (43) Mikami, K.; Terada, M.; Korenaga, T.; Matsumoto, Y.; Ueki, M.; Angelaud, R. *Angew. Chem., Int. Ed.* **2000**, *39*, 3532–3556.
- (44) Balsells, J.; Walsh, P. J. *J. Am. Chem. Soc.* **2000**, *122*, 1802–1803.
- (45) Davis, T. J.; Balsells, J.; Carroll, P. J.; Walsh, P. J. *Org. Lett.* **2001**, *3*, 2161–2164.
- (46) Costa, A. M.; Jimeno, C.; Gavenonis, J.; Carroll, P. J.; Walsh, P. J. *J. Am. Chem. Soc.* **2002**, *124*, 6929–6941.
- (47) Kitamura, M.; Suga, S.; Kawai, K.; Noyori, R. *J. Am. Chem. Soc.* **1986**, *108*, 6071–6072.
- (48) Noyori, R.; Suga, S.; Kawai, K.; Okada, S.; Kitamura, M. *Pure Appl. Chem.* **1988**, *60*, 1597–1606.
- (49) Noyori, R.; Kitamura, M. *Angew. Chem., Int. Ed. Engl.* **1991**, *30*, 49–69.
- (50) Kitamura, M.; Oka, H.; Noyori, R. *Tetrahedron* **1999**, *55*, 3605–3614.
- (51) Kitamura, M.; Suga, S.; Oka, H.; Noyori, R. *J. Am. Chem. Soc.* **1998**, *120*, 9800–9809.
- (52) Kitamura, M.; Suga, S.; Niwa, M.; Noyori, R. *J. Am. Chem. Soc.* **1995**, *117*, 4832–4842.
- (53) Goldfuss, B.; Houk, K. N. *J. Org. Chem.* **1998**, *63*, 8998–9006.
- (54) Goldfuss, B.; Steigelmann, M.; Khan, S. I.; Houk, K. N. *J. Org. Chem.* **2000**, *65*, 77–82.
- (55) Rasmussen, T.; Norrby, P.-O. *J. Am. Chem. Soc.* **2001**, *123*, 2464–2465.
- (56) Chen, Y. K.; Costa, A. M.; Walsh, P. J. *J. Am. Chem. Soc.* **2001**, *123*, 5378–5379.
- (57) Buono, F.; Walsh, P. J.; Blackmond, D. G. *J. Am. Chem. Soc.* **2002**, *124*, 13652–13653.
- (58) Kitamura, M.; Okada, S.; Suga, S.; Noyori, R. *J. Am. Chem. Soc.* **1989**, *111*, 4028–4036.
- (59) Girard, C.; Kagan, H. B. *Angew. Chem., Int. Ed.* **1998**, *37*, 2922–2959.
- (60) Pu, L.; Yu, H.-B. *Chem. Rev.* **2001**, *101*, 757–824.
- (61) Nugent, W. A. *J. Chem. Soc., Chem. Commun.* **1999**, 1369–1370.
- (62) Knowles, W. S. *Acc. Chem. Res.* **1983**, *16*, 106–112.
- (63) Knowles, W. S.; Sabacky, M. J.; Vineyard, B. D. *J. Chem. Soc., Chem. Commun.* **1972**, 10–11.
- (64) Dang, T. P.; Kagan, H. B. *J. Chem. Soc., Chem. Commun.* **1971**, 481–482.
- (65) Kagan, H. B.; Phat, D.-T. *J. Am. Chem. Soc.* **1972**, *94*, 6429–6433.
- (66) Miyashita, A.; Yasuda, A.; Takaya, H.; Toriumi, T.; Ito, K.; Souchi, T.; Noyori, R. *J. Am. Chem. Soc.* **1980**, *102*, 7932–7934.
- (67) Noyori, R.; Ohkuma, T. *Angew. Chem., Int. Ed.* **2001**, *40*, 40–73.
- (68) Noyori, R.; Yamakawa, M.; Hashiguchi, S. *J. Org. Chem.* **2001**, *66*, 7931–7944.
- (69) Ohta, T.; Takaya, H.; Noyori, R. *Inorg. Chem.* **1988**, *27*, 566–569.
- (70) Morton, D. A. V.; Orpen, A. G. *J. Chem. Soc., Dalton Trans.* **1992**, 641–653.
- (71) Brunner, H.; Winter, A.; Breu, J. *J. Organomet. Chem.* **1998**, *553*, 285–306.
- (72) Hao, J.; Hatano, M.; Mikami, K. *Org. Lett.* **2000**, *3*, 4059–4062.
- (73) Seebach, D.; Beck, A. K.; Heckel, A. *Angew. Chem., Int. Ed.* **2001**, *40*, 92–138.
- (74) Seebach, D.; Plattner, D. A.; Beck, A. K.; Wang, Y. M.; Hunziker, D.; Petter, W. *Helv. Chim. Acta* **1992**, *75*, 2171–2209.
- (75) Gothelf, K. V.; Hazzel, R. G.; Jørgensen, K. A. *J. Am. Chem. Soc.* **1995**, *117*, 4435–4436.
- (76) Braun, M. *Angew. Chem., Int. Ed. Engl.* **1996**, *35*, 519–522.
- (77) Muñoz, K.; Bolm, C. *Chem. Eur. J.* **2000**, *6*, 2309–2316.
- (78) Takahashi, H.; Kawakita, T.; Ohno, M.; Yoshioka, M.; Kobayashi, S. *Tetrahedron* **1992**, *48*, 5691–5700.
- (79) Takahashi, H.; Kawakita, T.; Yoshioka, M.; Kobayashi, S.; Ohno, M. *Tetrahedron Lett.* **1989**, *30*, 7095–7098.
- (80) Knochel, P.; Jones, P. *Organozinc Reagents*; Oxford University Press: Oxford, 1999.
- (81) Ostwald, R.; Chavant, P.-Y.; Stadtmüller, H.; Knochel, P. *J. Org. Chem.* **1994**, *59*, 4143–4153.
- (82) Pritchett, S.; Woodmansee, D. H.; Gantzel, P.; Walsh, P. J. *J. Am. Chem. Soc.* **1998**, *120*, 6423–6424.
- (83) Pritchett, S.; Gantzel, P.; Walsh, P. J. *Organometallics* **1999**, *18*, 823–831.
- (84) Royo, E.; Betancort, J. M.; Davis, T. J.; Walsh, P. J. *Organometallics* **2000**, *19*, 4840–4851.
- (85) Armistead, L. T.; White, P. S.; Gagné, M. R. *Organometallics* **1998**, *17*, 216–220.
- (86) Pritchett, S.; Woodmansee, D. H.; Davis, T. J.; Walsh, P. J. *Tetrahedron Lett.* **1998**, *39*, 5941–5944.
- (87) Evans, D. A.; Nelson, S. G. *J. Am. Chem. Soc.* **1997**, *119*, 6452–6453.
- (88) Takahashi, H.; Yoshioka, M.; Ohno, M.; Kobayashi, S. *Tetrahedron Lett.* **1992**, *33*, 2575–2578.
- (89) Takahashi, H.; Yoshioka, M.; Shibasaki, M.; Ohno, M.; Imai, N.; Kobayashi, S. *Tetrahedron* **1995**, *51*, 12013–12026.
- (90) Denmark, S. E.; O'Connor, S. P. *J. Org. Chem.* **1997**, *62*, 3390–3401.
- (91) Denmark, S. E.; O'Connor, S. P. *J. Org. Chem.* **1997**, *62*, 584–594.
- (92) Corey, E. J.; Sarshar, S.; Lee, D.-H. *J. Am. Chem. Soc.* **1994**, *116*, 12089–12090.
- (93) Ichihyanagi, T.; Shimizu, M.; Fujisawa, T. *J. Org. Chem.* **1997**, *62*, 7937–7941.
- (94) Denmark, S. E.; O'Connor, S. P.; Wilson, S. R. *Angew. Chem., Int. Ed.* **1998**, *37*, 1149–1151.
- (95) Brandt, P.; Södergren, M. J.; Andersson, P. G.; Norrby, P.-O. *J. Am. Chem. Soc.* **2000**, *122*, 8013–8020.
- (96) Evans, D. A.; Campos, K. R.; Tedrow, J. S.; Michael, F. E.; Gagné, M. R. *J. Am. Chem. Soc.* **2000**, *122*, 7905–7920.
- (97) Evans, D. A.; Campos, K. R.; Tedrow, J. S.; Michael, F. E.; Gagné, M. R. *J. Org. Chem.* **1999**, *64*, 2994–2995.
- (98) Mimoun, H.; Yves de Saint Laumer, J.; Giannini, L.; Scopelliti, R.; Floriani, C. *J. Am. Chem. Soc.* **1999**, *121*, 6158–6166.
- (99) von Zelewsky, A. *Stereochemistry of Coordination Compounds*; John Wiley & Sons Ltd.: West Sussex, 1996.
- (100) Brunner, H. *Angew. Chem., Int. Ed.* **1999**, *38*, 1194–1208.
- (101) Faller, J. W.; Parr, J. *Organometallics* **2000**, *19*, 1829–1832.
- (102) Faller, J. W.; Grimmond, B. J.; D'Allesci, D. G. *J. Am. Chem. Soc.* **2001**, *123*, 2525–2529.
- (103) Faller, J. W.; Parr, J. *Organometallics* **2001**, *20*, 697–699.
- (104) Faller, J. W.; Grimmond, B. J. *Organometallics* **2001**, *20*, 2454–2458.
- (105) Reetz, M. T.; Neugebauer, T. *Angew. Chem., Int. Ed.* **1999**, *38*, 179–181.
- (106) Clayden, J.; Johnson, P.; Pink, J. H.; Helliwell, M. *J. Org. Chem.* **2000**, *65*, 7033–7040.
- (107) Clayden, J. *Synlett* **1998**, 810–816.
- (108) Ahmed, A.; Bragg, R. A.; Clayden, J.; Lai, L. W.; McCarthy, C.; Pink, J. H.; Westlund, N.; Yasin, S. A. *Tetrahedron* **1998**, *54*, 13277–13294.
- (109) Rios, R.; Jimeno, C.; Carroll, P. J.; Walsh, P. J. *J. Am. Chem. Soc.* **2002**, *124*, 10272–10273.
- (110) Mino, T.; Kashiwara, K.; Yamashita, M. *Tetrahedron: Asymmetry* **2001**, *12*, 287–291.
- (111) Clayden, J.; Lai, L. W.; Helliwell, M. *Tetrahedron: Asymmetry* **2001**, *12*, 695–698.
- (112) Sibi, M. P.; Venkatraman, L.; Liu, M.; Jasperse, C. P. *J. Am. Chem. Soc.* **2001**, *123*, 8444–8445.
- (113) Vogl, E. M.; Groger, H.; Shibasaki, M. *Angew. Chem., Int. Ed.* **1999**, *38*, 1570–1577.
- (114) Kobayashi, S.; Ishitani, H. *J. Am. Chem. Soc.* **1994**, *116*, 4083–4084.
- (115) Kobayashi, S.; Hachiya, I.; Ishitani, H.; Araki, M. *Tetrahedron Lett.* **1993**, *34*, 4535–4538.
- (116) Ferreira, E. M.; Stoltz, B. M. *J. Am. Chem. Soc.* **2001**, *123*, 7725–7726.
- (117) Jensen, D. R.; Pugsley, J. S.; Sigman, M. S. *J. Am. Chem. Soc.* **2001**, *123*, 7475–7476.
- (118) Dearden, M. J.; Firkin, C. R.; Hermet, J.-P. R.; O'Brien, P. *J. Am. Chem. Soc.* **2002**, *124*, 11870–11871.
- (119) Mueller, J. A.; Jensen, D. R.; Sigman, M. S. *J. Am. Chem. Soc.* **2002**, *124*, 8202–8203.
- (120) Jensen, D. R.; Sigman, M. S. *Org. Lett.* **2003**, *5*, 63–65.
- (121) Keith, J. M.; Larrow, J. F.; Jacobsen, E. N. *Adv. Synth. Catal.* **2001**, *1*, 5–26.
- (122) Hashihayata, T.; Ito, Y.; Katsuki, T. *Tetrahedron* **1997**, *53*, 9541–9552.
- (123) Hashihayata, T.; Ito, Y.; Katsuki, T. *Synlett* **1996**, 1079–1081.
- (124) Zhang, W.; Loebach, J. L.; Wilson, S. R.; Jacobsen, E. N. *J. Am. Chem. Soc.* **1990**, *112*, 2801–2803.
- (125) Irie, R.; Noda, K.; Ito, Y.; Matsumoto, N.; Katsuki, T. *Tetrahedron Lett.* **1990**, *31*, 7345–7348.
- (126) Jacobsen, E. N.; Wu, M. H. Epoxidation of Alkenes Other than Allylic Alcohols. In *Comprehensive Asymmetric Catalysis*; Jacobsen, E. N., Pfaltz, A., Yamamoto, H., Eds.; Springer: Berlin, 1999; Vol. 2, pp 649–678.
- (127) Dalton, C. T.; Ryan, K. M.; Wall, V. M.; Bousquet, C.; Gilheany, D. G. *Top. Catal.* **1998**, *5*, 75–91.
- (128) Katsuki, T. Asymmetric Epoxidation of Unfunctionalized Olefins and Related Reactions. In *Catalytic Asymmetric Synthesis*, 2nd ed.; Ojima, I., Ed.; Wiley-VCH: New York, 2000; pp 287–326.
- (129) Palucki, M.; Finney, N. S.; Pospisil, P. J.; Güler, M. L.; Ishida, T.; Jacobsen, E. N. *J. Am. Chem. Soc.* **1998**, *120*, 948–954.
- (130) Feichtinger, D.; Plattner, D. A. *Angew. Chem., Int. Ed. Engl.* **1997**, *36*, 1718–1719.
- (131) Norrby, P.-O.; Linde, C.; Åkermark, B. *J. Am. Chem. Soc.* **1995**, *119*, 11035–11036.
- (132) Hamada, T.; Fukuda, T.; Imanishi, H.; Katsuki, T. *Tetrahedron* **1996**, *52*, 515–530.

- (133) Samsel, E. G.; Srinivasan, K.; Kochi, J. K. *J. Am. Chem. Soc.* **1985**, *107*, 7606–7617.
- (134) Pospisil, P. J.; Carsten, D. H.; Jacobsen, E. N. *Chem. Eur. J.* **1996**, *2*, 974–980.
- (135) Irie, R.; Ito, Y.; Katsuki, T. *Synlett* **1991**, 265–266.
- (136) Finney, N. S.; Pospisil, P. J.; Chang, S.; Palucki, M.; Konsler, R. G.; Hansen, K. B.; Jacobsen, E. N. *Angew. Chem., Int. Ed. Engl.* **1997**, *36*, 1720–1723.
- (137) Hughes, D. L.; Smith, G. B.; Liu, J.; Dezeny, G. C.; Senanayake, C. H.; Larsen, R. D.; Verhoeven, T. R.; Reider, P. J. *J. Org. Chem.* **1997**, *62*, 2222–2229.
- (138) March, J. *Advanced Organic Chemistry*, 4th ed.; Wiley and Sons: New York, 1992.
- (139) Sasaki, H.; Irie, R.; Hamada, T.; Suzuki, K.; Katsuki, T. *Tetrahedron* **1994**, *50*, 11827–11838.
- (140) Kagan, H. B. Asymmetric Oxidation of Sulfides. In *Catalytic Asymmetric Synthesis*, 2nd ed.; Ojima, I., Ed.; Wiley-VCH: New York, 2000; pp 327–356.
- (141) Kokubo, C.; Katsuki, T. *Tetrahedron* **1996**, *52*, 13895–13900.
- (142) Chavarot, M.; Byrne, J. J.; Chavant, P. Y.; Guindet, P.; Vallée, Y. *Tetrahedron: Asymmetry* **1998**, *9*, 3889–3894.
- (143) Mikami, K.; Matsukawa, S. *Nature* **1997**, *385*, 613–615.
- (144) Mikami, K.; Matsukawa, S.; Volk, T.; Terada, M. *Angew. Chem., Int. Ed. Engl.* **1997**, *36*, 2768–2771.
- (145) Terada, M.; Mikami, K.; Nakai, T. *J. Chem. Soc., Chem. Commun.* **1990**, 1623–1624.
- (146) Mikami, K.; Aikawa, K.; Ysa, Y.; Jordy, J. J.; Yamanka, M. *Synlett* **2002**, 1561–1578.
- (147) Bolm, C.; Beckmann, O. *Chirality* **2000**, *12*, 523–525.
- (148) Davis, T. J.; Carroll, P. J.; Walsh, P. J. *J. Organomet. Chem.* **2002**, *663*, 70–77.
- (149) Desponds, O.; Schlosser, M. *Tetrahedron Lett.* **1996**, *37*, 47–48.
- (150) Eliel, E. L.; Wilen, S. H. *Stereochemistry of Organic Compounds*; Wiley & Sons: New York, 1994.
- (151) Kurland, R. J.; Rubin, M. B.; Wise, W. B. *J. Chem. Phys.* **1964**, *40*, 2426–2431.
- (152) Müllen, K.; Heinz, W.; Klärner, F.-G.; Roth, W. R.; Kindermann, I.; Adamczak, O.; Wette, M.; Lex, J. *Chem. Ber.* **1990**, *23*, 2349–2371.
- (153) Iffland, D. C.; Siegel, H. *J. Am. Chem. Soc.* **1958**, *80*, 1947–1950.
- (154) Mislow, K.; Hyden, S.; Schaefer, H. *J. Am. Chem. Soc.* **1962**, *84*, 1449–1455.
- (155) Noyori, R.; Hashiguchi, S. *Acc. Chem. Res.* **1997**, *30*, 97–102.
- (156) Ohkuma, T.; Doucet, H.; Pham, T.; Mikami, K.; Korenaga, T.; Terada, M.; Noyori, R. *J. Am. Chem. Soc.* **1998**, *120*, 1086–1087.
- (157) Ohkuma, T.; Ooka, H.; Hashiguchi, S.; Ikariya, T.; Noyori, R. *J. Am. Chem. Soc.* **1995**, *117*, 2675–2676.
- (158) Ohkuma, T.; Ooka, H.; Ikariya, T.; Noyori, R. *J. Am. Chem. Soc.* **1995**, *117*, 10417–10418.
- (159) Doucet, H.; Ohkuma, T.; Murata, K.; Yokozawa, T.; Kozawa, M.; Katayama, E.; England, A. F.; Ikariya, T.; Noyori, R. *Angew. Chem., Int. Ed.* **1998**, *37*, 1703–1707.
- (160) Blackmond, D. G.; Rosner, T.; Neugebauer, T.; Reetz, M. T. *Angew. Chem., Int. Ed.* **1999**, *38*, 2196–2199.
- (161) Bolm, C.; Muniz, K.; Hildebrand, J. P. *Org. Lett.* **1999**, *1*, 491–494.
- (162) Balsells, J.; Walsh, P. J. *J. Am. Chem. Soc.* **2000**, *122*, 3250–3251.
- (163) Zhang, S. Y.; Girard, C.; Kagan, H. B. *Tetrahedron: Asymmetry* **1995**, *6*, 2637–2640.
- (164) Abdur-Rashid, K.; Faatz, M.; Lough, A. J.; Morris, R. H. *J. Am. Chem. Soc.* **2001**, *123*, 7473–7474.
- (165) Abdur-Rashid, K.; Clapham, S. E.; Hadzovic, A.; Harvey, J. N.; Lough, A. J.; Morris, R. H. *J. Am. Chem. Soc.* **2002**, *124*, 15104–15118.
- (166) Subongkoj, S.; Lange, S.; Chen, W.; Xiao, J. *J. Mol. Catal. A: Chemical* **2003**, *196*, 125–129.
- (167) Bandoli, G.; Dolmella, A. *Coord. Chem. Rev.* **2000**, *209*, 161–196.
- (168) Becker, J. J.; White, P. S.; Gagné, M. R. *Inorg. Chem.* **1999**, *38*, 798–801.
- (169) Becker, J. J.; White, P. S.; Gagné, M. R. *J. Am. Chem. Soc.* **2001**, *123*, 9478–9479.
- (170) Ghosh, A. K.; Matsuda, H. *Org. Lett.* **1999**, *1*, 2157–2159.
- (171) Mikami, K.; Aikawa, K.; Yusa, Y. *Org. Lett.* **2002**, *4*, 95–97.
- (172) Mikami, K.; Aikawa, K.; Yusa, Y.; Hatano, M. *Org. Lett.* **2002**, *4*, 91–94.
- (173) Koh, J. H.; Larsen, A. L.; Gagné, M. R. *Org. Lett.* **2001**, *3*, 1233–1236.
- (174) Tudor, M. D.; Becker, J. J.; White, P. S.; Gagné, M. R. *Organometallics* **2000**, *19*, 4376–4384.
- (175) Korenaga, T.; Aikawa, K.; Terada, M.; Kawachi, S.; Mikami, K. *Adv. Synth. Catal.* **2001**, *1*, 284–288.
- (176) Yamanaka, M.; Mikami, K. *Organometallics* **2002**, *21*, 5847–5851.
- (177) Mikami, K.; Aikawa, K.; Korenaga, T. *Org. Lett.* **2001**, *3*, 243–245.
- (178) Mikami, K.; Korenaga, T.; Ohkuma, T.; Noyori, R. *Angew. Chem., Int. Ed.* **2000**, *39*, 3707–3710.
- (179) Ohta, T.; Takaya, H.; Noyori, R. *Inorg. Chem.* **1988**, *27*, 566–569.
- (180) Ogasawara, M.; Yoshida, K.; Hayashi, T. *Organometallics* **2000**, *19*, 1567–1571.
- (181) Atwood, J. D. *Inorganic and Organometallic Reaction Mechanisms*, 2nd ed.; VCH Publishers: New York, 1997.
- (182) Bryndza, H. E.; Domaille, P. J.; Paciello, R. A.; Bercaw, J. E. *Organometallics* **1989**, *8*, 379–385.
- (183) Bryndza, H. E.; Fong, L. K.; Paciello, R. A.; Tam, W.; Bercaw, J. E. *J. Am. Chem. Soc.* **1987**, *109*, 1444–1456.
- (184) Caulton, K. G. *J. Am. Chem. Soc.* **1974**, *96*, 3005–3006.
- (185) James, B. R.; Markham, L. D. *Inorg. Chem.* **1974**, *13*, 97–100.
- (186) Crumpton, D. M.; Goldberg, K. I. *J. Am. Chem. Soc.* **2000**, *122*, 962–963.
- (187) Hartwig, J. F. *Angew. Chem., Int. Ed.* **1998**, *37*, 2047–2067.
- (188) Netherton, M. R.; Fu, G. C. *Org. Lett.* **2001**, *3*, 4295–4298.
- (189) Littke, A. F.; Dai, C.; Fu, G. F. *J. Am. Chem. Soc.* **2000**, *122*, 4020–4028.
- (190) Aranyos, A.; Old, D. W.; Kiyomori, A.; Wolfe, J. P.; Sadighi, J. P.; Buchwald, S. L. *J. Am. Chem. Soc.* **1999**, *121*, 4369–4378.
- (191) Stambuli, J. P.; Stauffer, S. R.; Shaughnessy, K. H.; Hartwig, J. F. *J. Am. Chem. Soc.* **2001**, *123*, 2677–2678.
- (192) Alcazar-Roman, L. M.; Hartwig, J. F. *J. Am. Chem. Soc.* **2001**, *123*, 12905–12906.
- (193) Beare, N. A.; Hartwig, J. F. *J. Org. Chem.* **2002**, *67*, 541–555.
- (194) Crabtree, R. H. *The Organometallic Chemistry of the Transition Metals*, 3rd ed.; John Wiley and Sons: New York, 2001.
- (195) Doherty, S.; Knight, J. G.; Robins, E. G.; Scanlan, T. H.; Champkin, P. A.; Clegg, W. *J. Am. Chem. Soc.* **2001**, *123*, 5110–5111.
- (196) Doherty, S.; Robins, E. G.; Nieuwenhuyzen, M.; Knight, J. G.; Champkin, P. A.; Clegg, W. *Organometallics* **2002**, *21*, 1383–1399.
- (197) Doherty, S.; Newman, C. R.; Hardacre, C.; Nieuwenhuyzen, M.; Knight, J. G. *Organometallics* **2003**, *22*, 1452–1462.
- (198) Ozawa, F.; Kubo, A.; Matsumoto, Y.; Hayashi, T.; Nishioka, E.; Yanagi, K.; Moriguchi, K. *Organometallics* **1993**, *12*, 4188–4196.
- (199) Knight, J. G.; Doherty, S.; Harriman, A.; Robins, E. G.; Betham, M.; Eastham, G. R.; Tooze, P. R.; Elsegood, M. R. J.; Champkin, P.; Clegg, W. *Organometallics* **2000**, *19*, 4957–4967.
- (200) Tissot, O.; Gouygou, M.; Dallemer, F.; Daran, J.-C.; Balavoine, G. G. A. *Angew. Chem., Int. Ed.* **2001**, *40*, 1076–1078.
- (201) Mercier, F.; Holand, S.; Mathey, F. *J. Organomet. Chem.* **1986**, *316*, 271–279.
- (202) Deschamps, E.; Mathey, F. *Bull. Soc. Chim. Fr.* **1992**, *129*, 486–489.
- (203) Tissot, O.; Gouygou, M.; Daran, J.-C.; Balavoine, G. G. A. *J. Chem. Soc., Chem. Commun.* **1996**, 2287–2288.
- (204) Egan, W.; Tang, R.; Zon, G.; Mislow, K. *J. Am. Chem. Soc.* **1971**, *93*, 6205–6216.
- (205) Gouygou, M.; Tissot, O.; Daran, J.-C.; Balavoine, G. G. A. *Organometallics* **1997**, *16*, 1008–1015.
- (206) Jacques, J.; Collet, A.; Wilen, S. H. *Enantiomers, Racemates, and Resolutions*; Wiley: New York, 1981.
- (207) Trost, B. M.; Van Vranken, D. L. *Chem. Rev.* **1996**, *96*, 395–422.
- (208) Pfaltz, A.; von Matt, P. *Angew. Chem., Int. Ed. Engl.* **1993**, *32*, 566–568.
- (209) Robin, F.; Mercier, F.; Ricard, L.; Mathey, F.; Spagnol, M. *Chem. Eur. J.* **1997**, *3*, 1365–1369.
- (210) Hayashi, T.; Yamamoto, A.; Hagihara, T.; Ito, Y. *Tetrahedron Lett.* **1986**, *27*, 191–194.
- (211) Mackenzie, P. B.; Whelan, J.; Bosnich, B. *J. Am. Chem. Soc.* **1985**, *107*, 2046–2054.
- (212) Hoveyda, A. H.; Morken, J. P. *Angew. Chem., Int. Ed. Engl.* **1996**, *35*, 1262–1284.
- (213) Hoveyda, A. H.; Morken, J. P. In *Metallocenes*; Togni, A.; Halterman, R. L., Eds.; Wiley-VCH: Weinheim, 1998; Vol. 2, p 625.
- (214) Halterman, R. L. *Chem. Rev.* **1992**, *92*, 965–994.
- (215) Halterman, R. L.; Ramsey, T. M. *Organometallics* **1993**, *12*, 2879–2880.
- (216) Mitchell, J. P.; Hajela, S.; Brookhart, S. K.; Hardcastle, K. I.; Henling, M. L.; Bercaw, J. E. *J. Am. Chem. Soc.* **1996**, *118*, 1045–1053.
- (217) Ellis, W. E.; Hollis, T. K.; Odenkirk, W.; Whelan, J.; Ostrander, R.; Rheingold, A. L.; Bosnich, B. *Organometallics* **1993**, *12*, 4391–4401.
- (218) Ringwald, M.; Stürmer, R.; Brintzinger, H. H. *J. Am. Chem. Soc.* **1999**, *121*, 1524–1527.
- (219) Huttenloch, M. E.; Diebold, J.; Rief, U.; Brintzinger, H. H.; Gilbert, A. M.; Katz, T. J. *Organometallics* **1992**, *11*, 3600–3607.
- (220) Huttenloch, M. E.; Dorer, B.; Rief, Proscenc, M.-H.; Schmidt, K.; Brintzinger, H. H. *J. Organomet. Chem.* **1997**, *541*, 219–232.
- (221) Willoughby, C. A.; Buchwald, S. L. *J. Am. Chem. Soc.* **1992**, *114*, 7562–7564.

- (222) Verdaguer, X.; Lange, U. E. W.; Buchwald, S. L. *Angew. Chem., Int. Ed.* **1998**, *37*, 1103–1107.
- (223) Hayashi, T.; Konishi, M.; Kobori, Y.; Kumada, M.; Higuchi, T.; Hirotsu, K. *J. Am. Chem. Soc.* **1984**, *106*, 158–163.
- (224) Clemente, D. A.; Corain, G. P.; Tiripicchio-Camellini, B. L. *Inorg. Chim. Acta* **1986**, *115*, L9–L11.
- (225) Longato, B.; Riello, L.; Bandoli, G.; Pilloni, G. *Inorg. Chem.* **1999**, *38*, 2818–2823.
- (226) Gusev, O. V.; Kalsin, A. M.; Peterleitner, M. G.; Petrovskii, P. V.; Lyssenko, K. A.; Akhmedov, N. G.; Bianchini, C.; Meli, A.; Oberhauser, W. *Organometallics* **2002**, *21*, 3637–3649.
- (227) Adams, J. J.; Berry, D. E.; Browning, J.; Burth, D.; Curnow, O. J. *J. Organomet. Chem.* **1999**, *580*, 245–256.
- (228) Togni, A. In *Metalloenes: Synthesis, Reactivity, and Applications*; Togni, A., Halterman, R. L., Eds.; Wiley-VCH: Weinheim, 1998; Vol. 2, pp 685–722.
- (229) Curnow, O. J.; Fern, G. M. *Organometallics* **2002**, *21*, 2827–2829.
- (230) Ganter, C. *J. Chem. Soc., Dalton Trans.* **2001**, 3541–3548.
- (231) Bellemin-Lapinaz, S.; Lo, M. M.-C.; Peterson, T. H.; Allen, J. M.; Fu, G. C. *Organometallics* **2001**, *20*, 3453–3458.
- (232) O'Connor, J. M.; Casey, C. P. *Chem. Rev.* **1987**, *87*, 307–318.
- (233) Hollis, K. T.; Wang, L.-S.; Tham, F. *J. Am. Chem. Soc.* **2000**, *122*, 11737–11738.
- (234) Hollis, T. K.; Ahn, Y. J.; Tham, F. S. *J. Chem. Soc., Chem. Commun.* **2002**, 2996–2997.
- (235) Atwood, D. A.; Cowley, A. H.; Dennis, S. M. *Inorg. Chem.* **1993**, *32*, 1527–1528.
- (236) Nief, F.; Mathey, F.; Ricard, L. *J. Organomet. Chem.* **1990**, *384*, 271–278.
- (237) McCullough, F.; Bailar, J. C. *J. Chem. Soc.* **1956**, *78*, 714–716.
- (238) Habu, T.; Bailar, R. C. *J. Am. Chem. Soc.* **1966**, *88*, 1128–1130.
- (239) Onaka, S.; Iwamoto, T.; Sasaki, Y.; Fujiwara, S. *Bull. Chem. Soc. Jpn.* **1967**, *40*, 1398–1402.
- (240) Kakazai, B. J. A.; Melson, G. A. *Inorg. Chim. Acta* **1970**, *4*, 360–364.
- (241) Kakazai, B. J. A.; Melson, G. A. *Inorg. Chim. Acta* **1968**, *2*, 186–190.
- (242) Tanimura, T.; Ito, H.; Fujita, J.; Saito, K.; Hirai, S.; Yamasaki, K. *J. Coord. Chem.* **1973**, *3*, 161–167.
- (243) Micu-Semeniuc, R.; Macarovici, C. G.; Bossanyi, M. *Rev. Roum. Chim.* **1974**, *19*, 1157–1167.
- (244) Jordan, W. T.; Lin, C.-Y.; Douglas, B. E. *J. Coord. Chem.* **1973**, *3*, 1–6.
- (245) Radlowski, C. A.; Liu, C. F.; Jun, M. J. *Inorg. Chim. Acta* **1984**, *86*, 101–106.
- (246) Radlowski, C.; Liu, C. F.; Kim, C. H.; Choi, S. R.; Jun, M. J. *Polyhedron* **1985**, 769–771.
- (247) Alguindigue, S. S.; Khan, M. A.; Ashby, M. T. *Organometallics* **1999**, *18*, 5112–5119.
- (248) Alguindigue, S. S.; Khan, M. A.; Ashby, M. T. *Inorg. Chim. Acta* **2000**, *310*, 156–162.
- (249) Perrin, C. L.; Dwyer, T. J. *Chem. Rev.* **1990**, *90*, 935–67.
- (250) Ottersen, T. *Acta Chem. Scand.* **1977**, *A 31*, 480.
- (251) Lew, D.; Amer, I. *Tetrahedron: Asymmetry* **1993**, *4*, 2147–2148.
- (252) Ashby, M. T.; Govindan, G. N.; Grafton, A. K. *Inorg. Chem.* **1993**, *32*, 3803–3804.
- (253) Yu, W.-Y.; Cheng, W.-C.; Che, C.-M.; Wang, Y. *Polyhedron* **1994**, *13*, 2963–2969.
- (254) Ashby, M. T.; Govindan, G. N.; Grafton, A. K. *J. Am. Chem. Soc.* **1994**, *116*, 4801–4809.
- (255) Ashby, M. T. *J. Am. Chem. Soc.* **1995**, *117*, 2000–2007.
- (256) Ashby, M. T.; Alguindigue, S. S.; Khan, M. A. *Organometallics* **2000**, *19*, 547–552.
- (257) Cheng, W.-C.; Yu, W.-Y.; Zhu, J.; Cheung, K.-K.; Peng, S.-M.; Poon, C.-K.; Che, C.-M. *Inorg. Chim. Acta* **1996**, *242*, 105–113.
- (258) Chelucci, G.; Cabras, M. S.; Saba, A.; Sechi, A. *Tetrahedron: Asymmetry* **1996**, *7*, 1027–1032.
- (259) Tsue, H.; Fujinami, H.; Itakura, T.; Tsuchiya, R.; Kobayashi, K.; Takahashi, H.; Hirao, K. *J. Chem. Soc., Perkin Trans. 1* **1999**, 3677–3683.
- (260) Tsue, H.; Fujinami, H.; Itakura, T.; Hirao, K. *Tetrahedron: Asymmetry* **1999**, *10*, 2975–2981.
- (261) Yamamoto, K.; Tateishi, H.; Wantanabe, K.; Adachi, T.; Matsumura, H.; Ueda, T.; Yoshida, T. *J. Chem. Soc., Chem. Commun.* **1995**, 1637–1638.
- (262) Cotton, F. A.; Wilkinson, G. *Advanced Inorganic Chemistry*, 5th ed.; John Wiley and Sons: New York, 1988.
- (263) Wang, X. C.; Cui, Y. X.; Mak, T. C. W.; Wong, H. N. C. *J. Chem. Soc., Chem. Commun.* **1990**, 167–169.
- (264) Botteghi, C.; Schiomato, A.; De Lucchi, O. *Synth. Commun.* **1991**, *21*, 1819–1823.
- (265) Ito, K.; Katsuki, T. *Tetrahedron Lett.* **1993**, *34*, 2661–2664.
- (266) Ito, K.; Katsuki, T. *Chem. Lett.* **1994**, 1857–1860.
- (267) Kwong, H. L.; Lee, W. S.; Ng, H. F.; Chiu, W. H.; Wong, W. T. *J. Chem. Soc., Dalton Trans.* **1998**, 1043–1046.
- (268) Collomb, P.; von Zelewsky, A. *Tetrahedron: Asymmetry* **1998**, *9*, 3911–3917.
- (269) Wong, H. L.; Tian, Y.; Chan, K. S. *Tetrahedron Lett.* **2000**, *41*, 7723–7726.
- (270) Bolm, C.; Zehnder, M.; Bur, D. *Angew. Chem., Int. Ed. Engl.* **1990**, *29*, 205–207.
- (271) Chelucci, G. *Gazz. Chim. Ital.* **1992**, *122*, 89–98.
- (272) Chelucci, G.; Thummel, R. P. *Chem. Rev.* **2002**, *102*, 3129–3170.
- (273) Milani, B.; Alessio, E.; Mestroni, G.; Zangrando, E.; Randaccio, L.; Consiglio, G. *J. Chem. Soc., Dalton Trans.* **1996**, 1021–1029.
- (274) Yu, W.-Y.; Fung, W.-H.; Zhu, J.-L.; Cheung, K.-K.; Ho, K.-K.; Che, C.-M. *J. Chin. Chem. Soc.* **1999**, *46*, 341–349.
- (275) Thummel, R. P. *Tetrahedron* **1991**, *47*, 6851–6886.
- (276) Belser, P.; von Zelewsky, A. *Helv. Chim. Acta* **1980**, *63*, 1675–1702.
- (277) Thummel, R. P.; Lefoulon, F. *J. Org. Chem.* **1985**, *50*, 666–670.
- (278) Draux, M.; Bernal, I.; Lefoulon, F.; Thummel, R. *Inorg. Chim. Acta* **1985**, *104*, 203–210.
- (279) Thummel, R. P.; Lefoulon, F. *Inorg. Chem.* **1987**, *26*, 675–680.
- (280) Thummel, R. P.; Lefoulon, F.; Korp, J. D. *Inorg. Chem.* **1987**, *26*, 2370–2376.
- (281) Wang, X. C.; Wong, H. N. C.; Mak, T. C. W. *Tetrahedron Lett.* **1987**, *28*, 5833–5836.
- (282) Wang, X. C.; Wong, H. N. C. *Pure Appl. Chem.* **1990**, *62*, 565–568.
- (283) Jaime, C.; Font, J. *J. Org. Chem.* **1990**, *55*, 2637–2644.
- (284) Rashidi-Ranjbar, P.; Sandström, J.; Wong, H. N. C.; Wang, X. C. *J. Chem. Soc., Perkin Trans. 2* **1992**, 1625–1628.
- (285) Moya, S. A.; Guerrero, J.; Pastene, R.; Schmidt, R.; Sariego, R.; Sartori, R.; Sanz-Aparicio, J.; Fonseca, I.; Martinez-Ripoll, M. *Inorg. Chem.* **1994**, *33*, 2341–2346.
- (286) Wang, X. C.; Wong, H. N. C. *Tetrahedron* **1995**, *51*, 6941–6960.
- (287) Jahng, Y.; Hazelrigg, J.; Kimball, D.; Riesgo, E.; Wu, F.; Thummel, R. P. *Inorg. Chem.* **1997**, *36*, 5390–5396.
- (288) Leung, W.-P.; Poon, K. S. M.; Mak, T. C. W.; Wang, R.-J.; Zhou, Z.-Y. *Organometallics* **1997**, *16*, 4839–4844.
- (289) Klein, R. A.; vanBelzen, R.; Vrieze, K.; Elsevier: C. J.; Thummel, R. P.; Fraanje, J.; Goubitz, K. *Collect. Czech. Chem. Commun.* **1997**, *62*, 238–256.
- (290) Riesgo, E. C.; Hu, Y.-Z.; Bouvier, F.; Thummel, R. P.; Scaltrito, D. V.; Meyer, G. J. *Inorg. Chem.* **2001**, *40*, 3413–3422.
- (291) Thummel, R. P.; Jahng, Y. *Inorg. Chem.* **1986**, *25*, 2527–2534.
- (292) Ohba, S.; Sato, S.; Saito, Y. *Acta Crystallogr.* **1979**, *B35*, 957–959.
- (293) Ohba, S.; Miyamae, H.; Sato, S.; Saito, Y. *Acta Crystallogr.* **1979**, *B35*, 1470–1472.
- (294) Sato, S.; Saito, Y. *Acta Crystallogr.* **1978**, *B34*, 3352–3354.
- (295) Long, G. V.; Boyd, S. E.; Harding, M. M.; Buys, I. E.; Hambley, T. W. *J. Chem. Soc., Dalton Trans.* **1993**, 3175–3180.
- (296) Fontes, M.; Verdaguer, X.; Solà, L.; Vidal-Ferran, A.; Reddy, K. S.; Riera, A.; Pericàs, M. A. *Org. Lett.* **2002**, *4*, 2381–2383.
- (297) Almenningen, A.; Bastiansen, O.; Cyvin, B. N.; Samdal, S. J. *Mol. Struct.* **1985**, *128*, 59–76.
- (298) Hlsw, K.; Glass, M. A. W.; Hopps, H. B.; Simon, E.; Wahl, G. H. *J. Am. Chem. Soc.* **1964**, *86*, 1710–1733.
- (299) Rebek, J. J.; Costello, T.; Wattlely, R. *J. Am. Chem. Soc.* **1985**, *107*, 7487–7493.
- (300) Rebek, J. J. *Acc. Chem. Res.* **1984**, *17*, 258–264.
- (301) Rebek, J. J.; Trend, J. E. *J. Am. Chem. Soc.* **1978**, *100*, 4315–4316.
- (302) Rebek, J. J.; Marshall, L. *J. Am. Chem. Soc.* **1983**, *105*, 6668–6670.
- (303) Westheimer, F. H. In *Steric Effects in Organic Chemistry*; Newman, M. S., Ed.; John Wiley: New York, 1956; Chapter 12.
- (304) Cheng, C. P.; Plankey, B.; Rund, J. V.; Brown, T. L. *J. Am. Chem. Soc.* **1977**, *99*, 8413–8417.
- (305) Greenberg, A.; Lieberman, J. *Strained Organic Molecules*; Academic Press: New York, 1978; pp 148–163.
- (306) Reedijk, J. In *Comprehensive Coordination Chemistry*; Wilkinson, G., Ed.; Pergamon Press: Oxford, 1987; Vol. 2, pp 73–98.
- (307) Knapp, S.; Keenan, T. P.; Zhang, X.; Fikar, R.; Potenza, J. A.; Schugar, H. J. *J. Am. Chem. Soc.* **1987**, *109*, 1882–1883.
- (308) Knapp, S.; Keenan, T. P.; Liu, J.; Potenza, J. A.; Schugar, H. J. *Inorg. Chem.* **1990**, *29*, 2189–2191.
- (309) Knapp, S.; Keenan, T. P.; Zhang, X.; Fikar, R.; Potenza, J. A.; Schugar, H. J. *J. Am. Chem. Soc.* **1990**, *112*, 3452–3464.
- (310) Imai, Y.; Zhang, W.; Kida, T.; Nakatsuji, Y.; Ikeda, I. *J. Org. Chem.* **2000**, *65*, 3326–3333.
- (311) Uozumi, Y.; Kato, K.; Hayashi, T. *J. Org. Chem.* **1998**, *63*, 5071–5075.
- (312) Andrus, M. B.; Asgari, D.; Sclafani, J. A. *J. Org. Chem.* **1997**, *62*, 9365–9368.
- (313) Uozumi, Y.; Kato, K.; Hayashi, T. *J. Am. Chem. Soc.* **1997**, *119*, 5063–5064.
- (314) Imai, Y.; Zhang, W.; Kida, T.; Nakatsuji, Y.; Ikeda, I. *Tetrahedron Lett.* **1997**, *38*, 2681–2684.
- (315) Knapp, S.; Albaneze, J.; Schugar, H. J. *J. Org. Chem.* **1993**, *58*, 997–998.
- (316) Knochel, P. *Chemtracts. Org. Chem.* **1995**, *8*, 205–221.
- (317) Knochel, P.; Vettel, S.; Eisenberg, C. *Appl. Organomet. Chem.* **1995**, *9*, 175–188.

- (318) Berrisford, D. J.; Bolm, C.; Sharpless, K. B. *Angew. Chem., Int. Ed. Engl.* **1995**, *34*, 1059–1070.
- (319) Balsells, J.; Betancort, J. M.; Walsh, P. J. *Angew. Chem., Int. Ed.* **2000**, *39*, 3428–3430.
- (320) Bradley, D. C.; Mehrotra, R. C.; Rothwell, I. P.; Singh, A. *Alkoxo and Aryloxo Derivatives of Metals*; Academic Press: London, 2001.
- (321) Alberts, A. H.; Wynberg, H. *J. Am. Chem. Soc.* **1989**, *111*, 7265–7266.
- (322) Soai, K.; Shibata, T.; Morioka, H.; Choji, K. *Nature* **1995**, *378*, 767–768.
- (323) Bolm, C.; Bienewald, F.; Seger, A. *Angew. Chem., Int. Ed. Engl.* **1996**, *35*, 1657–1659.
- (324) Balsells, J.; Costa, A. M.; Walsh, P. J. *Isr. J. Chem.* **2001**, *41*, 251–261.
- (325) Mikami, K.; Angelaud, R.; Ding, K. L.; Ishii, A.; Tanaka, A.; Sawada, N.; Kudo, K.; Senda, M. *Chem. Eur. J.* **2001**, *7*, 730–737.
- (326) Geerts, R. L.; Huffman, J. C.; Caulton, K. G. *Inorg. Chem.* **1986**, *25*, 1803–1805.
- (327) Darensbourg, D. J.; Zimmer, M. S.; Rainey, P.; Larkins, D. L. *Inorg. Chem.* **1998**, *37*, 2852–2853.
- (328) Cummins, C. C. In *Three-Coordinate Complexes of "Hard" Ligands: Advances in Synthesis, Structure and Reactivity*; Karlin, K. D., Ed.; Progress in Inorganic Chemistry 47; John Wiley and Sons: New York, 1998; pp 685–836.
- (329) Müllen, K.; Heinz, W.; Klärner, F.-G.; Roth, W. R.; Kindermann, I.; Adamczak, O.; Wette, M.; Lex, J. *Chem. Ber.* **1990**, *123*, 2349–2371.
- (330) Muñoz-Muñiz, O.; Juaristi, E. *J. Org. Chem.* **2003**, asap.
- (331) van der Linden, A.; Schaverien, C. J.; Meijboom, N. *J. Am. Chem. Soc.* **1995**, *117*, 3008–3021.
- (332) Corazza, F.; Floriani, C.; Chiesi-Villa, A. *Inorg. Chem.* **1991**, *30*, 145–148.
- (333) Floriani, C.; Corazza, F.; Lesueur, W.; Chiesi-Villa, A.; Guastini, C. *Angew. Chem., Int. Ed. Engl.* **1989**, *28*, 66–67.
- (334) Okuda, J.; Fokken, S.; Kang, H.-C.; Massa, W. *Chem. Ber.* **1995**, *128*, 221–227.
- (335) Sernetz, F. G.; Mülhaupt, R.; Fokken, S.; Okuda, J. *Macromolecules* **1997**, *30*, 1562–1569.
- (336) Takeuchi, D.; Nakamura, T.; Aida, T. *Macromolecules* **2000**, *33*, 725–729.
- (337) Gielen, E. E. C. G.; Dijkstra, T. W.; Berno, P.; Meetsma, A.; Hessen, B.; Teuben, J. H. *J. Organomet. Chem.* **1999**, *591*, 88–95.
- (338) Soai, K.; Niwa, S. *Chem. Rev.* **1992**, *92*, 833–856.
- (339) Yamakawa, M.; Noyori, R. *Organometallics* **1999**, *18*, 128–133.
- (340) Zhang, F.-Y.; Yip, C.-W.; Cao, R.; Chan, A. S. C. *Tetrahedron: Asymmetry* **1997**, *8*, 585–589.
- (341) Mori, M.; Nakai, T. *Tetrahedron Lett.* **1997**, *38*, 6233–6236.
- (342) Balsells, J.; Davis, T. J.; Carroll, P. J.; Walsh, P. J. *J. Am. Chem. Soc.* **2002**, *124*, 10336–10348.

CR0000630